TKK Dissertations 206
Espoo 2009

METHOD AND DEVICE FOR IN SITU RUNOUT MEASUREMENT OF CALENDER THERMO ROLLS

Doctoral Dissertation

Panu Kiviluoma

Helsinki University of Technology
Faculty of Engineering and Architecture
Department of Engineering Design and Production

TKK Dissertations 206
Espoo 2009

METHOD AND DEVICE FOR IN SITU RUNOUT MEASUREMENT OF CALENDER THERMO ROLLS

Doctoral Dissertation

Panu Kiviluoma

Dissertation for the degree of Doctor of Science in Technology to be presented with due permission of the Faculty of Engineering and Architecture for public examination and debate in Auditorium K216 at Helsinki University of Technology (Espoo, Finland) on the 18th of December, 2009, at 12 noon.

Helsinki University of Technology
Faculty of Engineering and Architecture
Department of Engineering Design and Production

Teknillinen korkeakoulu
Insinööritieteiden ja arkkitehtuurin tiedekunta
Koneenrakennustekniikan laitos

Distribution:
Helsinki University of Technology
Faculty of Engineering and Architecture
Department of Engineering Design and Production
P.O. Box 4100 (Otakaari 4)
FI - 02015 TKK
FINLAND
URL: http://edp.tkk.fi/en/
Tel. +358-9-47001
E-mail: panu.kiviluoma@tkk.fi

ISBN 978-952-248-259-4
ISBN 978-952-248-260-0 (PDF)
ISSN 1795-2239
ISSN 1795-4584 (PDF)
URL: http://lib.tkk.fi/Diss/2009/isbn9789522482600/

TKK-DISS-2703

Picaset Oy
Helsinki 2009

ABSTRACT OF DOCTORAL DISSERTATION	HELSINKI UNIVERSITY OF TECHNOLOGY P.O. BOX 1000, FI-02015 TKK http://www.tkk.fi

Author Panu Kiviluoma

Name of the dissertation

Method and device for *in situ* runout measurement of calender thermo rolls

Manuscript submitted 7th of September, 2009	Manuscript revised 1st of December, 2009
Date of the defence 18th of December, 2009	
☒ Monograph	☐ Article dissertation (summary + original articles)

Faculty	Faculty of Engineering and Architecture
Department	Department of Engineering Design and Production
Field of research	Paper machinery technology
Opponent(s)	Prof. Rene Theska and D.Sc. (Tech.) Juha Lipponen
Supervisor	Prof. Petri Kuosmanen
Instructor	Prof. Petri Kuosmanen

Abstract

Geometric and rotational errors of the paper machine rolls have a direct influence on the quality of the finished paper and may also weaken the runnability of the machine. In the calender section where the paper gets the final structure and finish, the surface temperature of a thermo roll may be 250 °C or even more. High temperature causes roll deformations such as bending and so-called polygon effect.

The measurements of the roll geometry are usually carried out in the workshop conditions. However, to find out the true dynamic behavior of the rolls requires that the measurements should be done in the real operating conditions during the process. This is difficult and often impossible to do because of the harsh environment and issues with the sensor mounting. Many conventional displacement measuring methods are sensitive to either the target material properties or to the environment.

In this study, a device and a method for the *in situ* measurement of a roll shell runout based on the measurement of radial acceleration of the surface was described. In this method, an acceleration sensor attached to a sliding probe is held against the rotating roll surface. Acquired acceleration signal is averaged and double integrated using a computer to get the surface displacement, i.e., runout. A number of measurements were done to demonstrate the applicability of the method. The laboratory measurements showed that it was possible to measure runout with an adequate accuracy. The case measurements showed that by using the method it was possible to detect and measure phenomena in the rotating rolls that were difficult or impossible to measure earlier. The method can be used, for example, for applications related to problem solving in the paper quality and runnability issues, online geometry measurement and balancing.

Keywords paper machine, roll geometry, roundness, dynamic error, thermal deformation, measuring

ISBN (printed) 978-952-248-259-4	ISSN (printed) 1795-2239
ISBN (pdf) 978-952-248-260-0	ISSN (pdf) 1795-4584
Language English	Number of pages 98

Publisher Helsinki University of Technology, Department of Engineering Design and Production

Print distribution Helsinki University of Technology, Department of Engineering Design and Production

☒ The dissertation can be read at http://lib.tkk.fi/Diss/2009/isbn9789522482600/

VÄITÖSKIRJAN TIIVISTELMÄ	TEKNILLINEN KORKEAKOULU PL 1000, 02015 TKK http://www.tkk.fi

Tekijä Panu Kiviluoma

Väitöskirjan nimi

Menetelmä ja laite kalanteritermotelojen ajonaikaiseen heiton mittaukseen

Käsikirjoituksen päivämäärä 7.9.2009	Korjatun käsikirjoituksen päivämäärä 1.12.2009

Väitöstilaisuuden ajankohta 18.12.2009

☒ Monografia	☐ Yhdistelmäväitöskirja (yhteenveto + erillisartikkelit)

Tiedekunta	Insinööritieteiden ja arkkitehtuurin tiedekunta
Laitos	Koneenrakennustekniikan laitos
Tutkimusala	Paperikonetekniikka
Vastaväittäjä(t)	Prof. Rene Theska ja TkT Juha Lipponen
Työn valvoja	Prof. Petri Kuosmanen
Työn ohjaaja	Prof. Petri Kuosmanen

Tiivistelmä

Paperikoneen telojen ympyrämäisyys- ja pyörimisvirheet vaikuttavat suoraan valmistettavan paperin laatuun ja ne voivat myös aiheuttaa ajettavuusongelmia koneella. Kalanteriosalla, jossa paperi saa lopullisen rakenteensa ja pinnanlaatunsa, käytetään termoteloja, joiden pintalämpötila voi olla jopa 250 °C. Näin korkeat lämpötilat aiheuttavat telojen taipumista sekä ns. piparkakkuilmiötä.

Telojen mittaukset suoritetaan yleensä konepajaolosuhteissa. Telojen todellisen dynaamisen käyttäytymisen selvittäminen edellyttäisi kuitenkin telojen mittaamista ajon aikana todellisissa prosessiolosuhteissa. Käytännössä tällaisten mittausten suorittaminen on usein hankalaa tai jopa mahdotonta vaikeiden olosuhteiden ja anturien asentamiseen liittyvien ongelmien vuoksi. Monet perinteiset siirtymäanturit ovat herkkiä joko kohteen materiaalin tai ympäristöolosuhteiden suhteen.

Tässä tutkimuksessa on esitetty telavaipan ajonaikaisen heiton mittaamiseen soveltuva laite ja menetelmä, joka perustuu pinnan säteensuuntaisen kiihtyvyyden mittaamiseen. Menetelmässä pyörivän telan pintaa vasten pidetään liukupalaa, johon on kiinnitetty kiihtyvyysanturi. Tallennetusta kiihtyvyyssignaalista saadaan keskiarvostamisen ja kaksinkertaisen integroinnin avulla telapinnan siirtymä eli heitto. Menetelmän toimivuutta on tutkittu kokeellisesti lukuisten mittausten avulla. Laboratoriomittaukset osoittivat, että menetelmällä on mahdollista mitata heittoa riittävällä tarkkuudella. Paperitehtaissa suoritetut mittaukset puolestaan osoittivat, että menetelmällä on mahdollista todeta ja mitata teloissa esiintyviä ilmiöitä, joiden mittaaminen ei aikaisemmin ole ollut mahdollista. Menetelmää voidaan käyttää mm. paperin laatuun tai koneen ajettavuuteen liittyvien ongelmien selvittämiseen, telojen ajon aikaisen muodon mittaamiseen sekä tasapainotukseen.

Asiasanat paperikone, telageometria, ympyrämäisyys, dynaaminen virhe, lämpömuodonmuutos, mittaaminen

ISBN (painettu)	978-952-248-259-4	ISSN (painettu)	1795-2239
ISBN (pdf)	978-952-248-260-0	ISSN (pdf)	1795-4584
Kieli	englanti	Sivumäärä	98

Julkaisija TKK, Koneenrakennustekniikan laitos

Painetun väitöskirjan jakelu TKK, Koneenrakennustekniikan laitos

☒ Luettavissa verkossa osoitteessa http://lib.tkk.fi/Diss/2009/isbn9789522482600/

Preface

The method for *in situ* measurement of paper machine rolls has been developed during the past years in the research projects funded by TEKES and Finnish paper industry. I wish to thank all the participants, and especially the research group of Paper Machinery, for the opportunity to make this thesis on the subject. Thanks to Esa Porkka for the original idea and many other good advice, Jukka Pirttiniemi for the construction and the long hours of measurement and Jari Toiva for solutions to the challenges in the analysis. Thanks to Thomas Widmaier and Jari Juhanko for the feedback on the manuscript. I would also like to thank all the colleagues and co-workers, former and present, back then in the Laboratory of Machine Design and, now, in the Department of Engineering Design and Production for the inspiration and support. It's been a long way here.

Professor Petri Kuosmanen deserves thanks for giving the possibility to finish this thesis and for the endless trust and support during this project. Thanks to Vesa Saikko for the invaluable comments on the manuscript.

Thanks to my parents for over four decades of support. It is fairly possible now that there will be a doctor in the family. And finally, thanks again to Anne, Sara, Iiris and Mari for the love, support and understanding through all these years even though, I'm afraid, you had no idea what I was doing.

Helsinki, December 2009 Panu Kiviluoma

Contents

Introduction

1.1 Background

In a paper machine (Figure 1) there are hundreds of rolls for various tasks. The sizes, geometries and materials of the rolls vary depending on the tasks. Most of the rolls support and guide the paper web during the process while some have a direct influence on the properties of the paper. In the press section the paper web is mangled between two rolls under high pressure to remove water from the web and to compress it. In the coating section the backing roll acts as a counter face for the applied coating which improves the look and printing properties of the paper. In the calender the web is again pressed between a pair or multiple pairs of rolls to give paper desired structure and finish.

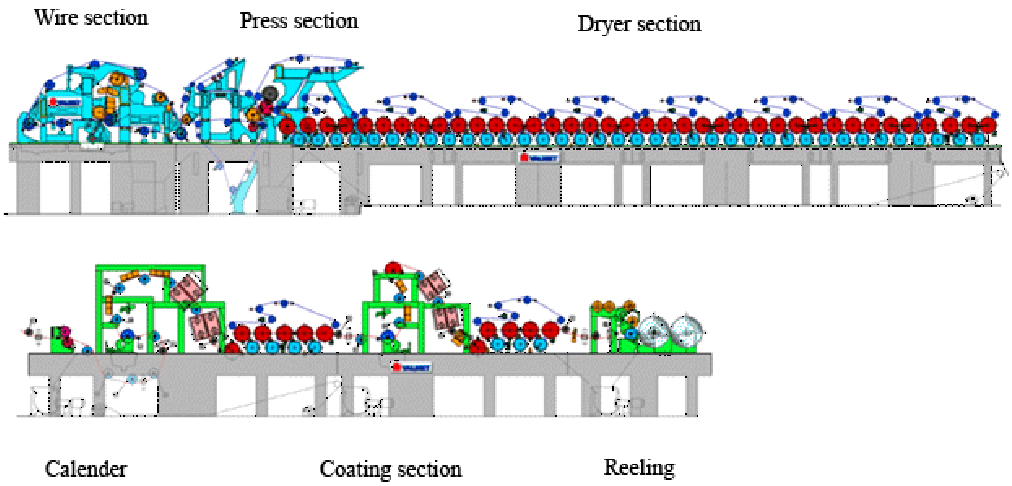

Figure 1. Main sections of modern LWC paper machine (Metso Paper 2009).

The contact zone between two rolls is called a nip (Figure 2). In the nip the paper web is pressed between two rotating rolls under heavy load and, especially in calendering, under high temperature. The temperature in the nip is controlled using heated rolls, thermo rolls.

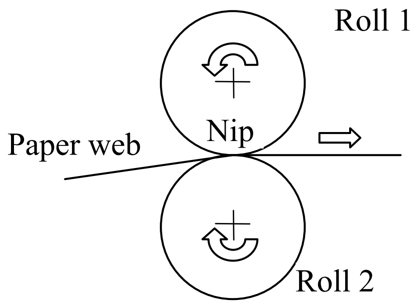

Figure 2. In a nip paper web travels between two rolls.

There may be one or several nips in a calender depending on the paper grade and calender location in the paper machine line. In a typical soft calender there is a roll with a soft polymer cover against a heated hard cover thermo roll. Soft calender is usually an on-line calender, that is, the paper is calendered at the process speed before reeling. There may also be two consecutive roll pairs for calendering both sides of the paper. A multinip supercalender (Figure 3) is installed off-line and has typically a stack of 9 to 12 alternating hard and soft rolls. There are on-line multinip calenders with 6 to 14 rolls in one or two stacks as well.

Figure 3. Roll stack of a supercalender.

The nip-rolls have a direct influence on the paper quality. Geometric errors on the rolls cause variation in the nip pressure which may affect the paper web. Since the main target of calendering is to modify the surface structure and caliper of the paper (Jokio 1999), problems in rolls may cause several different calendering problems such as profile problems (gloss, caliper, moisture) and barring (Vinicki 2001). Barring appears as a periodic variation on the paper web in the machine direction. Calendering is usually the final step in the papermaking process, and it has a decisive influence on many end-use properties. Coated papers are calendered to increase gloss, which is considered to be the most important surface property (Larsson et al. 2007).

In modern papermaking industry production rates are improved by increasing the speed of the machines and making the machines wider which results in long and slim, and therefore fairly flexible, rolls. High demands are made on the dynamic properties of the rolls. The rolls leave the manufacturer in good condition qualifying the geometrical tolerances and other demands. In their lifetime the rolls go through many maintenance operations and worn surfaces will be reground or recovered. Consequently the geometrical properties may change gradually. The behaviour of the roll also depends on the support. The bearing and other supporting structures on the machine change the dynamic properties of the roll assembly compared with those in the workshop. Typical causes of vibrations in paper machines are rolls that have rotational errors such as runout. Especially sensitive to problems caused by runout are nip-rolls because they are in contact with other rolls and the paper web. Vibrations in paper machines do not only have an effect on the end-product quality but they reduce the runnability of the paper machine by limiting the allowable running speed and causing extra breaks.

Some of the problems with rolls can be detected by condition monitoring systems which are widely used in paper industry. On-line condition monitoring systems are typically based on vibration measurements of the roll support. In most cases the measurement is done by accelerometers attached to the bearing houses at the roll ends. In this way, increased vibration levels can be detected and vibration appearing at the frequency of the rotation speed of a roll or its multiple can be related to a specific roll. The cause for vibration may still remain unknown. Indirect measurement of the vibration through the bearing houses does not provide enough information about the behaviour of the roll body during the operation and about the causes for the vibration. To find out why a specific roll vibrates or excites vibration it would be useful to be able to study the dynamic behaviour of the roll in the installation position during the papermaking process.

Besides problem solving, the *in situ* measurement of roll body dynamics has many other applications. The roll behaviour is vital information for the process development purposes. If the running speed of the machine is to be raised, it is necessary to find out the rolls that may become bottlenecks because of excessive vibration. Measurements can also be used to detect the need for roll maintenance for example due to shape deformations. Information about the runtime geometry and behaviour can be used for the planning of the required maintenance operations such as grinding or balancing.

1.2 Research problem

The measurements of roll geometry are usually done in the workshop conditions during the normal maintenance operations. For example, the roundness measurement of the roll can be done in the grinding machine at low speed (Kuosmanen and Väänänen 1996). Using special workshop test equipment the dynamic behavior of a roll can be measured at higher speeds (Juhanko 1999). However, in order to find out the actual dynamic behaviour and run-time roll geometry, the rolls should be measured in conditions that are equivalent to those during the papermaking process. Then, for example, the bending of the roll caused by unbalance or high temperature would correspond to the bending that becomes evident in the process conditions. Some of the conditions that are essential for the behaviour are rotation frequency, temperature and support of the rolls, i.e., bearings and supporting structures. The running speed of a modern paper machine may be between 1000 and 2000 m/min which corresponds to a typical roll rotation frequency of 5 to 10 Hz depending on the roll diameter. The surface temperature of a thermo roll may be 250 °C or even more. The paper web transfers a part of the thermal energy from the roll surface possibly changing the surface temperature of the roll. The paper web may act as a source for excitation in the form of periodic thickness variations.

With nip rolls, the contact with an other roll will have its own influence on the behaviour of the roll. The research group at Tampere University of Technology (TUT) has built a half-scale nip test unit (Kivinen 2001) in the laboratory to study the effect of nip contact on the system dynamics. Despite of the mathematical models and laboratory and on-site measurements, a full understanding about the dynamics of nip contact has still not been achieved (Cotsaftis et. al. 2005, Yuan et. al. 2006, Järvenpää et. al. 2007). Many modes of vibration can however be related to the geometrical errors of the rolls. Most of the measurements have been done using accelerometers placed on the bearing houses of the rolls.

The above-mentioned run-time conditions are expensive and difficult or sometimes impossible to reproduce in the workshop. High temperature, for example, may damage or impair the accuracy of high precision machine tools or measuring instruments. In order to solve problems related to rolls, it is often necessary to change running parameters such as speed or temperature to see what is their influence on the behaviour of the rolls. This is usually not possible during the papermaking process, so the tests should be done during the maintenance breaks. These breaks are typically very tightly scheduled and there is not much time to set up the measuring instruments.

In *in situ* measurements, the biggest difficulties arise from the support or fixture of the sensors. The sensor should be placeable close to the surface of the roll and yet the support of the sensor should be rigid. Some sensors require calibration to the measured surface. The vibrations conducting through the sensor support may distort the signal which calls for measures to compensate the movement of the sensor from the signal. These measures further complicate the measurement arrangement and add inaccuracy to the results. The sensors may be subjected to harsh environmental conditions such as heat, moisture or impacts. Yet the measuring system should be flexible and mobile enough to make it possible to take several measurements in different cross-sections and positions in a short period of time during the process. One possible problem when measuring nip rolls is the fact that the rolls will be moving relative to each other during the process. Usually, the nip is held open until the paper web is running and, in case of web break, the nip will be opened again.

There are many different sensors that can be used for the measurement of surface displacement. Contact-based displacement sensors, such as dial indicators or LVDT sensors (Linear Variable Differential Transformer) are best suited for measurements in workshop or laboratory conditions where rotation speed of the target is low. At higher speeds the dynamics of mechanics, wear of the gauge or warming up may decrease the accuracy. These problems could partly be avoided by using non-contact sensors. They have the benefit of not damaging the surface under measurement. Optical, eddy current and capacitive sensors all have adequate accuracy for runout measurements. These sensors do however have properties that make their use in runtime conditions inconvenient. Inductive or eddy current based sensors, for example, may be sensitive to inhomogeneties in the target material or surface geometry such as the curvature of roll surface. They require a calibration on the target material and geometry which may be difficult or impossible to do in process conditions and with moving targets. Problems may arise from a short measuring range and, especially with optical sensors, stability of the medium, changes in surface reflectivity or contamination.

1.3 Aim of the research

The objective of this research is to confirm experimentally that with the developed device and method it is possible to measure the runout of paper machine rolls in process conditions with accuracy in the scale of a few micrometers. The method is utilised to perform on-line measurements of phenomena in rotating rolls in a frequency range up to a few hundred Hertz that were difficult or impossible to measure earlier.

1.4 Scope of the research

This research is restricted to the measurement of radial runout of a cylindrical object. The research will focus on the measurement of frequency and amplitude of the runout. Usually for problem solving purposes it is enough to find out the frequencies in runout that have the highest amplitudes. The magnitude and phase of the runout are needed, for example, if any corrections for the geometry of the roll are planned using 3D-grinding methods. The magnitude and phase of the first harmonic component of the runout is the basis for roll balancing. No error separation methods will be used to separate roundness and eccentricity in the runout signal.

1.5 Research methods

A measuring device was constructed and its operation was verified experimentally in the laboratory and process environment in selected paper mills. The laboratory measurements were compared with other measurement methods. The *in situ* measurements could not be verified but the results were analyzed taking into consideration literary references.

The analysis of the measured signals used mathematical methods like FFT-based synchronous averaging and double integration of acceleration to displacement in the frequency domain.

1.6 Contribution

This work showed that the slide pad based displacement measurement method was applicable in runout measurement of thermo rolls in process conditions. It showed that this method can be used to measure phenomena in rolls that would otherwise be difficult or impossible to detect. With *in situ* runout measurements it is possible to determine, for example, how the temperature distribution in a roll cross section, change of temperature or unbalance affect the deflection of the roll or roll surface. The method can be used as a tool to analyse and solve problems related to the paper quality or runnability of the paper machine.

2 Runout of thermo rolls

The movement of a surface of a roll or any other rotating object in relation to a fixed datum is called runout (Figure 4). The motions of a surface are a combination of both the physical properties of the target such as eccentricity or surface geometry and vibrations. This must be taken into account when analysing runout. Runout is a very practical parameter and directly measurable. It can be used as a tool for many purposes such as condition monitoring and balancing.

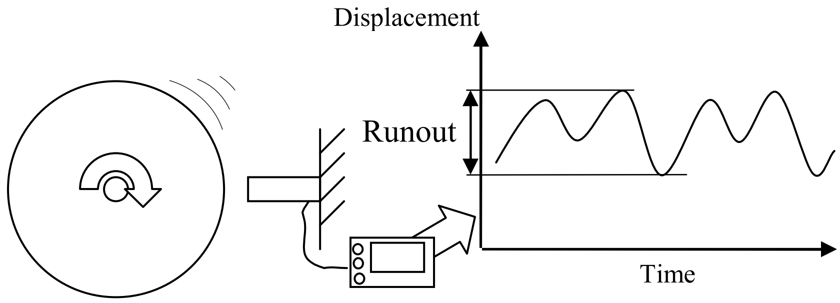

Figure 4. Runout is the movement between a surface and a fixed datum.

2.1 Definition of runout

According to the ISO 1101 standard circular runout is defined within any cross-section (*b*) perpendicular to the datum axis (*a*) as the radial difference (*t)* between two concentric circles centred on the datum point and drawn such that one coincides with the nearest and the other with the farthest point on the profile (Figure 5). So runout is defined with respect to a fixed point and is the difference between the nearest and furthest point on a profile from that point. The term runout is occasionally referred to as *total indicated reading* or *total indicated runout* (TIR) (Smith 2002).

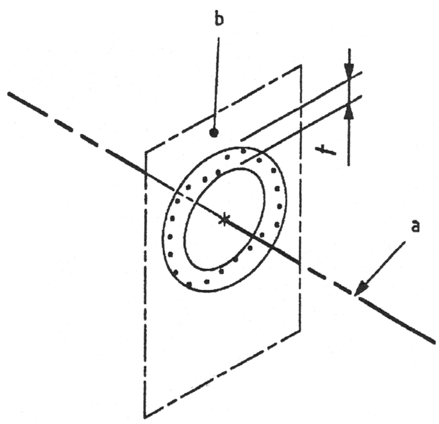

Figure 5. Definition of runout (ISO 1101).

2.2 Analysis of runout

A very useful measure for runout is the maximum value of runout measured during one rotation of the workpiece (Figure 6). To add reliability to the measurement, several rotations can be measured and the data averaged. The runout can be displayed either in polar or cartesian coordinates where the displacement trace is plotted against the phase angle. The polar plot is fairly descriptive but can sometimes cause the runout to get mixed with the geometrical shape of the workpiece.

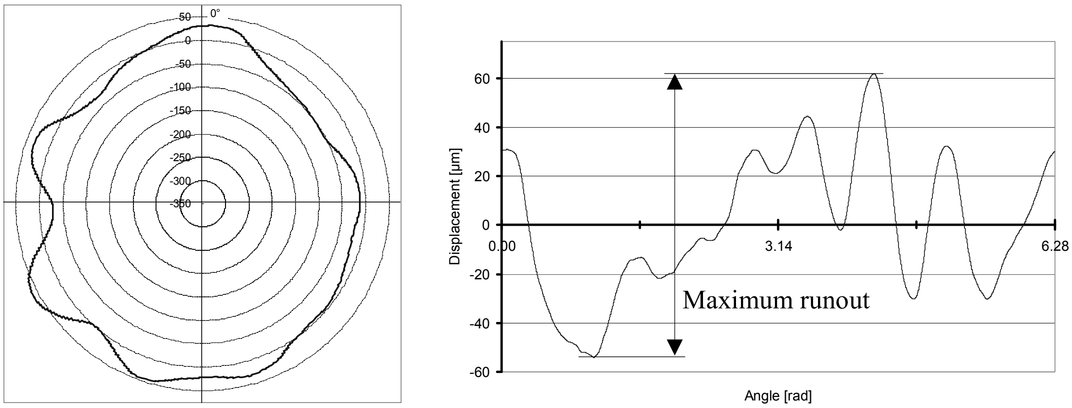

Figure 6. Runout derived from the displacement displayed in polar (left) and cartesian coordinates (right).

Often it is more useful to analyse runout by the harmonic content of the signal (Figure 7). According to the Fourier theorem, a periodic function can be represented as a sum of sinusoidal components at equally spaced frequencies kf_1 where f_1 is the reciprocal of the periodic time and k is an integer. The frequency of the k^{th} component $f_k = kf_1$ is called the k^{th} harmonic of f_1 (Randall 1987). Therefore the harmonics are multiples of the basic frequency. When analysing rotating objects this basic frequency is the rotation frequency of the target and the harmonics are multiples of that frequency. On a circular profile the harmonics can be considered uniform waveforms (sine waves) that are superimposed onto the surface of the part.

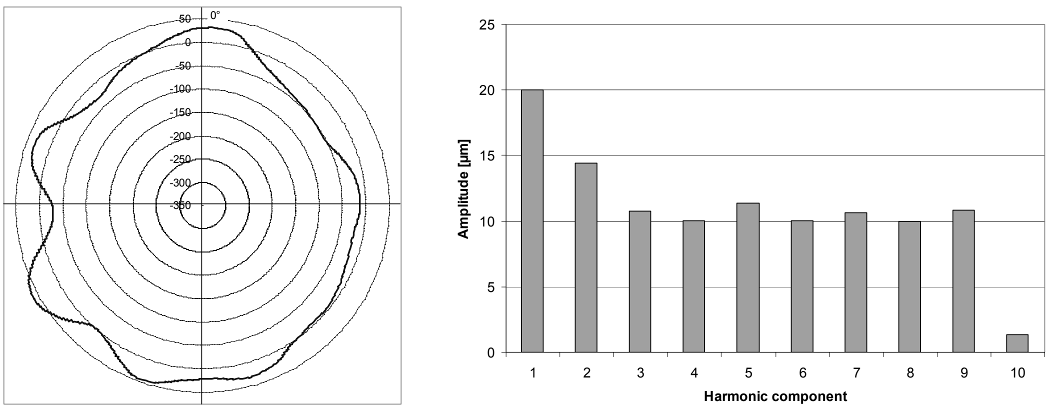

Figure 7. Amplitudes of the harmonics (right) occurring on the measured runout profile(left).

The harmonic analysis is useful in determining the cause of possible problems as different issues produce different harmonics. Vibration or runout due to imbalance appears at the rotation frequency, i.e., 1^{st} harmonic. Vibration appearing at twice the rotation frequency (2^{nd} harmonic) can be excited for example by stiffness asymmetry, misalignment or journal ovality. The harmonic behaviour can also be related to either the manufacturing process of the component or its measurement (Smith 2002). The amplitude of the 1^{st} harmonic (1 undulation per revolution, upr) is equal to the eccentricity of the part, relative to the spindle axis of the roundness instrument. The 2^{nd} harmonic (2 upr) is generally called ovality and can be caused either by a setting-up error of the roundness instrument, or the part being machined out-of-square to its axis of revolution. The harmonics from the 3^{rd} to the 7^{th} are normally introduced by the work-holding technique during the manufacture. If a three-jaw chuck was used to hold the part and an excessive clamping force was employed, then upon machining and removal of the clamping forces a three-lobed part would have been produced. Harmonics from the 15^{th} upwards are usually introduced to the part by either machine instability (self-exciting vibration – chatter) or by the reaction of the materials used in the component, cutting tool and lubricant (Smith 2002). The higher harmonics could be the result of instrument noise or vibration.

Harmonic features are normally calculated using Fast Fourier Transform (FFT), which breaks down the measured data into its constituent waveforms and calculates both the amplitude and phase angle of each harmonic (Smith, 2002). FFT is an algorithm for obtaining the Discrete Fourier Transform (DFT). DFT takes a discrete signal in the time domain and transforms that signal into its discrete frequency domain representation. The basic prerequisites by the algorithm for the data to be analyzed are that the signal must be periodic and, for the most efficient FFT algorithms, the number of sampled points must equal to a power of 2. When measuring a rotating object, the data is inherently periodic unless external, non-synchronous disturbance, affects the measurement. These disturbances can be minimized by averaging. If the number of samples does not equal to a power of the 2, the data set can be extended by adding zeros to the end of the data until the number of points is correct. Some modern algorithms, used for example in *Matlab* (Mathworks 2007), do no longer require a power-of-two length data set.

2.3 Causes of runout of thermo rolls

Leaving aside the externally excited vibrations, the runout of thermo rolls is caused by roundness errors and rotational errors. These errors can further be divided into static and dynamic errors and errors caused by uneven thermal expansion. Static errors are due to eccentricity, surface errors, initial curvature and errors in bearing for example. Dynamic errors are caused by dynamic bending or deflection of roll shell under a centrifugal force. Also asymmetric support of the roll or asymmetric or inhomogeneous structure of the roll body affects the dynamic runout. Uneven thermal expansion is caused by either uneven heat distribution or material inhomogeneity. Typical for the dynamic runout is its relation to the rotation frequency of the roll. The runout caused by thermal deflection or unbalance appears normally in the rotation frequency while runout caused by roundness errors may appear at higher frequencies. There are also form errors that are caused by other reasons such as the time-dependent alteration of material properties.

2.3.1 Roundness errors

The static roundness errors of rolls result from the changing distance between the workpiece centre axis and the tool during the machining process (Kuosmanen 2004). The workpiece may have rotational error caused by a changing flexural stiffness or errors in the bearing arrangement. Also the workpiece or tool vibrations during the machining may cause roundness errors. Any roundness profile will consist of a series of sine waves that are combined to form the overall roundness shape. These undulations are synchronized with the rotation frequency including integer multiples of the rotation frequency.

2.3.2 Unbalance

The unbalance is caused by uneven distribution of mass on the rotational part. The centrifugal force F_c is proportional to the unbalance mass *m*, the radius of location of unbalanced mass *e* and to the square of angular velocity ω

$$F_c = me\omega^2 \tag{1}$$

Since the rotation frequencies of the rolls are continuously increasing, any residual unbalance will result in a significant centrifugal force that will cause vibrations and elastic deformation of the roll at high frequencies. The response caused by the unbalance will be seen on the 1st harmonic component of the runout as the centrifugal force has the same rotation frequency as the roll. When a roll is balanced, the response is typically measured at the roll support, i.e., the bearing, using a dedicated balancing machine.

2.3.3 Thermal deformations

In calender thermo rolls the thermal fluid transfers heat to the roll surface. A typical peripherally drilled type calender thermo roll consists of a peripherally drilled cast iron roll body and bolted-on flanged journals (Figure 8). The peripherally drilled fluid passages are usually 20…60 mm below the outer surface of the roll (Jokio 1999). The manufacturers have designed and patented different configurations for the fluid passages ranging from one peripheral bore per pass to three adjacent bores in parallel with the two outer bores flowing out and returning in the middle hole at twice the velocity (Figure 9). Peripheral holes are normally drilled from both ends of the roll body and they meet in the middle of the roll body. Bending of the boring rod and variation in the roll hardness may cause variation in the distance between the bore and the roll surface. This and possible misalignment of the bores may cause surface temperature deviations.

Figure 8. Structure of peripherally bored calender thermo roll (SHW Casting Technologies, Inc. 2009).

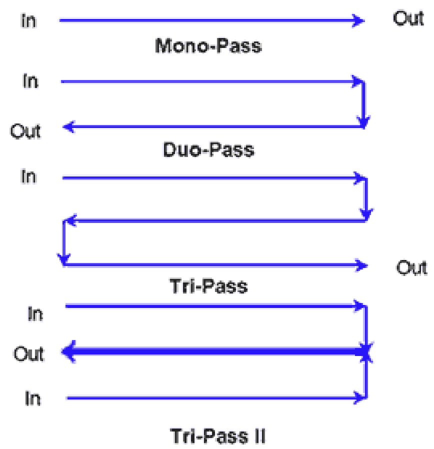

Figure 9. Flow configurations for thermo roll body (SHW Casting Technologies, Inc. 2009).

The difference in temperature between adjacent bores causes a periodic circumferential pattern on roll surface. According to manufacturer (SHW 2003) with Duo-Pass configuration there is 10 °C temperature drop between adjacent bores on the tending side of the roll in a multinip calender with a throughput of 20 litres per second and a heat load of 800 kW. This is enough to cause temperature distortions in the circumferential direction called polygon effect. Another manufacturer (Wirtz 2002/Walzen Irle) claims that with their peripherally bored thermo roll concept it is possible to obtain a radius deviation in the roll less than 1 µm and a temperature difference of less than 2 °C between adjacent bores (Figure 10).

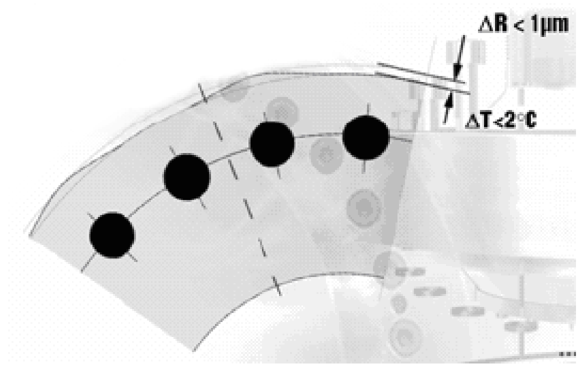

Figure 10. Temperature uniformity and the roll shape of a Walzen Irle Roll (Wirtz 2002).

Zaoralek (1991) used finite element analysis to show that according to the thermal pattern a slight polygon shape is generated by thermal expansion with peaks between 2 and 3 µm. There are no reports to show that anyone has actually measured the polygon shape caused by thermal expansion. Zaoralek (2004) also stated that the inherent shortcomings with respect to the straightness and the precision of the bores can cause roll surface temperature variations and imbalance and vibration which as a result cause operating and paper quality problems. The scattering of bores directly affects the mass distribution within the roll body and results in unbalance. The variation of the distance of the peripheral bores from the roll surface affect the circumferential temperature distribution which due to thermal expansion may deflect the roll centre.

Rothenbacher et al. (1985, 1986) listed three essential causes for an uneven mass distribution in chilled cast-iron rolls. Firstly, since the cast-iron roll consists of three different zones, the hard, wear resistant white iron, consisting of iron carbide, must be concentrically arranged around the grey cast-iron core that provides stability to the rolls. The concentric transition zone between the white and the grey zones is a mixture of grey cast iron and iron carbide that binds the core and the shell together (Figure 11). An uneven mass distribution occurs if these three zones with their different specific weights are not completely concentric.

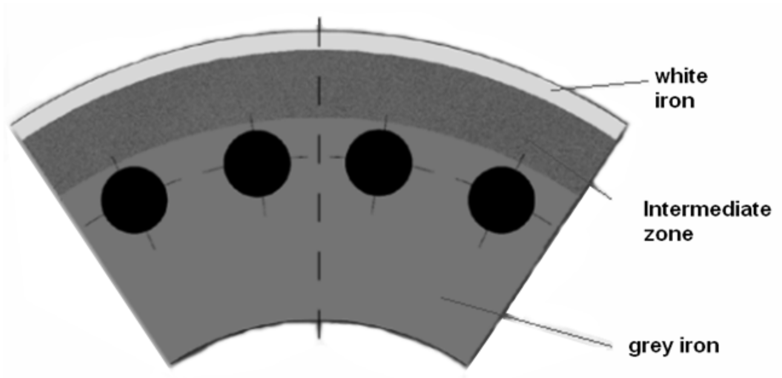

Figure 11. Zones of cast iron roll shell (Wirtz 2002).

Secondly, the grey and white constituents of chilled cast-iron rolls have different thermal coefficients of expansion, with the expansion coefficient of grey cast-iron about 10 % higher than that of the white cast iron. This may cause a so-called bimetallic effect, where the roll body, originally machined as an exact cylinder at room temperature, becomes deformed at higher temperatures because of the different coefficients of expansion (Figure 12). The grey and white irons have also different thermal conductivities (Brierley et al. 1977) which may cause the white iron zone to act as an insulating layer. Thickness variation in the white iron zone may thereby cause uneven thermal expansion.

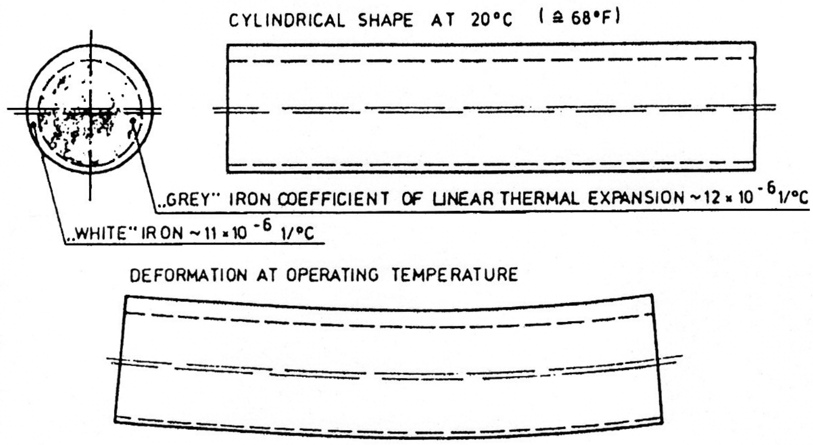

Figure 12. Deformation of a chilled cast-iron roll with uneven chill depth (Rothenbacher 1986).

The variation of the chill layer may be caused by the imperfection of the roll body casting and subsequent machining (SHW 2005). If the cast-iron body is bent before machining the result may be two differently behaving rolls depending on the way the cylindrical machining is done. When the ends of the roll are true running in the faceplates of the lathe, there will be great variation of the chill layer in the middle of the roll (Figure 13) and the roll will be bending upwards when heated (in the direction, where the white iron layer is thinner). When machined with the roll centre true running, a different distribution of the chilled layer will be achieved (Figure 14) and the roll will be bending downwards at the increased temperature.

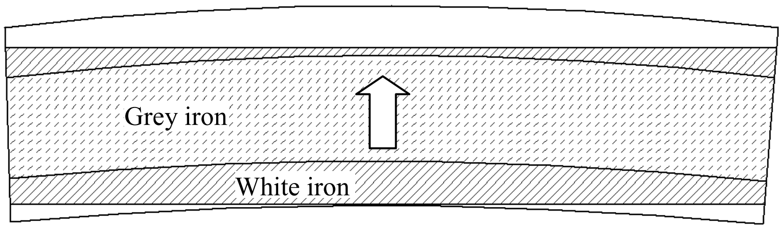

Figure 13. Bent casting machined with the ends true running (SHW 2005).

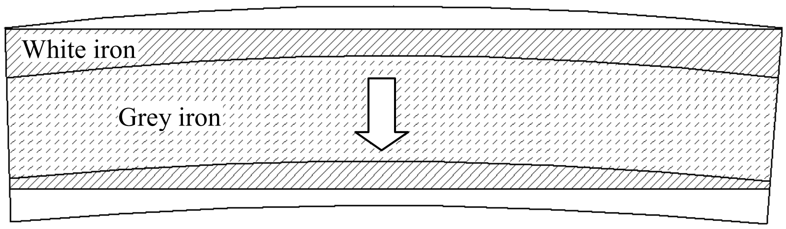

Figure 14. Bent casting machined with the roll centre true running (SHW 2005).

The third reason for an uneven mass distribution in the middle of the roll face is imperfect bores (Figure 15). All chilled cast-iron rolls are provided with bores of varying sizes. If the central or even the peripheral bores are not carefully executed, especially in bores close to the surface or in conjunction with differences in the chill depth, a centre deviation can occur when boring from both sides, resulting in an uneven mass distribution in the middle of the roll face. The runout of peripheral bores will bend the roll during operation because of temperature non-uniformity on the circumference (Figure 16) (SHW 2003). This property can be used to reduce runout of the roll by adjustment of the flow of the liquid heat transfer medium on different sides of the roll.

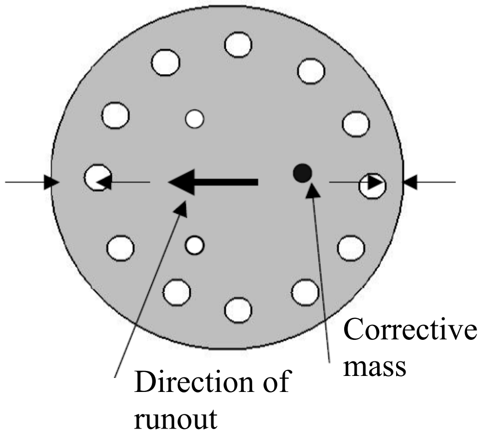

Figure 15. Runout caused by uneven mass distribution due to imperfect peripheral bores (SHW 2003).

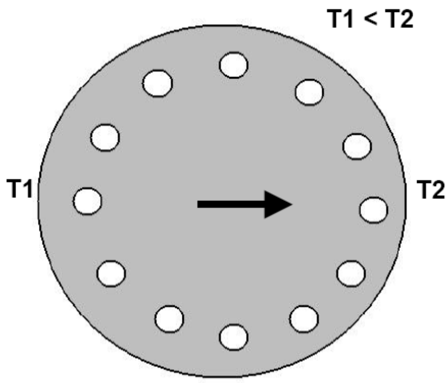

Figure 16. Runout caused by uneven temperature (T1,T2) distribution due to imperfect peripheral bores (SHW 2003).

Manufacturer Walzen Irle (Wirtz 2002) reported the runout deviation of a thermo roll heated up to 150 °C (Figure 17). The thermo roll had a diameter of 1067 mm and length of 6900 mm. The amplitude of the runout of the roll was measured to be 80 μm at a temperature of 150 °C. While cold, runout deviations of less than 3 μm were typical values for larger rolls.

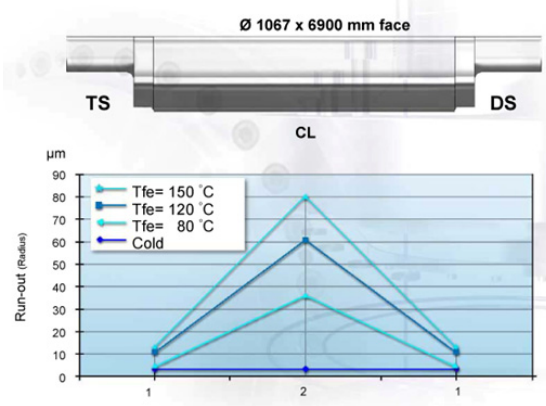

Figure 17. Runout of a thermo roll at different oil temperatures (Wirtz 2002).

2.4 Measurement of runout

Measurement of runout can basically be done by any linear displacement measurement method including both contact based methods such as dial gauge and LVDT sensors and noncontact methods such as inductive and optical sensors. Contact sensors have a measuring head that is in contact with the surface and measures the direct movement of surface. Typically in workshops runout of a workpiece is measured by a dial gauge held against the part while it is rotated at slow speed. Noncontact sensors measure the gap between the surface and the stationary sensor head. Inductance and eddy current probes are one of the most common instruments used to measure rotor vibrations in rotating machinery (Flack et al. 1981). The accuracy of most of these methods is good enough for the runout measurement; reasons to select a specific type of sensor may mostly depend on the environment or the properties of the target.

Even if there are several methods to measure runout and displacement, very little or no research is reported about the methods for measuring of runout of large cylindrical objects such as paper machine rolls. This may be due to the fact that runout is usually of no special interest itself but it is used as a tool for balancing or measuring roundness (Gao 1997, Jeong 2005) or some other geometrical properties of the rolls. In the workshop conditions at low rotation speeds the measurement is considered an easy task. More interest in runout measurement has been in the field of precision engineering. Computer hard drives operate at very high rotation speeds and while the data transfer rates and packaging density are continuously increased the requirement for very low runout is obvious (Jang 1999, Okuyama 2007). In the high speed machining the runout of the spindle or tool will directly be seen on the quality of the workpiece surface (Albrecht 2005, Tatar 2007). Runout will cause excessive wear of the tool and may damage or break the tool. In the above-mentioned applications runout is typically measured using capacitive or inductive displacement sensors but laser and laser vibrometry are used as well. There are also some commercial tools available for spindle runout measurement and analysis. They are typically based on non contact measurement by capacitive or eddy current sensors. Although the measurement of runout of the disk drives and spindles is basically similar to paper machine rolls the conditions and properties of the workpiece differ greatly from each other. The measurements with disk drives and spindles are usually done in controlled laboratory or workshop conditions. The dimensions of the workpieces are significantly smaller, the support of the workpiece is different and masses and forces related to the measurements are of totally different magnitude. Spindles and disks have much higher rotation velocities and phenomena such as non-repeatable runout (NRRO) may become important. NRRO is the radial displacement of the spindle that is not synchronous with the rotation frequency.

2.4.1 Contact sensors

Contact sensors, as the name implies, make physical contact with the surface being measured. The typical sensor is a mechanical dial gauge (Figure 18) which is very often used for centring or aligning the workpiece before machining. It is also used to verify the geometrical tolerances of the workpiece. The principle of the dial gauge is based on a plug gauge, which is pushed into a housing against a spring force. This moves an indicator, displaying the measurement value on a scale.

Figure 18. Dial gauge.

If higher accuracy is needed, a LVDT sensor is typically used. The Linear Variable Differential Transformer is based on the principle of electromagnetic induction (Figure 19). A ferro-magnetic core moves within the hollow core of coils without making physical contact. The hollow core consists of a primary ac (alternating current) excited coil and two secondary coils. The ferro-magnetic core induces a voltage which depends on the position of the core in the secondary coils. The accuracy and resolution of LVDT sensor is virtually limited by the signal condition electronics.

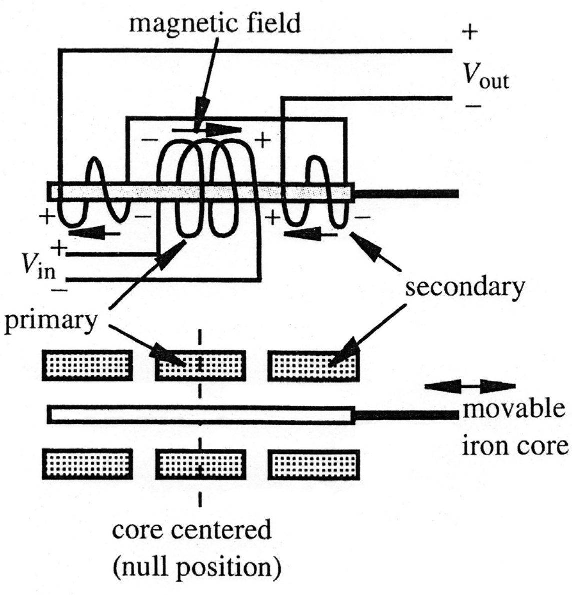

Figure 19. Operating principle of an LVDT sensor (Alciatore 2007).

Physical contact with the surface is the most significant drawback of contact-based methods. The tip of the probe is subjected to wear and warming up. A soft surface, such as polymer coated roll surface, could be marked or damaged by the probe. Any discontinuities on the surface could damage the sensor head. Because of the high surface velocity and high temperature of the paper machine rolls, conventional contact based methods are not applicable in the production environment.

2.4.2 Noncontact sensors

One advantage of noncontact measuring is that the speed of the target surface is insignificant within the limits of the sensor bandwidth. There is no friction or wear. Noncontact measuring does not cause any deformation to the target surface. Tian et al. (1997) and Charles (2000) presented application criteria for noncontact displacement sensors. Noncontact displacement sensors can be grouped into three categories, based on eddy current, capacitive and optical principles. The eddy current sensor is insensitive to environmental influences such as oil, dirt, water and electromagnetic fields but electrical runout, caused by target material inhomogeneities, will disturb the propagation of the eddy currents and will affect the transducer output, which in turn results in noise and degraded resolution. A capacitive sensor has the smallest nominal distance and the smallest measuring range. It is sensitive to changes of dielectric in the measurement gap, and can only be used in clean and dry environments. Because of its low signal-to-noise ratio, the sensor cable length is restricted. Optical techniques are available for both geometry and profile measurements. Their drawbacks are size, alignment complications (particularly in a high vibration environment) and the random effects of debris in the optical path. Laser sensors measure a very small target area, whereas capacitive and eddy current sensors average a circular area slightly larger than the probe tip diameter thereby making them slightly less affected by surface roughness and waviness. Next, the operating principles of noncontact sensors are described in more detail (Slocum 1992, Bolton 1997, Onwubolu 2005, Bishop 2008).

Capacitive sensors

Capacitive sensors are based on the capacitance between the face of the probe and the target surface. Capacitance for a parallel plate capacitor is defined as

$$C=\varepsilon_r\varepsilon_0 A/d \qquad (2)$$

where ε_r is the relative permittivity of the dielectric between the plates, ε_0 is the permittivity of free space, A is the area of overlap of two plates and d is the separation between the plates. ε_r is dependent on temperature, pressure, humidity and media type.

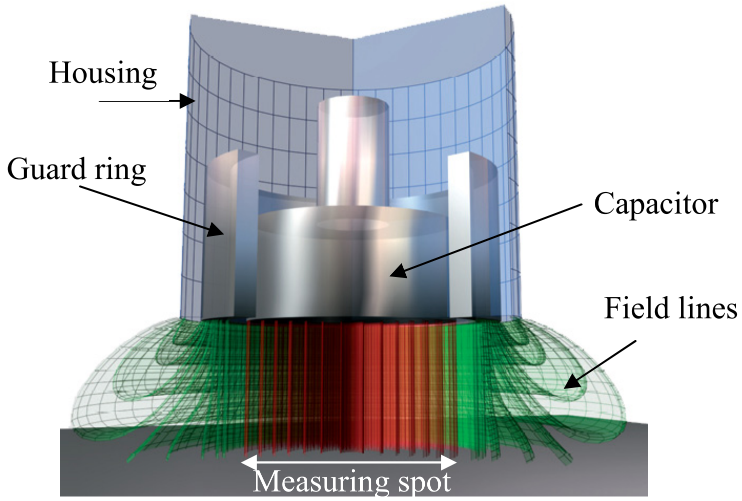

Figure 20. Measuring principle of a capacitive sensor (Micro-epsilon 2009).

The typical configuration has one plate of the capacitor inside a probe and the external target object forms the other plate of the capacitor. An electrical field is created in the gap between the probe tip and the surface. As the gap between the target and the probe tip changes, the modulated capacitive current is measured and linearised. The method is suitable for a wide range of material types including metals, dielectrics and semiconductors. The output of the sensor is affected by the type of material but not by any microstructures such as alloy constituencies or grain size. The technology is independent of magnetic fields. The shape of the face of the probe and the target has an effect on the accuracy and linearity of the sensors. Capacitive sensors are said to have the best resolution of analogue sensors. Capacitance is measured over an area which will average the result to some extent. Because the capacitance is dependent on the properties of the medium between the sensor and the target, capacitive measurement is sensitive to disturbances such as dirt, moisture, temperature variation or liquids. This may weaken the possibilities to use capacitive methods in a plant environment.

Smith et al. (2005) studied the effect of a cylindrical target on the error of capacitive displacement measurement. They detected that as the diameter of the target is reduced, the sensitivity increases, the sensing range decreases, the sensing range shifts towards the target, and the sensor becomes increasingly nonlinear. However these effects are significant only when measuring nanometre displacements. The diameters of the rolls are so large that the error is negligible. The error caused by a cylindrical target can be reduced by calibrating sensors with the correct target surface or by determining corrections for post-processing data.

Eddy current sensors

An eddy current sensor consists of a coil wound around a ferrite core (Figure 21). A high frequency ac current in the coil creates an electromagnetic field. When a metallic object enters the field, eddy currents are induced in the target surface. These eddy currents produce a secondary magnetic field that interacts with the originating field. This will change the effective inductance of the sensor coil resulting in an oscillator frequency shift or amplitude change which can be detected and converted into an output signal proportional to the gap between the sensor and the target.

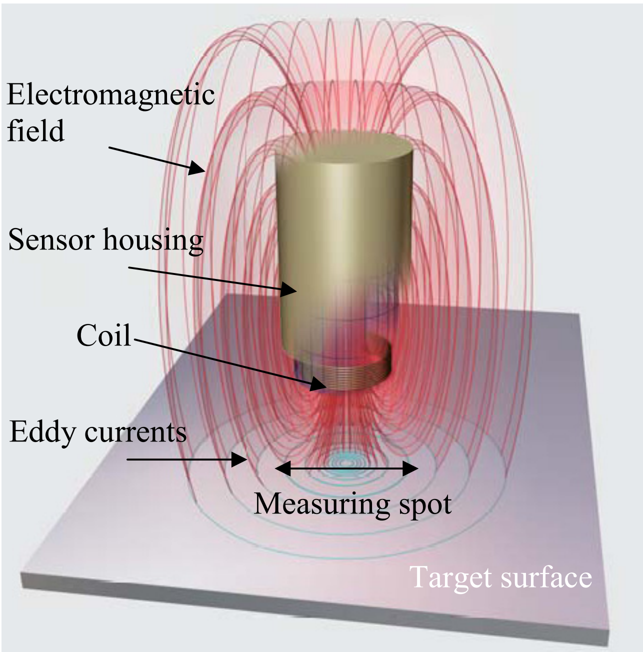

Figure 21. Measuring principle of an eddy current sensor (Micro-epsilon 2009).

Inductance relates electrical flux to current. The inductive reactance of a coil is a measure of the inductive effect and is expressed as:

$$X = 2\pi fL, \tag{3}$$

where X is the inductive reactance, f is the frequency of the applied voltage and L is the inductance of a coil. The inductance of a coil is dependent, among other things, on the permeability of the flux path. This means that besides the actual displacement, varying properties of the material can also affect the permeability and thus cause sensor to measure apparent displacement of the target. This can be caused for example by inhomogeneities of heat treatment or hardness, residual magnetism or impurities or defects under the surface such as slag, inclusions or voids (Campbell 1983, Doebelin 1990). The grain size and grain boundaries of the microstructure of ferrous materials can also locally affect the permeability. This apparent displacement is sometimes referred to as electrical runout compared with the actual mechanical runout. Inductance based sensors can only be used with conductive metals, ferrous and non-ferrous. It is best suited for good conductors with uniform electrical properties and low magnetic permeability. On the other hand, oil, dirt or dust do not affect the accuracy.

Lin et al. (1998) conducted a set of tests comparing the performance of capacitive vs. eddy current proximity probes by measuring the slow-roll electrical runout of a large motor rotor. Eddy current type proximity probes have been the standard for non-contacting proximity measurement for decades. The capacitive and eddy current probes were alternately paired with an LVDT probe to observe the motion of the rotor shaft. The difference between the readings taken by the LVDT transducer and each proximity probe is by definition the level of electrical runout for that proximity probe. According to the results the waveform of the eddy-current probe signal did have the same general shape as the LVDT signal but appeared to lag the movement of the shaft. There also seemed to be significant electrical noise from the eddy current probe signal and the electrical runout level was fairly high. On the other hand, the capacitive probe tracked the motion of the shaft quite closely and without the phase lag exhibited by the eddy-current probe. It would seem reasonable to infer from those test results that the capacitive proximity probe is immune to electrical runout.

An eddy current sensor would seem fairly suitable for roll runout measurements because of its robustness against environmental disturbances. However, the inhomogeneity of the roll material may cause erroneous results. A significant disadvantage is the need for calibration for certain target material and surface geometry which may be impossible to carry out in a hasty measurement situation.

Optical sensors

Optical sensors operate upon several different principles. Typically there are both light transmitting and receiving components in the probe. The emitted light is reflected by the target surface. The majority of the probes nowadays are based on laser as a light source because of the coherent nature of the light.

Optical triangulation is a measuring principle where a laser diode projects a visible spot of light onto the target surface. The reflected light is directed through an optical receiving system onto a position-sensitive element (Figure 22). When the target moves, the reflected light spot changes its position on the receiving element which can be evaluated.

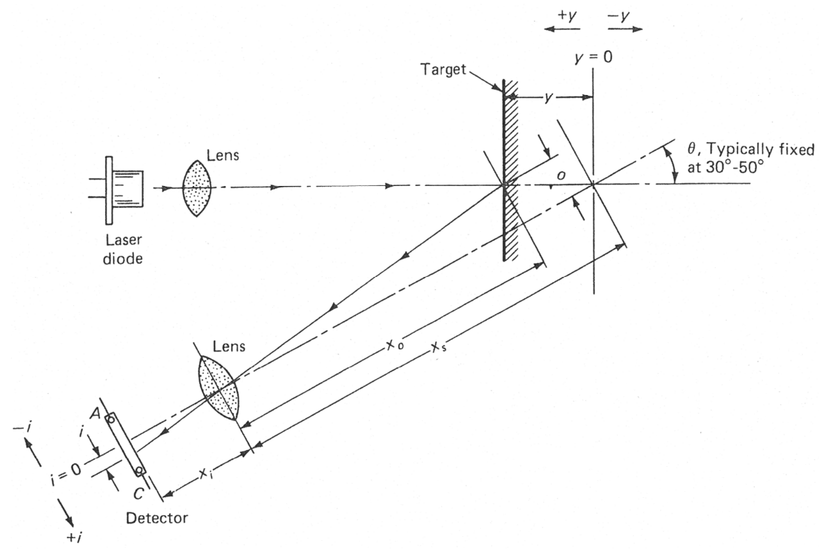

Figure 22. Optical triangulation (Doebelin 1990).

In interferometric methods two beams of light are transmitted simultaneously and, by using a beam splitter and mirrors, one of them has a constant path while the other is reflected from the moving target. At the detector the two light beams have a phase difference that depends on their optical path lengths (Figure 23). This phase shift causes alternate reinforcement and interference of the two beams. One complete cycle of the intensity modulation corresponds to a target movement of half the wavelength of the light. By counting the number of illumination cycles, the distance between any two positions of the moving target can be calculated. This principle was introduced by Michelson in the 1890s.

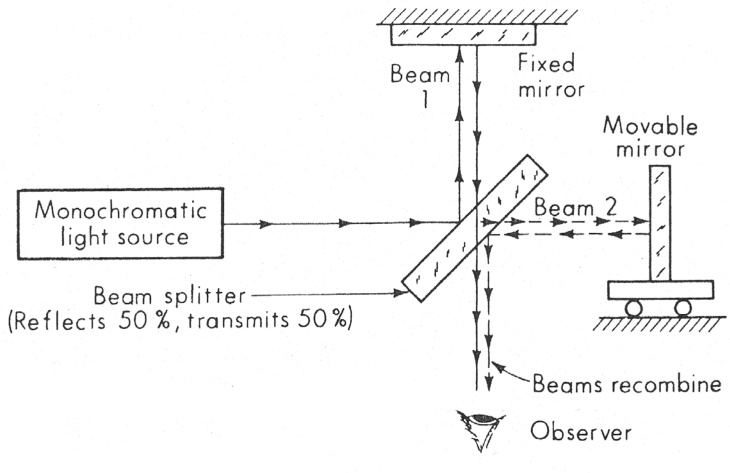

Figure 23. Michelson interferometer (Doebelin 1990).

Laser Doppler Vibrometers (LDV) are based on the same principle but instead of counting interference lines they detect the apparent frequency change in reflected light beam caused by the moving target. Typical applications for LDVs include vibration measurements on rotating surfaces. According to Gatzwiller et al. (2003), LDV-based measurement does not interpret any changes in the geometry of the shaft as a vibration, but only vibrations of the centre of the rotation of the shaft, in the direction of the laser beam. This presumes however that the laser beam is aligned so that it lies in a straight line passing through the centre of the shaft.

Optically rough (in terms of the wavelengths of light) surface causes the reflected light to have a granular appearance, referred to as a laser speckle pattern (Gatzwiller 2003). As the beam moves to a different point on the surface the speckle pattern changes. This effect gives rise to the so-called laser speckle noise. Measuring perpendicular to the surface minimizes speckle noise while the moving surface will raise the level of noise. This makes it important that the alignment of the laser is done carefully. Contrary to the claims of the manufacturers, the measurement of moving targets with machined surfaces may still be problematic. For example for spindle rotation error measurements, sometimes a masterball, a glass ball with superior surface finish, is used as a target surface (Castro 2008).

One advantage of optical methods is that the measurement can be done from a distance. Capacitive and inductive sensors have to be taken fairly near to the target surface. The measuring ranges are also longer than those of the capacitive and inductive methods.

There are methods that are based on the measurement of light intensity. In the simplest implementations, the displacement produces a change of the optical power reaching the detector (Girão 2001). Wang et al. (1994) developed a reflective fibre optic displacement sensor to gauge form and axis position of shafts during rotation. Because cylindrical parts are involved, the curvature of parts under inspection has certain effects on the sensing process. Inside the illuminating spot, the proximity changes due to surface curvature. Moreover, because the reflection of the cylindrical parts acts much like a convex cylindrical mirror, it will make the reflected beam more divergent. The effect of this phenomenon is a modification to the sensor response curves: specifically, the maximum response moves to the direction of smaller proximity. Finally, the variation of reflectance around the shaft surface has to be taken into account. For cylindrical shafts, it is necessary to calibrate the sensor on the particular shaft diameter being measured. For larger cylinders, such as paper machine rolls, the effect of cylindrical surface could once again be thought to be less significant.

2.4.3 *In situ* measurement of rolls

Charles (2000) described a measurement system for Operating Surface Topography (OST) of Yankee dryers (Figure 24). In this system a steel cable is stretched between two pulleys and used to mount the measurement sensor for traversing under the dryer. A non-contact type sensor can be used for the measurement. The effects of cable sag and deformation due to the pressure roll line load must be corrected in the measured signal. The cable-pulley system could be replaced with a fixed beam equipped with a linear guide for the probe. Guide errors and inevitable beam vibrations should anyhow be corrected. The fixed system can be expected to be prone to contamination.

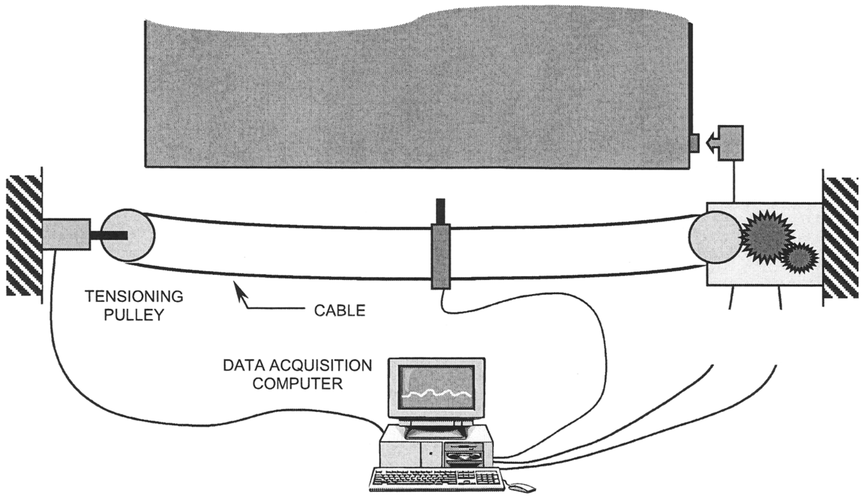

Figure 24. Measurement system for Operating Surface Topography of Yankee dryers (Charles 2000).

There are only few references to slider-type measurement of runout in literature. Möhle et al. (1970) studied vibrations on paper winders using a strain gage based measuring device in contact with the paper roll (Figure 25). The method appears to be based on the measurement of the deflection of the supporting arm caused by the movement of the measuring head in contact with the target surface.

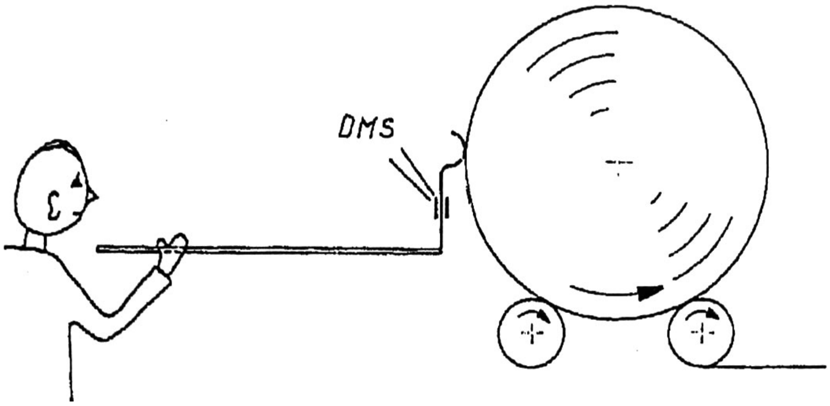

Figure 25. Strain gage (DMS) based measuring device in contact with the paper roll (Möhle et. al. 1970).

The research group at TUT used sensors inside the roll to measure vibrations and vibrations modes of rolls (Järvinen et al. 2001). Accelerometers and strain gauges were attached to the inner surface of roll shell and the data were transmitted outside using wireless communication. As an additional measurement method they used an accelerometer with Teflon plate in sliding contact with the roll cover to measure the movements of the roll shell (Figure 26). No results of these measurements were presented. The structure or operational principles of either of the devices were not further described.

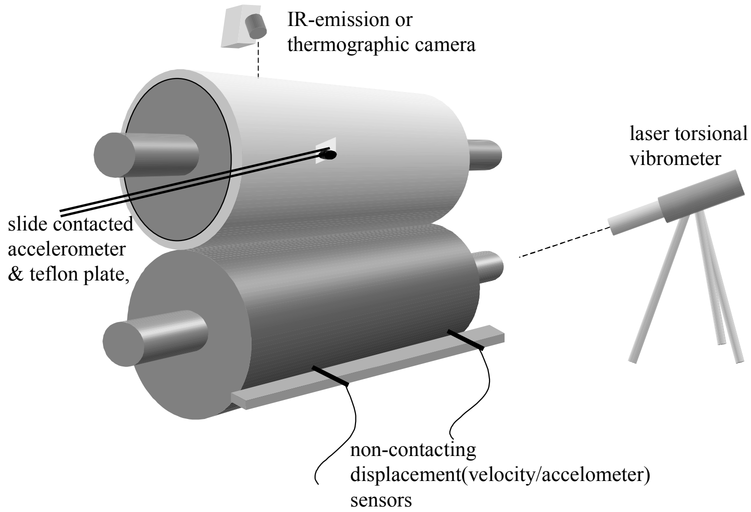

Figure 26. Accelerometer with Teflon plate in sliding contact with roll cover (Järvinen et al. 2001).

The idea of using an accelerometer with a sliding plate in contact with the surface is clearly not a novel one. It is possible that the method has been used for quick "check outs" to see what is happening or is something happening on the target. There is no indication of a systematic use to be found in the literature. Nor has there been any knowledge of the use of this method among the paper making industry or the paper machine industry.

2.4.4 Summary of the measurement methods

A considerable amount of research has been done and is being done to improve the performance of different types of displacement sensors which however are best suited for laboratory conditions or otherwise controlled environments. The accuracy and band width of the typical displacement sensors are adequate to the runout measurement. There are some other issues that may be more important when choosing the measurement method (Table 1).

Table 1. Comparison of the typical displacement measurement methods.

Method	Advantages	Disadvantages
Contact sensors		
Dial gauge, LVDT	Easy to use No calibration to the target needed	Wear, warming-up May damage the surface Only for slow speeds
Noncontact sensors		
Capacitive	Suitable for a range of different materials Insensitive to the material properties	Sensitive to the properties of the medium (dirt, dust)
Eddy current	Insensitive to the environment	Electrical runout Only for conductive metals Calibration to the target needed
Optical	Long measuring distance and range	Speckle noise Sensitive to dirt and dust Careful alignment needed

As it would seem, the capacitive measurement could be the best candidate as a method for the *in situ* measurement of the roll runout. There are however, besides environmental limitations, practical issues such as mounting and manoeuvrability, which limit the possibilities to use the conventional methods for the *in situ* measurements.

The two methods, based on the principle of the probe with a sliding contact to the surface and a method for detecting the movement of the probe, solve at least some of the problems. As hand-held devices they are quick and easy to take in use and to move to different locations. No supports or fixtures are needed either. Measurement can be made from a longer distance and the environmental conditions and the target properties do not have as much influence on the measurement as they would have with the conventional methods. Warming-up of the sliding probe does not have a direct effect on the measurement as does the warming-up of the probe in the LVDT sensor, for example. On the other hand, these methods require that the target is accessible by the measurer. Any dirt or other surface irregularities will have an effect on the measurement. Accuracy and performance of the methods must also be studied.

3 Device, method and measurements

A device and a method for the *in situ* measurement of a roll shell runout based on the measurement of radial acceleration of the surface is described. A number of measurements have been done to demonstrate the applicability of the method.

3.1 Device

The basic operation principle of the method is the one in a cam mechanism (Figure 27). Cams are used to convert rotary motion into reciprocating motion. As the cam turns, the cam follower traces the surface of the cam transmitting its motion to the required mechanism. Between the rotational input θ and linear output y there is a functional relationship

$$y = y(\theta). \tag{4}$$

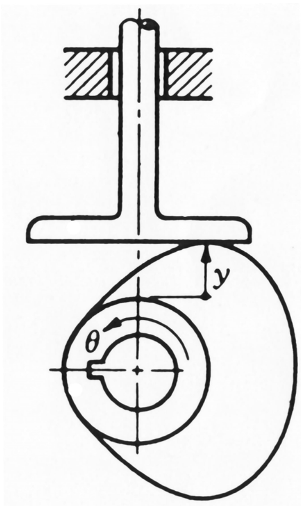

Figure 27. Cam mechanism with flat-faced follower (Shigley 1981).

The flat-faced follower can be replaced by a hand-held slide pad while the roll surface acts as a circular or eccentric cam with very small undulations. The measurement of the radial displacement of the slide pad yields the runout of the roll.

An accelerometer is one of the most often used sensors in condition monitoring applications. Accelerometers are very sensitive instruments and can detect even the smallest vibrations on any surface. As vibrations are always related to the movement of the media, it is possible to obtain the displacement of the surface by measuring its acceleration. Attached to a slide pad which is in sliding contact with the roll surface, the movement of the surface can be measured with an accelerometer (Figure 28). The velocity and displacement can be obtained by integrating the acceleration.

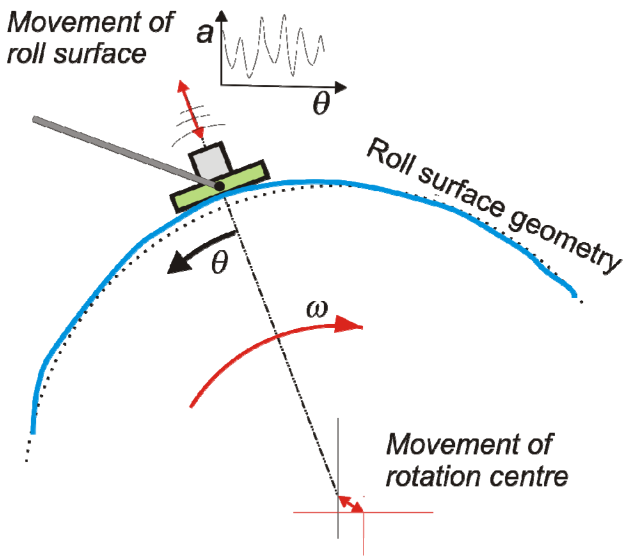

Figure 28. The basic operation principle of the measurement.

Thus the device consists of a polymer based slide pad which is in contact with the moving surface, an accelerometer attached to the slide pad and an extension handle for the user to hold the device on the target surface (Figure 29).

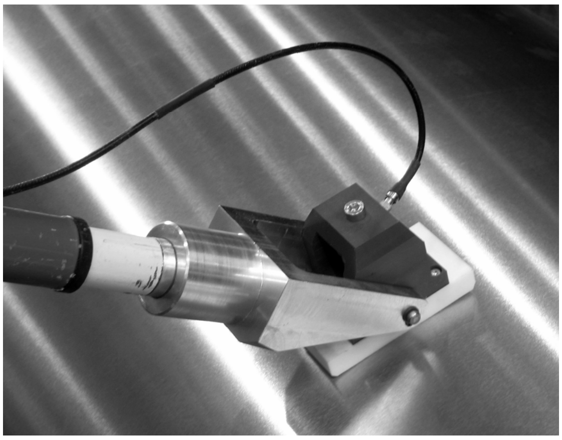

Figure 29. Device on roll surface.

The benefit of this method compared with conventional methods is that there is no need for vibration sensitive holding fixtures or supports for the probe. The reference of the measurement will be the shell of the roll itself instead of a fixed datum. The body of the user will efficiently dampen possible vibration arising from the environment. It is possible to quickly carry out measurements in numerous positions and inconvenient locations such as working platforms or service elevators.

3.1.1 Body and slide pad

When the measurer places the slide pad on the target surface, the slide pad should orientate itself tangential to the surface and be stable, in contact with the surface even if the measurer moves a little. The device will be subjected to high surface velocities (up to 2000 m/min) and high surface temperatures (up to 250 °C). The material used for the slide pad has been selected to have low coefficient of friction, good wear resistance and high heat distortion temperature. In the first versions of the device the body and the slide pad were separate parts made of different materials. The sliding surface was made of reinforced PTFE while the body was made of a common engineering plastic. Both of these materials proved to soften at high temperatures causing the dampening of the acceleration signal as can be seen in the following series of graphs (Figure 30).

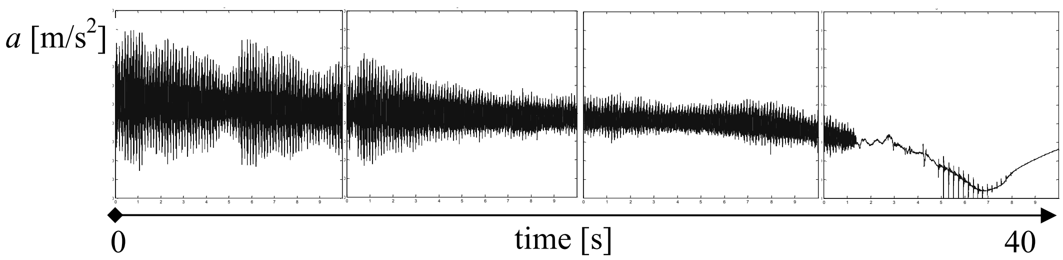

Figure 30. Effect of high temperature on the measurement. A series of 10 second measurements of acceleration.

Figure 30 represents a 40 second measurement of acceleration on a hot roll surface (about 200 °C). It can be seen that the softening of the device material first dampen the measured signal until the signal becomes totally distorted. As a consequence the material was replaced by a one of a higher grade and the whole structure was made of a single block. The new material is PEEK (polyetheretherketone) which is a polymer used in demanding engineering applications. The glass fibre enforced PEEK should keep its mechanical properties in temperatures up to 300 °C.

The connection of the slide pad to the extension handle has been implemented with two joints which make it possible for the slide pad to self-align itself on the target surface (Figure 31). A fork wrench allows the pitch movement with the hinge joint (1) while the pivot joint (2) with a journal bearing allows the slide pad to rotate along the axis of the handle, roll. The pin of the fork wrench is located as close to the slide surface as possible to make the device stable. The details of the structure are represented in Figure 32.

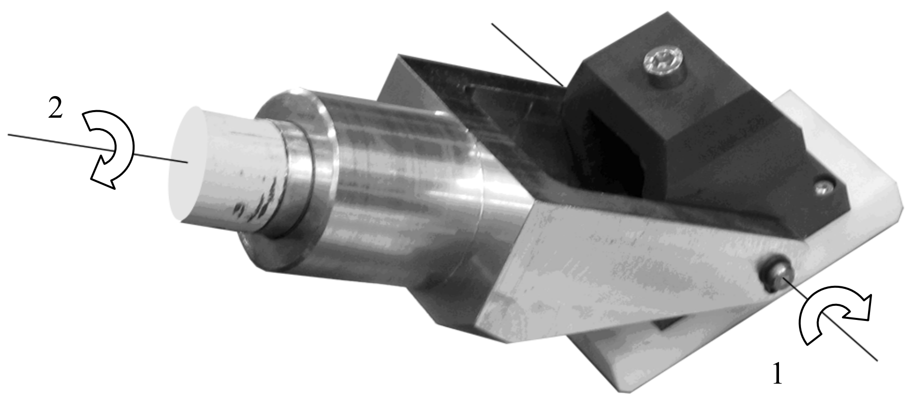

Figure 31. The two joints of the slide pad assembly.

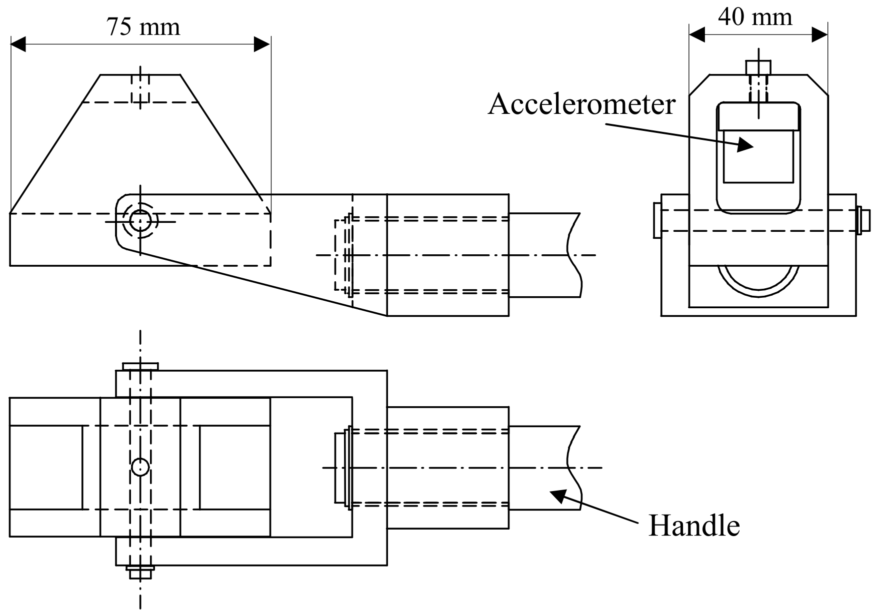

Figure 32. Details of the device

As the slide pad is able to rotate around the pin it will tend to align itself automatically tangentially on the surface. The structural force F_N (Figure 33) from the pin will always be in the direction of the normal of the target surface. The smaller the target diameter is, the more unstable the slide pad is. The friction force F_R between the surface and the slide pad may slightly tilt the pad.

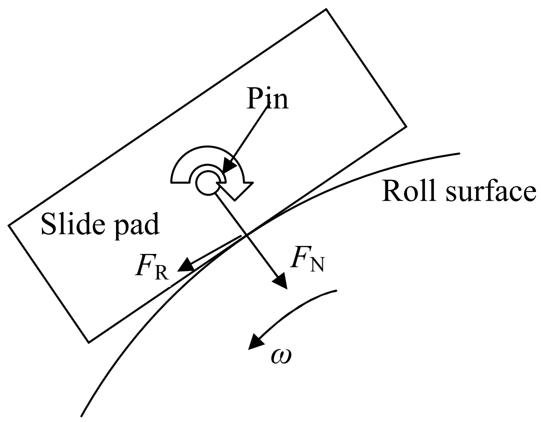

Figure 33. Forces acting on the slide pad.

There is a line contact between the slide surface and the roll surface. The width of the contact line depends on the curvature of the roll, the materials of the contacting surfaces and the force with which the slide pad is pressed against the roll surface. The width of the contact can be approximated using theories for Hertzian contact between two parallel cylinders (Stachowiak 2005). The half-width b of the contact is

$$b = \sqrt{\frac{4F_N R'}{\pi L E'}} \tag{5}$$

where

$$\frac{1}{E'} = \frac{1-\nu_1^2}{E_1} + \frac{1-\nu_2^2}{E_2} \tag{6}$$

and

$$\frac{1}{R'} = \frac{1}{R_1} + \frac{1}{R_2}. \tag{7}$$

E is Young's modulus and v is Poisson's ratio of the material in the contact, R is the radius of the curvature of the surface (∞ for flat surface) and L is the length of the contact. Subindexes 1 and 2 refer to the two objects in the contact.

For reinforced PEEK (E = 10.3 GPa, v = 0.4 (Matbase 2009)), the width of the contact (= $2b$) is about 0.5 mm for a 300 mm diameter steel target and 0.8 mm for a 1000 mm diameter steel target with an average holding force of 50 N. This means that the width of the contact has no filtering effect on the lower harmonic components of the surface geometry, because the width of the contact is significantly smaller than the wavelength of the undulations.

3.1.2 Accelerometer

An accelerometer measures directly the acceleration related to the motion of the surface to which it is attached. Typically an accelerometer consists of a mass that is free to move along a sensitive axis within a case (Figure 34). The acceleration is acquired by measuring the displacement of the mass. In a piezoelectric accelerometer, which is used in this case, the mass is in direct contact with a piezoelectric component (Figure 35). When a varying motion is applied to the accelerometer, the piezoelectric crystal experiences a varying force excitation which in turn will cause an electric charge to be developed. A charge conditioning amplifier is needed to obtain more useful voltage signal. Piezoelectric accelerometers have no dc response so they can only be used for dynamic measurements. For the same reason the position of the sensor does not have an influence on the output of the sensor.

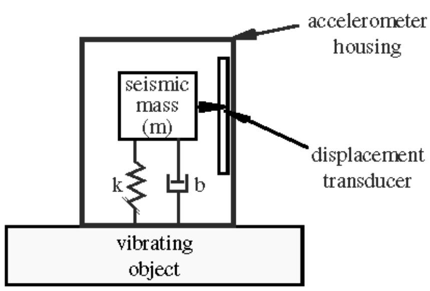

Figure 34. Operation principle of an accelerometer.

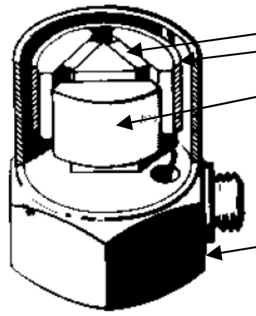

Figure 35. Delta Shear® -type accelerometer (Brüel & Kjær 1987).

The accelerometer should be mounted so that the desired measuring direction coincides with its main sensitivity axis. Accelerometers are slightly sensitive to vibrations in the transverse direction, but this can normally be ignored (Brüel & Kjær 1982). The accelerometer must be mounted with a close mechanical contact with the surface to which it is to be attached. In this case the accelerometer is mounted with a threaded stud and, to ease the installation, it is installed upside down to the slide pad.

The accelerometer used is a piezoelectric-type acceleration sensor Type 4381 by Brüel & Kjær (Table 2).

Table 2. Specifications for charge accelerometer Type 4381 (Brüel & Kjær).

Characteristic	**Value**	**Unit**
Charge sensitivity	98 ± 2	pC/*g*
Mounted resonance frequency	16	kHz
Amplitude response	0.1 to 4800	Hz
Transverse sensitivity	4	%
Temperature range	-74 to 250	°C
Thermal transient sensitivity	0.002	*g*/°C
Max. operational acceleration	2000	*g*

3.2 Measurement procedure

The measurement procedure is:

1. Trigger sensor is installed on the target
2. Slide pad is set on the surface
3. Data collection is started
4. Slide pad is held on the surface during the measurement
5. Data collection is stopped
6. Slide pad is lifted

During the measurement, the measurer positions the slide pad on the surface of the target using the extension handle and keeps the probe still with light pressure for the duration of the measurement (Figure 36). The measurement is not started until the acceleration sensor has settled after the impact caused by the first contact to the surface. This takes normally a few seconds. The measurement should not start until the measurer has a stable hold of the device. Depending on the location, the measurer can hold the device reliably stable for about 30 to 60 seconds. A typical duration of one measurement is 10 seconds which should be repeated for a few times. The longer the measurement is, the more reliable the result is.

Normally two operators are needed for the measurement. One is operating the device and the other is operating the measurement computer. In this way, the device operator can focus on holding the slide pad on the surface while the other operator can check the validity of the data. This will also improve the safety in the process conditions.

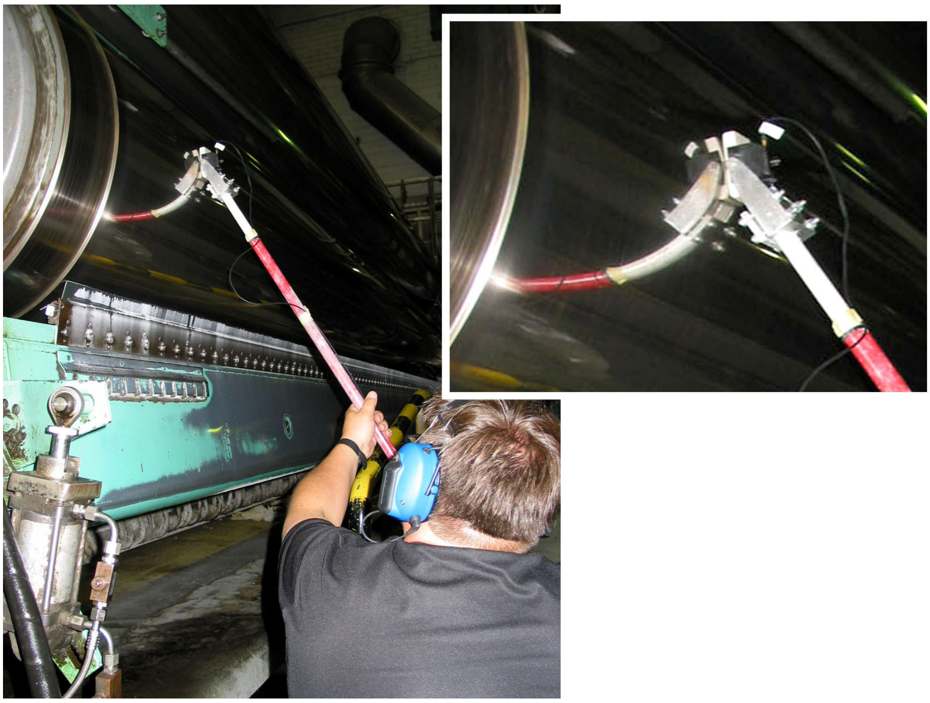

Figure 36. The measurer holding the probe on the roll surface

3.3 Signal processing and data handling

The output of the measurement is acceleration (Figure 37). As the runout is usually viewed as displacement, the acceleration signal must be integrated twice into displacement. As usual in the measurement of rotating targets the output signal will be averaged to remove random errors. All the signal analysis is done after the measurements for the saved data using Matlab software.

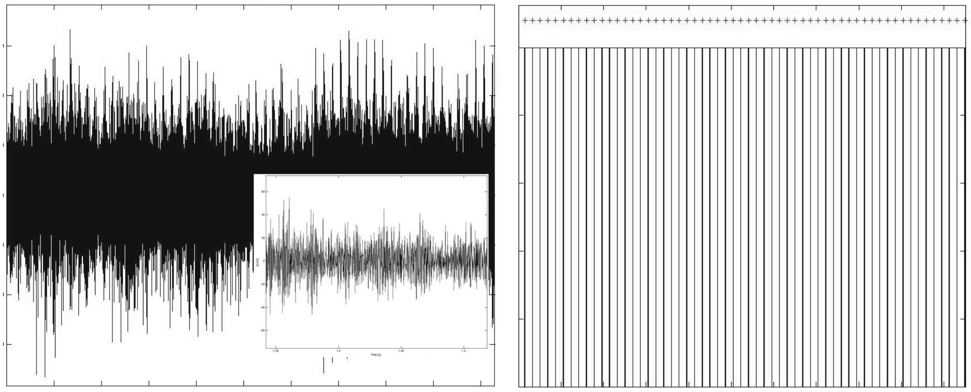

Figure 37. Left: acceleration signal of a 10 second measurement and detail of acceleration of length about one revolution of the target (small picture), right: trigger signal of one measurement.

Two signals are saved simultaneously during the measurement: acceleration and trigger. The trigger data consist of pulses that appear once on every revolution. The signal processing flow is represented in Figure 38.

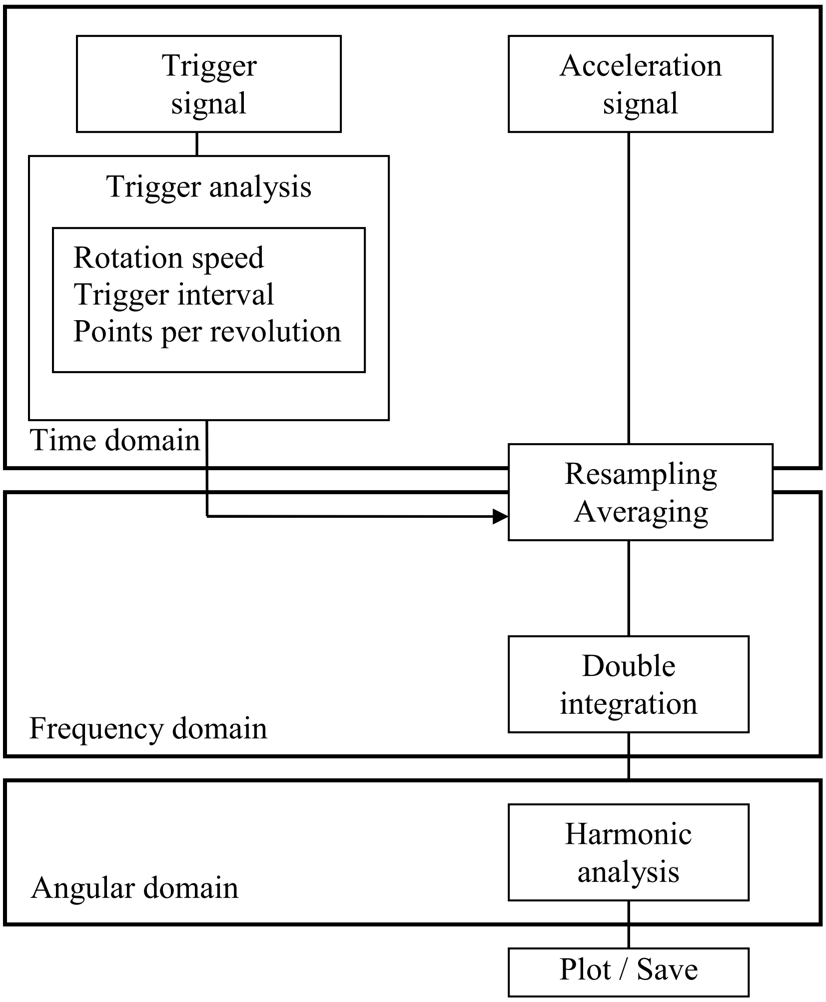

Figure 38. Signal flows in the measurement.

The analysis is based on the averaging and synchronisation of the displacement to one revolution of the target. Hence a trigger signal of good quality is needed. As a result of the trigger analysis, the rotation frequency of the target and average number of measured points per revolution are found out. The acceleration data are divided to sequences of one revolution using the trigger signal. To be able to average the data that is measured during consequent revolutions, the number of points per revolution should be the same. Therefore the data is resampled and a certain number of equally spaced points are interpolated for each rotation. Finally, the averaged data is double integrated using FFT to get the displacement signal. FFT is also used to analyse the harmonic content of the signal.

3.3.1 Data acquisition

The accelerometer used with the device is a piezoelectric-type acceleration sensor Bruel&Kjaer type 4381 with Nexus 2692 OI4 charge amplifier. The data are acquired using a 14-bit analogue-to-digital board located in a personal computer with a sampling rate of 10 kHz (Figure 39). The input range for the A/D-board is ±5 Volts. An analogue filter with a low pass to 2.5 kHz is used before sampling to avoid aliasing. The measurements are triggered using a laser-type photoelectric sensor (Omron E3C-LD11) with reflective tape glued on the roll axis or surface. The duration of one measurement is typically 10 seconds. Each measurement is repeated at least three times. After each measurement the data are saved to a file.

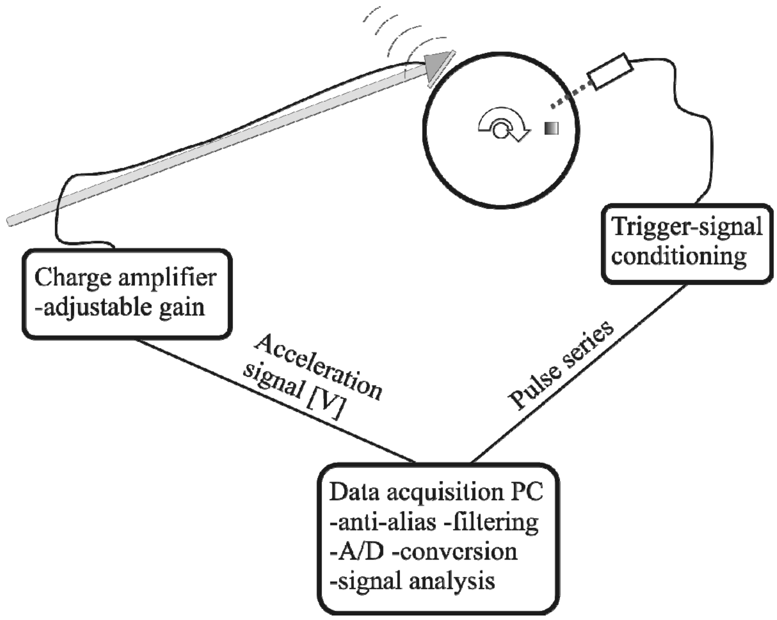

Figure 39. Components of the measurement system.

3.3.2 Triggering

The measurement is synchronized using the trigger signal. The trigger signal is first checked to see if there are missing pulses. If the signal is of poor quality, the measurement is rejected. If there are only a few missing pulses, the trigger signal may still be useful; only the missing trigger intervals are rejected. If the phase of the signal is not of interest, it is enough that the trigger signal remains stable during the measurement. Either the rising or lowering edge of the pulse can be used. With nip rolls, the runout measurement is often done in the direction of the nip and the trigger is installed at a convenient point. Therefore there will usually be an angular difference in their positions. When the angular location, i.e., the phase, for example of a high or low place on the roll surface is required, the locations of the trigger and acceleration transducer must be known. Based on Figure 40, it is easy to see that, if there is a high place at zero angle it would appear at an angle of θ in the measurement. The measurement starts when the zero marker passes the trigger and after turning for an angle of θ, the high place will hit the transducer. In order to obtain the actual angle between the zero angle marker and the high place, the angle between the trigger and the transducer in the direction of the rotation must be subtracted from the measured angle. Taylor (2003) gives a general rule for this: always add the angle in the direction of rotation between the transducer and the trigger to the measured angle of the irregularity. If the sum is greater than 360 degrees, subtract 360 degrees.

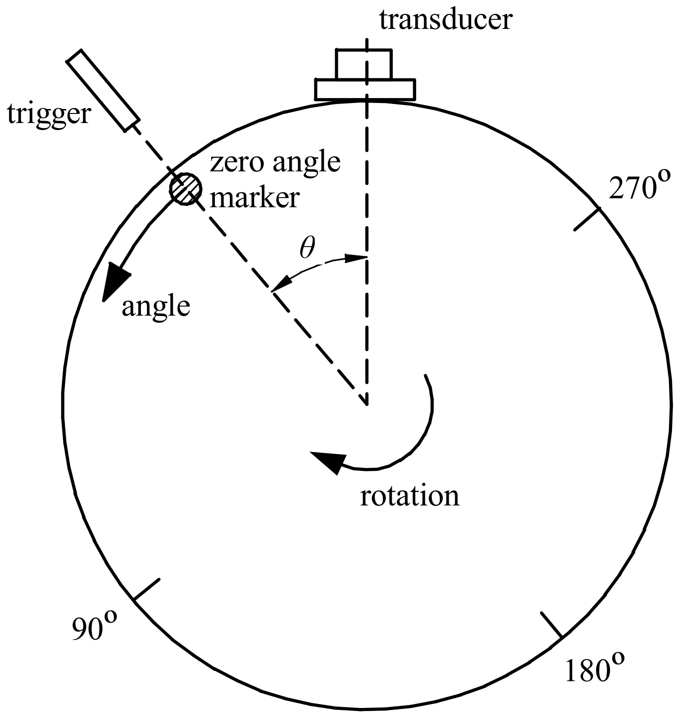

Figure 40. The angle θ between the trigger and the transducer must be known if the phase analysis is done.

To verify this it is possible to measure a bump (for example a piece of tape) in a known location on the surface and compare it to the position of the transducer. Measuring of a known bump makes it possible to verify the direction (polarity) of the acceleration signal.

The usage of the trigger sensor usually requires stopping the machine for the glueing of the reflecting tape. In some occasions, it is possible to use some distinguishable points, such as bolt heads, on the target for triggering.

There are different practices concerning, for example, the direction of the peripheral angle, whether it is counted clockwise or anti-clockwise and is looked from the drive side or the tending side of the roll. It is very important that the people doing the measurements and the people in the workshop have the same understanding about the angle.

3.3.3 Equalisation and averaging

Using a photoelectric sensor and a piece of reflecting tape on the roll shaft as a trigger, numerous signal periods are collected and averaged over many rotations of the roll (Figure 41). The number of rotations in one measurement depends on the rotation frequency of the target and the duration of the measurement. Using this synchronous averaging over numerous rotation periods, the vibration frequencies that are not specific to the rotation period of the roll are eliminated.

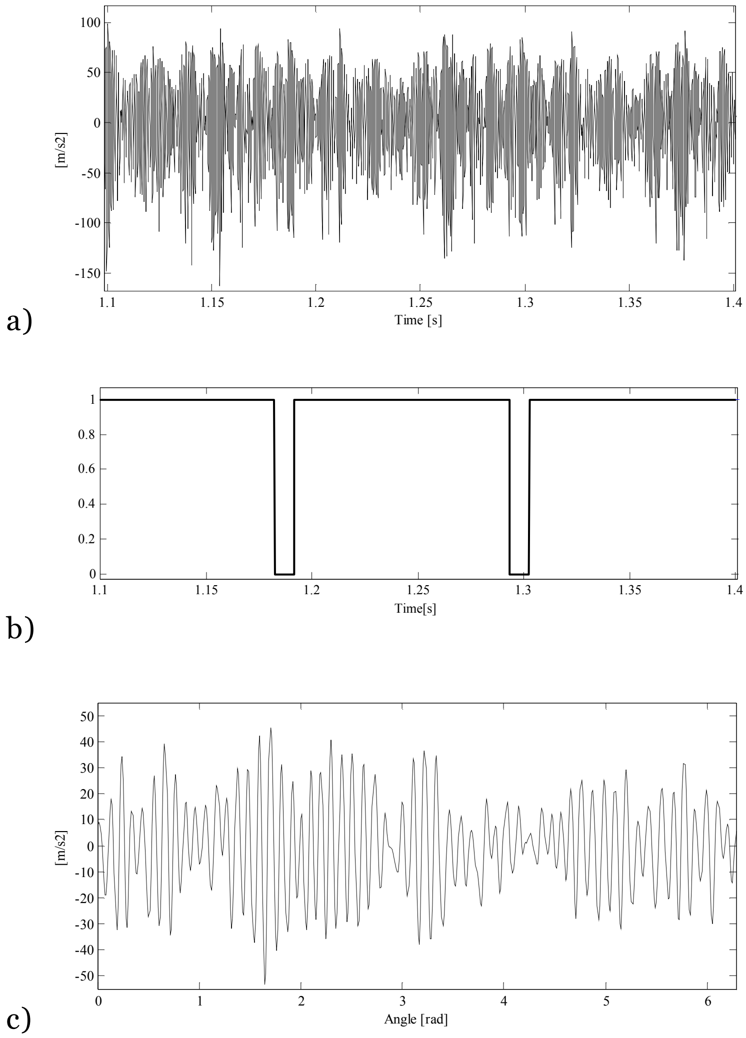

Figure 41. A sample of acceleration signal of test disk measurement (a), trigger signal (b) and averaged (89 rotations) acceleration signal (c).

The number of sampled data points varies on each rotation depending, for example, on how the sampling interval coincides with the edge of the trigger tape, on the quality of the trigger signal or on the possible fluctuation of the rotation frequency. If the triggering works precisely and the rotation frequency is stable, the variation in the number of points should be within a single measurement point. Therefore it is necessary to equalise the number of data points before averaging. This is done by interpolation of points for each rotation if necessary. The number of points is determined by the maximum of all rotations. If the number of points on a single rotation differs too much from the average for some reason, that rotation will be rejected from averaging. The interpolation is done using the Matlab function *interpft*, which uses the FFT method transforming the measured data vector to the Fourier domain and then back with desired number of points (Mathworks 2007). After that the data is averaged for one rotation using a simple arithmetic mean.

3.3.4 Integration

Sinusoidal linear movement can be described as

$$x(t) = A\sin\omega t \tag{8}$$

where x is displacement, A is the amplitude, ω is angular velocity ($=2\pi f$) and t is time. Derivation of movement in relation to time yields velocity and acceleration

$$v(t) = \dot{x}(t) = \omega A\cos\omega t = \omega A\sin\left(\omega t + \frac{\pi}{2}\right) \tag{9}$$

$$a(t) = \ddot{x}(t) = -\omega^2 A\sin\omega t = \omega^2 A\sin(\omega t + \pi) \tag{10}$$

This means that is possible to integrate acceleration to displacement simply by dividing the acceleration by the negative angular velocity squared

$$x(t) = \frac{a(t)}{-\omega^2} \tag{11}$$

The frequency of the movement remains unchanged, only the phase is shifted 180 degrees (Figure 42).

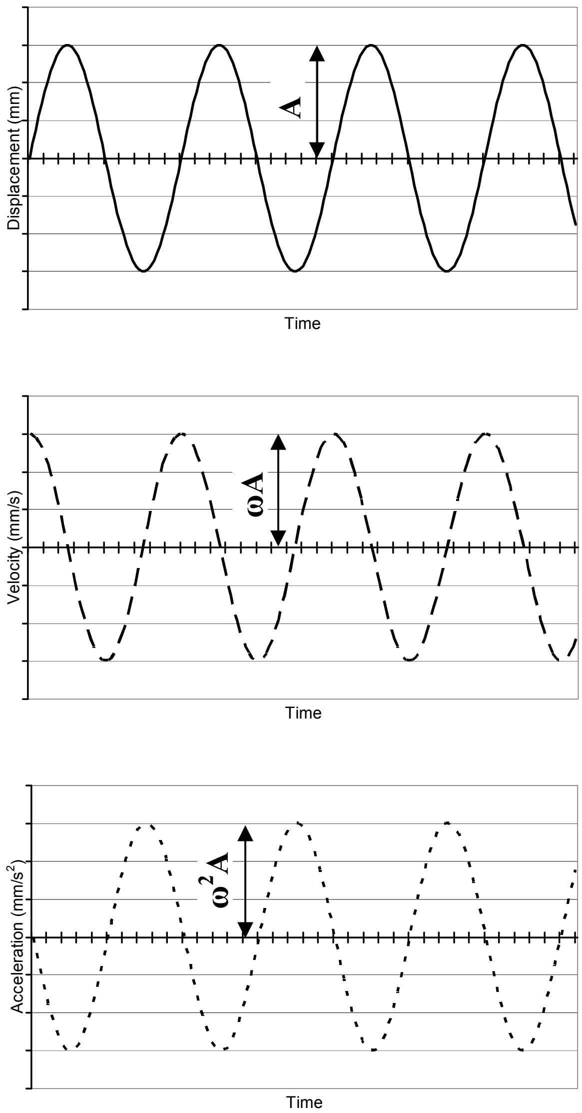

Figure 42. Derivation of displacement into acceleration.

In the frequency domain the integration is done by diving each spectral line by corresponding angular velocity. With complex numbers Equation 11 equals

$$x(\omega) = \frac{a(\omega)}{(j\omega)^2} \tag{12}$$

Integrating acceleration twice yields the displacement signal (Figure 43). Thereby the final result of the analysis is the averaged displacement of the roll surface over one rotation period of roll, i.e., the runout. In Figure 44 is an example of a measurement where there were two pieces of tape glued to the roll surface on the path of the slide pad. The two bumps resulting from the impact are clearly visible in both the acceleration and the displacement signal. This “tape test” can be used to verify the phase angle and direction of the displacement.

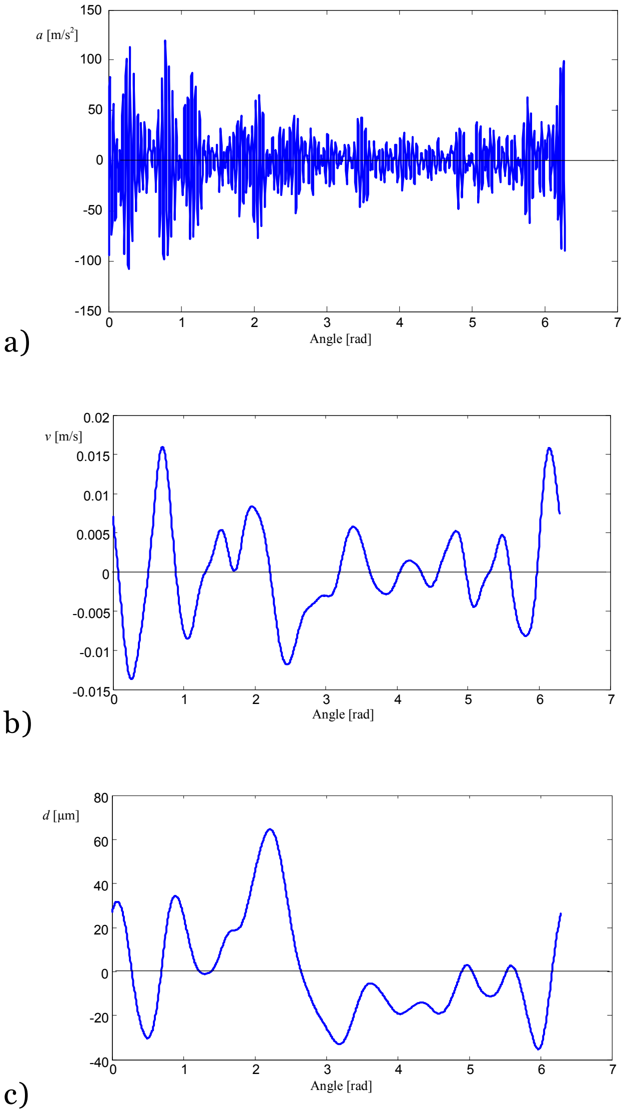

Figure 43. Acceleration (a), velocity (b) and displacement (c) signals.

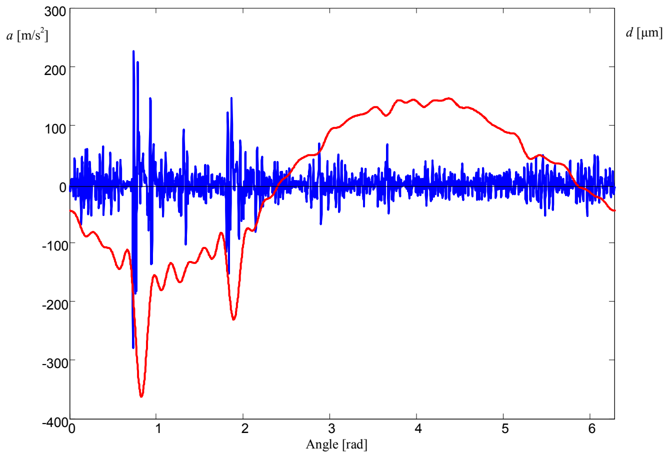

Figure 44. Acceleration signal (blue) integrated into displacement (red). There are two clearly noticeable bumbs caused by tape glued on the surface.

3.3.5 Harmonic analysis

After averaging and integration the signal contains the displacement of the target surface for one revolution. This displacement can be analyzed as it is but it is usually more useful to study the phenomena that are synchronous with the rotation frequency. Using FFT for the displacement data yields the harmonic components of the runout, i.e., the first harmonic is the displacement that occurs once on every revolution, the second harmonic twice etc. The number of harmonic components, analogous to the number of lines in the frequency domain, depends on the total number of points measured during one revolution.

3.4 Measurements

A series of laboratory and *in situ* measurements were done to study the performance of the method in measuring the runout of cylindrical and rotationally symmetrical objects. Firstly, a series of laboratory measurements for a workpiece with a known geometry were done to study the accuracy and functionality of the method. Secondly, a series of *in situ* measurements in paper mills were done to study the usability of the method in actual cases.

3.4.1 Laboratory measurements

The test disk

The first measurements were done with a steel disk having a diameter of 250 mm and width of 17 mm and a certain number of undulations machined on its surface. The measured surface is ground and nitrogen hardened. The roundness profile of the disk was measured with a Taylor Hobson Talyrond 31C roundness geometry measurement system (Figure 45). A roundness measurement involves the rotation of the part on a highly accurate spindle that provides the reference for the circular datum while keeping the contact based measuring transducer fixed. One measurement lasted about 1 minute and the disk rotated at a slow speed about 5 revolutions during the measurement. Simultaneously with the roundness measurement, the runout of the disk was measured using an eddy current measuring system eddyNCDT 3300 with an ES4 sensor by Micro-epsilon. This was done in order to find out how the eddy current sensor measures relative to the precision roundness measurement system. The eddy current sensor would later be used as a reference for the slide pad measurements.

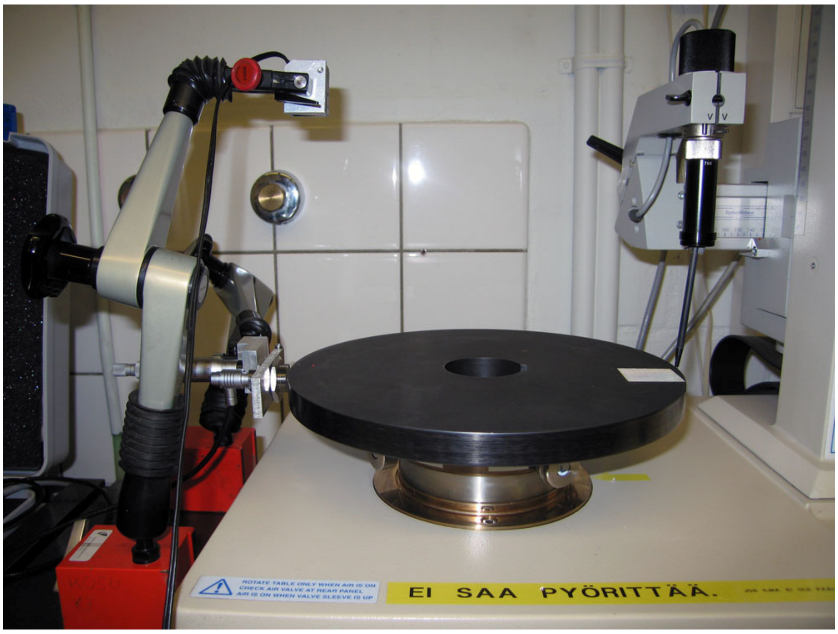

Figure 45. Roundness measurement and simultaneous eddy current measurement of the test disk.

Test disk measurements in the lathe

For the measurements the disk was attached to a lathe chuck with a stub shaft (Figure 46). The disk was centred using a dial gauge. Measurements were triggered using a laser-type photoelectric sensor (Omron E3C-LD11) with reflective tape glued on the side of the disk. The trigger position remained the same during all the measurements.

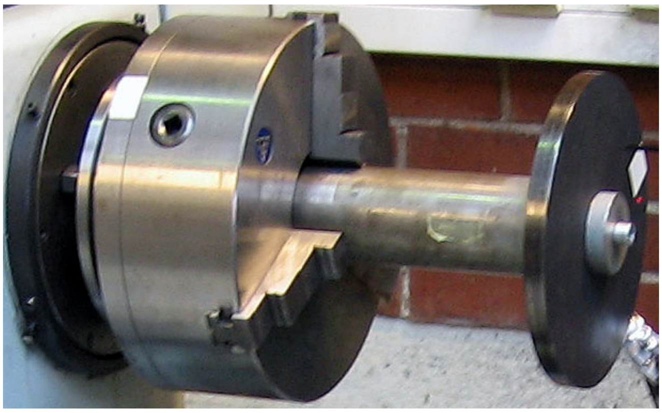

Figure 46. The disk attached to a lathe chuck.

LVDT measurements

First the runout of the disk was measured using a LVDT sensor (Figure 47). The LVDT sensor was a HBM W5TK with a ±5 mm measuring range. A HBM KWS 3073 measurement amplifier was used with the sensor. The sensor was calibrated for a range of ±1 mm with a Mitutoyo digital micrometer calibrated by MIKES, *Centre for metrology and accreditation*. During the measurement the disk was rotated in the clockwise and counter clockwise directions with rotation frequencies of about 0.5 Hz and 0.3 Hz, respectively. To obtain a sufficient number of revolutions, each measurement lasted for about 50 seconds. The measurement was repeated 10 times.

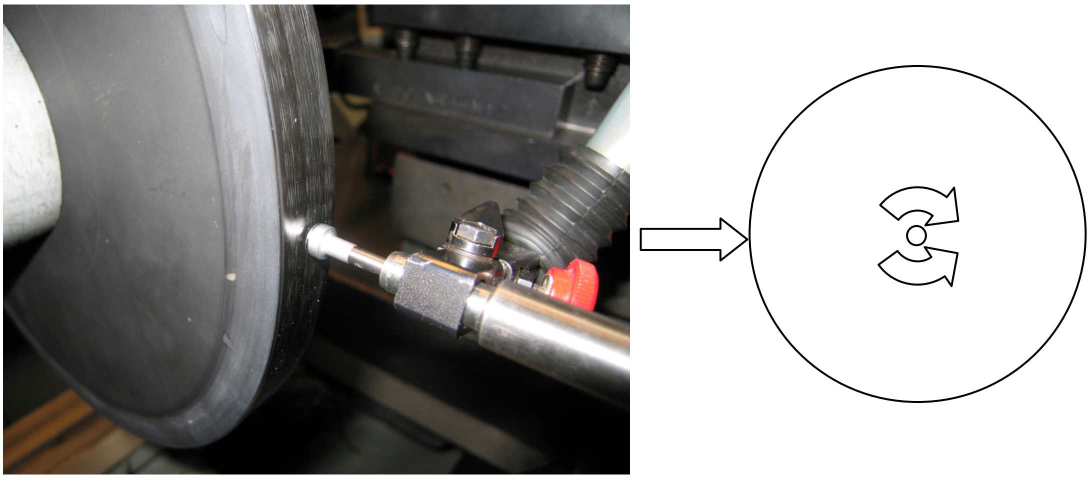

Figure 47. LVDT measurement and the measurement direction.

Eddy current measurements

Secondly, the LVDT measurement procedure was repeated with the eddy current sensor. The sensor was calibrated for the disk on the measurement position (1). In addition, the runout was measured in two additional directions (Figure 48); first in the direction where the slide pad measurement would be done (2) and second opposite to that (3). The latter two measurements were done with the rotation frequencies of 2.2, 4.5, 9.0 and 18 Hz in the clockwise rotation direction.

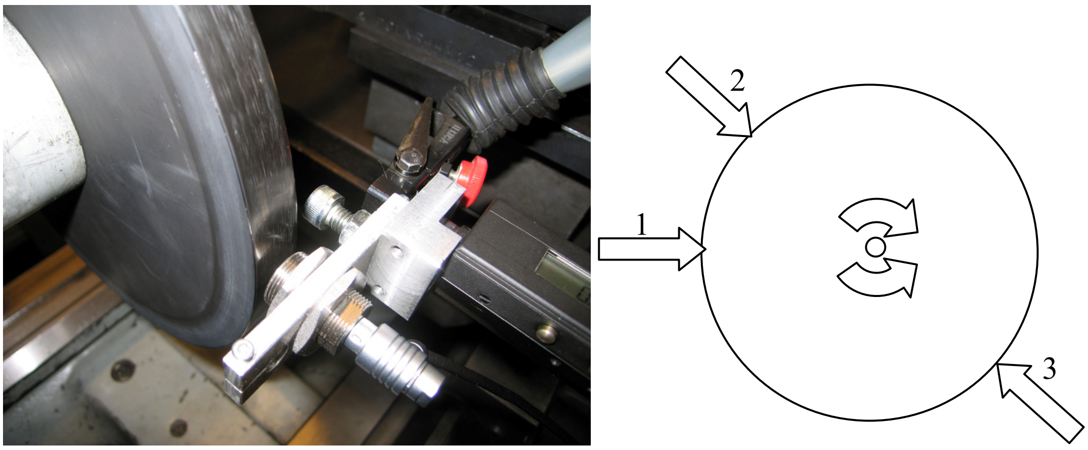

Figure 48. Eddy current measurement and the measurement directions.

Slide-pad measurements

The slide pad measurements were done the slide pad positioned at the position seen in Figure 49. The disk was rotating in the clockwise direction at four different frequencies: 2.2, 4.5, 9.0 and 18 Hz. The runout was measured using the slide pad simultaneously with the eddy-current sensor on the opposite side of the disk. The eddy-current sensor was calibrated to disk in the measurement position. The same trigger signal was used for both measurements.

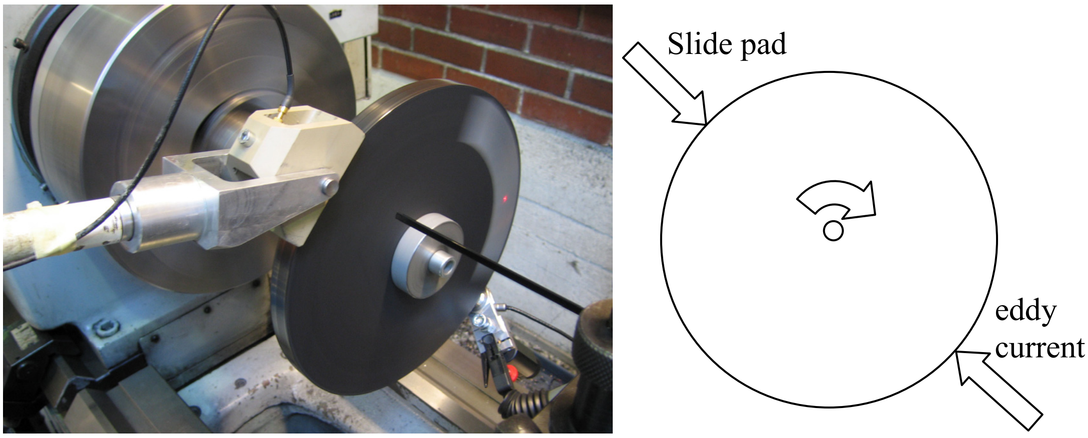

Figure 49. Slide pad measurement of the disk and the measurement directions.

Test roll measurement

The width of the test disk used for the measurements is only about one third of the slide pad which makes it difficult to hold the device on the surface on a stable position. To achieve better measurement conditions some tests were done with a test roll which was mounted on the grinding machine in the laboratory (Figure 50). The diameter of the roll was 1400 mm and the length 8 m. On the surface of the roll there were 40 undulations per revolution machined using a 3D grinding technology (Widmaier et al. 2009). The setting in the grinding for the amplitude of the undulations was 5 µm but the actual amplitude could not be verified.

The runout of the surface was measured using both slide pad and eddy-current probes in the same cross section; there was, however, a difference in their angular positions (Figure 50). In the first measurement the rotation frequency of the roll was 5 Hz. In the second measurement the roll was measured at different rotation frequencies from 0.5 to 7.2 Hz to see how this affects the results.

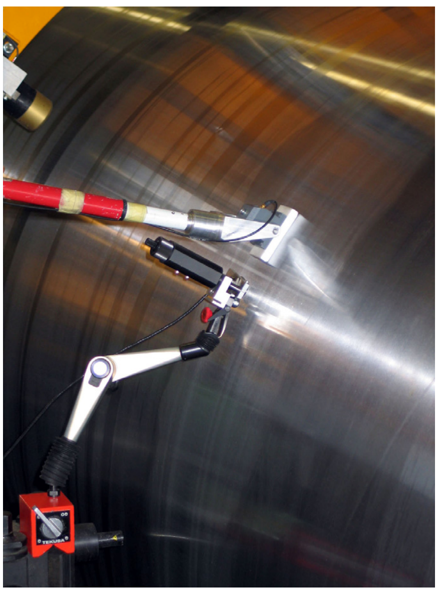

Figure 50. Runout measurement of the test roll in the laboratory.

3.4.2 Measurements in paper mills

The objective of the on-site measurements was to find out how the calender thermo rolls behave in the papermaking process when heated. There were two main effects to look for: thermal bending and possible undulations on the roll surface where the heating bores are located. The measurements were done during scheduled maintenance breaks. No reference measurements could be done in process conditions due to difficult accessibility and limited time frame set by the maintenance programs.

Table 3. Properties of case calenders.

	Case 1	**Case 2**	**Case 3**
Calender type	On-line soft calender	Off-line multinip calender	On-line multinip calender
Number of Thermorolls	1	5	4
Thermoroll material	Cast iron	Forged steel	Cast iron
Number of bores	40 (duo-pass)	24 (duo-pass)	32 (DuoTherm)
Heating oil temperature [º C]	220	110…220	257
Thermo roll diameter [mm]	1066	630	813
Web speed [m/min]	1164	450	1220
Roll rotation frequency [Hz]	5.8	5.3	8.0

Case 1 - Thermal bending of thermo-roll

The target of this measurement was to find out the possible bending of an oil-heated, peripherally bored cast iron thermo roll in an on-line soft calender (Figure 51) at different temperatures. The bending of the roll should be evident on the first harmonic of the runout. The measured thermo roll had 40 peripheral bores (duo-pass type). The counter roll was polymer coated.

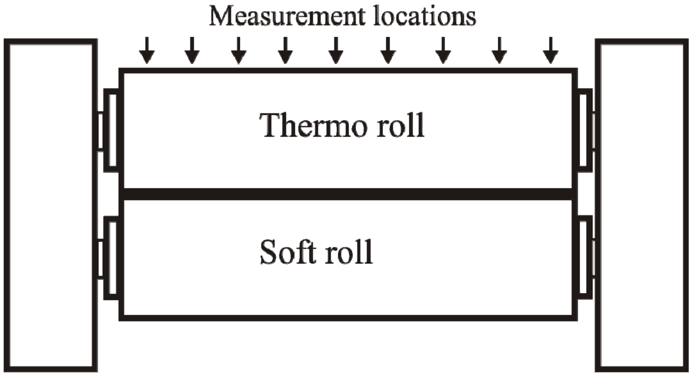

Figure 51. Basic layout of soft calender (case 1).

Total of four different sets were measured:

Measurement 1, *Process condition*

- Normal operation, nip closed, paper web on
- Web speed 1164 m/min

Measurement 2, Web break

- Nip open
- Web speed 1164 m/min

Measurement 3, Varying speed

- Nip open
- Web speeds 616 m/min and 1169 m/min

Measurement 4, Varying temperature

- Nip open
- Web speed 1164 m/min
- Oil inlet temperatures 50…220º C

Firstly, the runout of the roll was measured during the papermaking process to find out the behaviour of the roll during normal operation. The measurement was triggered using the same reflector on the roll drive shaft that the process control is using. Immediately after a web break preceding the maintenance break the runout was measured in the centre cross section of the roll when the nip was just opened. This was done to see if the paper web has any significant effect on the roll temperature during the process and thereby on the runout. During the maintenance break the runout was first measured at two different running speeds and second with varying heating oil inlet temperatures at nine different cross-sections. Two different running speeds were measured to find out if there would be any dynamic bending in the roll caused by unbalance. The measurements with varying temperatures were all done with a fixed running speed. The nip was open during these measurements and the paper web was not present. The measurement was done at the upper side of the thermo roll in the direction of the nip. In addition, the vibrations of the support in the direction of the nip were measured using accelerometers attached to the bearing houses of the rolls.

Case 2 & 3 - Thermal expansion of thermo roll

The main target of these measurements was to find out if it would be possible to detect the expected thermal expansion caused by heated peripheral bores. This should be seen as a harmonic component on the runout at a frequency related to the number of bores.

Case 2: Off-line multinip calender with forged steel thermo rolls

The measurements were done in an off-line multinip calender with a total of five oil-heated, peripherally bored forged steel thermo rolls (Figure 52). The structure of the forged steel roll is more uniform than that of the cast iron rolls which should reduce thermal bending. The forged steel thermo rolls make it possible to use higher temperatures during the calendering which on the other hand may amplify the effects of thermal behaviour. The heating oil inlet temperatures of individual rolls varied from 110 to 220 °C so that when the paper web enters the calender the first thermo rolls have the highest temperatures. The thermo rolls have 24 peripheral bores (duo-pass). All the thermo rolls have the same structure. A total of nine cross-sections of each roll were measured consecutively during the calendering process while the process parameters, web speed, nip pressure and oil temperatures, remained unchanged. All the rolls were measured from the same side approximately perpendicular to the direction of the nip.

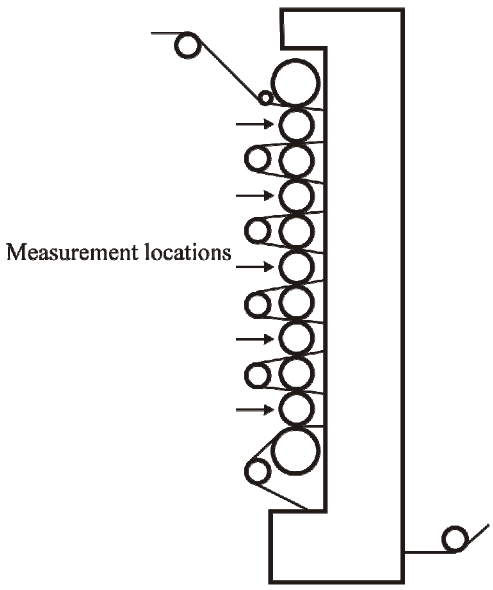

Figure 52. Basic layout of multinip calender stack (case 2).

Case 3: On-line multinip calender with cast iron thermo rolls

The measurements were done in an on-line multinip calender with four oil-heated, peripherally bored cast iron thermo rolls in two stacks (Figure 53). Only one of the thermo rolls was accessible for the measurement. The measurement direction was perpendicular to the nip direction. The thermo roll had 32 peripheral bores (DuoTherm).

At first, the runout of the roll was measured nip open. Secondly, the runout was measured during the papermaking process. The temperature of the heating oil inlet during the process was 257 °C. The temperature of the roll during the first measurement was unknown but the roll had cooled down during the maintenance break.

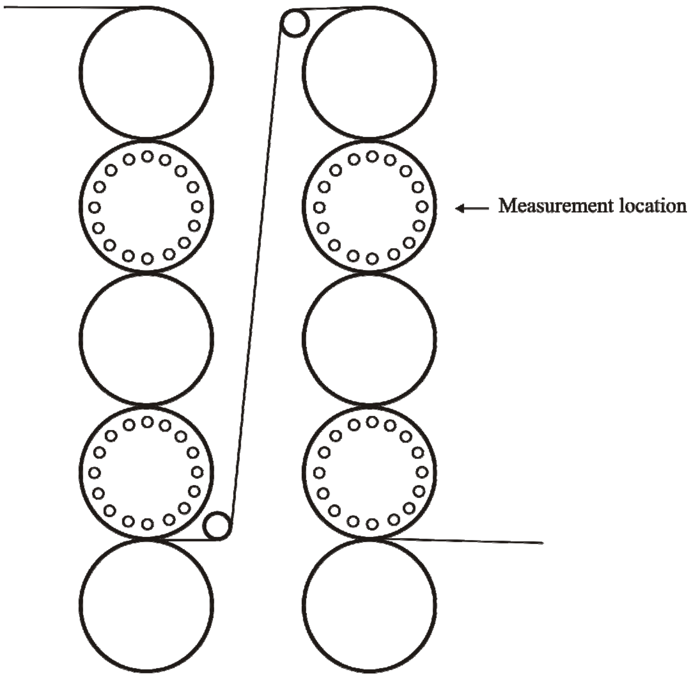

Figure 53. Basic layout of multinip calender roll stacks (case 3).

There were also a number of machine direction (MD) paper samples taken from the paper manufactured with the same rolls and parameters as were used during the measurements. These samples were analysed using the Tapio Paper Machine Analyzer to measure the thickness and gloss variation of the paper. The analysis was done in the laboratory of the plant.

3.4.3 Uncertainty of the measurement

The method is based on the principle that the measurer holds the device by hands during the measurement. This will naturally add uncertainty to the measurement. To some extent, the result will be depended on the skills and experience of the measurer. This makes it difficult to determine the exact quantitative properties of the method concerning its precision and accuracy.

Calibration of the LVDT and eddy current sensors

The LVDT and eddy current sensors were calibrated using a calibrated digital micrometer with a resolution of 1 μm. A calibration procedure of measuring both rising and lowering values repeatedly within the measuring range was done. The eddy current sensor was calibrated with the test disk to take into account the material and the geometry of the target. In each measurement position the eddy current sensor was calibrated using the built-in calibration system of the sensor amplifier. The maximum standard deviations for the calibration measurements were 0.2 % for the LVDT and 0.4 % for the eddy current sensor. The square root of the sum of the squares was used to calculate the combined uncertainty. Considering the reading and sampling accuracies, the combined uncertainties for the measurements are 0.8 % for LVDT and 1 % for eddy current sensor (k=2).

Possible error sources

There are some factors that can be seen as potential sources for either systematic or random errors. Systematic errors affect the result the same way for each of the repeated measurements. If known, the systematic errors can be corrected before or after the measurement. Random errors cause the result to be randomly different for each of the repeated measurements. The random errors can be minimised, for example, by averaging.

Possible sources of the systematic errors are

- Measurement equipment
    - Amplifier and sensor bias and linearity
    - Errors in amplification and sensitivities
    - Drift
- Ambient conditions, such as temperature
- Measurement method
    - Mechanical properties of the slider
        - Friction
        - Inertia
        - Elasticity
        - Damping
    - Alignment and position
    - Holding force
- Signal processing
    - Filtering
    - Sampling
    - Integration
    - Averaging

The magnitude response of the accelerometer was measured by MIKES (Centre of Metrology). The result for the frequencies from 10 to 400 Hz is shown in Figure 54 as an error in sensitivity of the sensor. The frequencies under 10 Hz could not be measured but it is obvious that the error increases at lower frequencies.

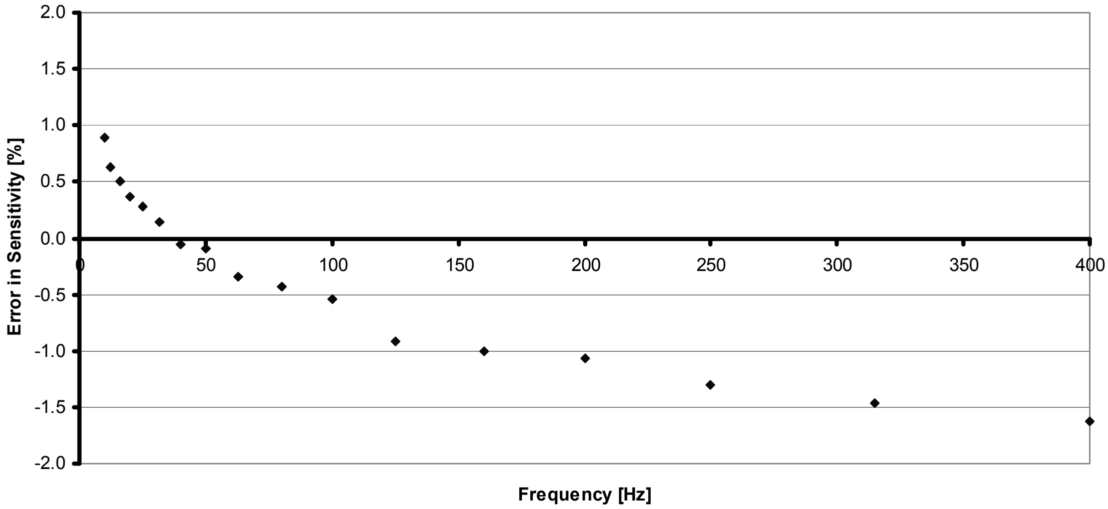

Figure 54. The magnitude response of the accelerometer.

Amplification coefficient of the accelerometer amplifier is set experimentally before the measurement to have the full benefit of the input range of the A/D-board. The amplification coefficient is saved in a measurement file along with the data. The sensitivity of the accelerometer is set by the manufacturer specification. The sensitivity is temperature dependent. According to the manufacturer, the sensitivity deviation at 100 °C is about +3 % and at 200 °C about +10 % compared with the room temperature. The actual temperature of the sensor in a process environment is not known but it can be assumed to be less than 100 °C because of the shield provided by the slide pad structure and the cooling effect of the air flow around the roll. It has been possible to hold the sensor with bare hands immediately after the measurements.

The contact between the slide pad and the target surface during the measurement is of vital importance. The slide pad must be in a continual contact with the surface. This is ensured by applying an adequate handling force to the device. If the slide pad should disengage from the surface during the measurement, the measurer would feel it in his hands. A poor contact between the slide pad and the surface will also be clearly seen in the acceleration signal, typically as raised levels and repetitive impacts. The width of the contact line between the slide pad and the surface is fairly narrow, as stated earlier, and it should not affect the harmonic components in the region of interest, that is, usually under 50. The slide pad should align itself on the surface but the friction or friction changes between the surfaces may have a tilting effect on the pad. If the accelerometer is tilted by an angle α relative to the normal of the surface (Figure 55), the measured acceleration in the radial direction is reduced by a factor 1/cos α. Even when the angle α is $5°$, the measured acceleration is reduced only by 0.4 %. The transverse sensitivity of the sensor is 1.7 % which means that the transverse acceleration caused by an angular error of the accelerometer alignment is negligible.

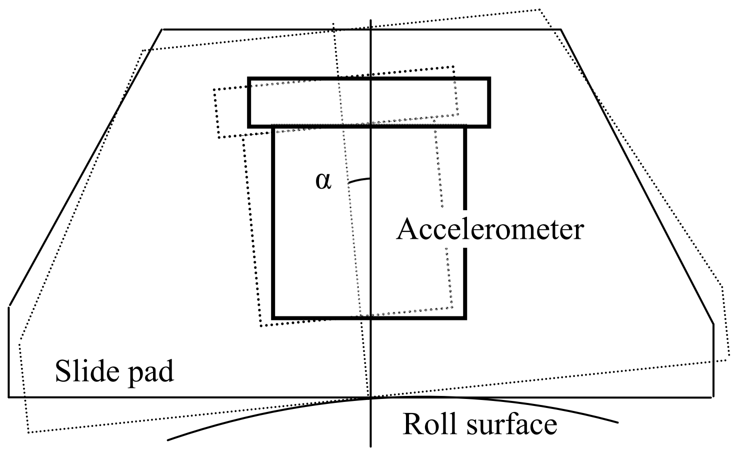

Figure 55. Tilting angle α of the accelerometer.

If the slide pad moves along the circumference during the measurement, the apparent phase of the vibration will change slightly between consecutive revolutions. The averaging will even out the variation but the amplitudes of the vibration may decrease slightly. The effect is stronger at the higher frequencies. When the measurement is done carefully the movement of the slide pad is fairly small compared to the circumference and the effect to the measurement negligible.

The random errors may be caused, for example, by

- Electrical noise
    - Cabling and grounding
    - Amplifier and sensor
- Fluctuation in ambient conditions
- Variation in process conditions
    - Speed
    - Temperature
    - External excitations
    - Contamination
- Wear of the contact face
- Data acquisition
    - Triggering
    - Sampling
    - AD-conversion
- Sensor position (location, angle)

The effect of electrical noise is minimised using high-grade, allocated cables and connectors. The noise caused by the amplifiers and other data acquisition components is minimal compared with the other sources of errors.

Rotation frequency measurement

Rotation frequency measurement is based on the once-per-revolution pulse obtained from the photoelectric trigger sensor. Rapid fluctuations in the speed of the target are unlikely due to the large inertia. Possible variation in speed measurement is most probably caused by the sampling interval. There are a variable number of sampled points on each revolution. The averaging of revolutions will even out the variation. The maximum speed variation in the measurements has been less than 0.1 %.

Analogue to digital conversion

With a 14-bit AD conversion and a ±5 V input range the resolution of the ADC is 0.61 mV. The maximum error of a single sample is then ±0.31 mV. The actual error in acceleration depends on the amplification of the signal, i.e., how well the input range of the ADC has been utilised. Assuming that only half of the range is used, the maximum error of the sampling is ±0.61 mV which is 0.012 % of the range. Compared with other error sources, this is negligible.

Equalisation of the number of the sampled points per revolution

Before averaging the data are resampled using a FFT-based interpolation method to have an equal number of points on each revolution. The variation in the number of points is within a few points whereas the number of points per a revolution is typically 1000-2000 at the minimum. Therefore the effect of the interpolation on the content, i.e., shape of the data, is minimal.

Integration

The displacement error depends on the error in the acceleration and the error in the rotation frequency. The effect of these factors on the total error can be analysed using partial differentiation. From Equation 12 using partial differentiation yields

$$\Delta x(\omega) = \left|\frac{\partial x}{\partial a}\right| da + \left|\frac{\partial x}{\partial \omega}\right| d\omega = \frac{1}{\omega^2}\Delta a(\omega) + \frac{2a}{\omega^3}\Delta\omega(\omega) \qquad (13)$$

It can be seen that the effect of the errors both in the acceleration and in the rotation frequency decreases rapidly as the rotation frequency increases. It means also that the effect of the errors diminishes on the higher harmonic components of the runout.

Combined standard uncertainty of the slide pad method

The estimated standard uncertainty for the measurement is based on the laboratory measurements. The estimated standard uncertainty for the accelerometer is based on the calibration done by MIKES. These and the other, above-mentioned, factors are combined using the square root of the sum of the squares to calculate the combined uncertainty.

The uncertainty of the method is, to some extent, dependent on the frequency. On low frequencies, that is, low rotation frequencies and lower harmonic components up to 2 Hz, the uncertainty of the method is more than 10 %. It is not advisable to use the method on the frequencies this low. The combined standard uncertainty of the method for the frequencies from 2 to 5 Hz is 4.5 % (k=2) and for the higher frequencies 3 % (k=2).

4 Results

The results in this chapter are mostly presented as the harmonic components of the runout. In rotating machinery, especially with paper machines, the vibration problems are usually viewed as multiples of the rotation frequency because the phenomena causing the vibration are typically periodic.

4.1 Laboratory measurements

4.1.1 Roundness measurement of the disk

The roundness of the disk was measured with a Taylor Hobson Talyrond 31C roundness geometry measurement system. The roundness profile of the disk based on one measurement is shown in Figure 56. Numerical values (average value of 5 measurements) of the amplitudes of the lowest 10 harmonic components are presented in Table 4. The amplitudes of the higher harmonic components are all less than 1 µm.

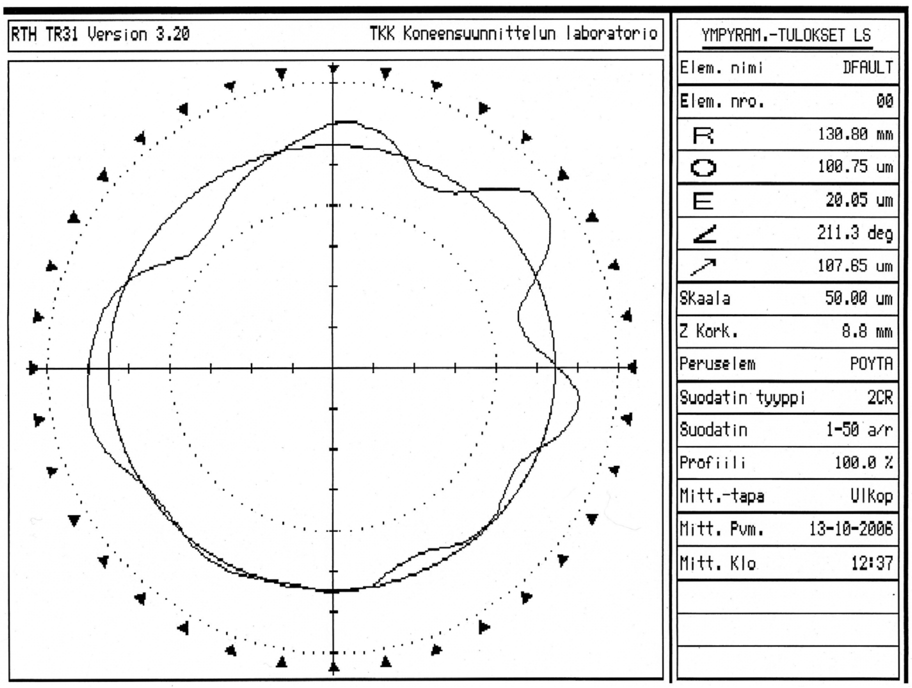

Figure 56. Roundness profile of the disk.

The roundness (Least square circle) of the disk is 100.75 µm, total runout 107.65 µm and eccentricity 20.05 µm, i.e., the centre of the disk is 20.05 µm off the rotation axis of the spindle.

Table 4. The lowest 10 harmonic components of roundness measurement of the test disk.

# of harmonic	1	2	3	4	5	6	7	8	9	10
Amplitude [µm]	20.0	14.5	10.8	10.1	11.4	10.1	10.7	10.0	10.9	1.35

The runout of the disk was measured simultaneously with the eddy current probe. The lowest 15 harmonics of the runout measured with the eddy current probe are compared to lowest 15 harmonics of the roundness in Figure 57. The result of the eddy current measurement is the average of 10 measurements. Both the roundness profile and the runout were measured at the centre circumference of the disk.

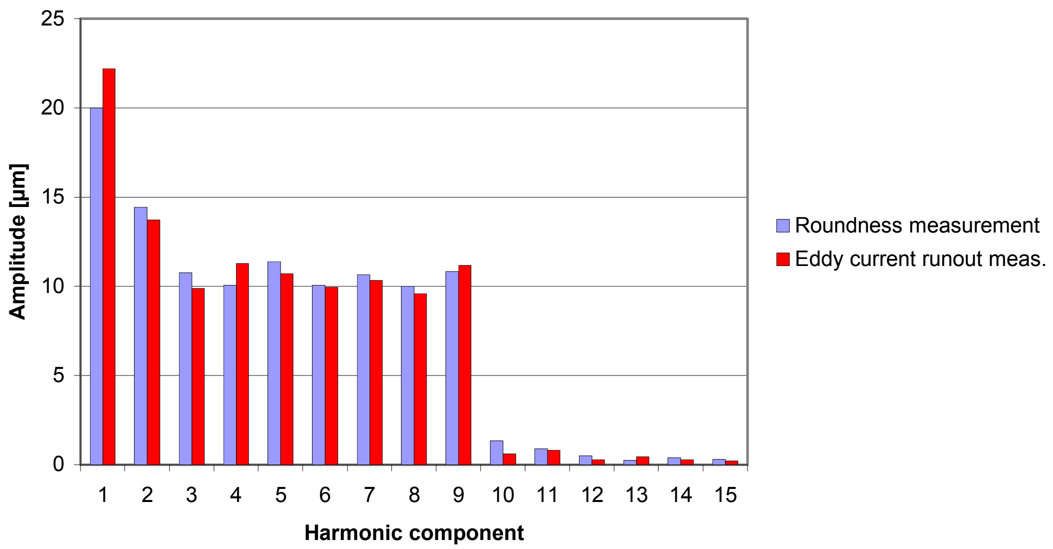

Figure 57. The lowest 15 harmonics of runout measured with eddy current probe compared with roundness measurement.

The runout measured with the eddy current probe is very close to the roundness profile which indicates that the spindle error of the roundness measurement device is very low. Most of the runout is caused by the geometry of the disk.

4.1.2 LVDT and eddy current measurements

The test disk was rotated in a lathe and the runout was measured with a contact based LVDT sensor and an eddy current sensor. The measurements are compared to see if there would be differences in their readings indicating possible electrical runout of the eddy current sensor. The rotation frequencies were very slow during the measurement. The results are an average of 10 measurements.

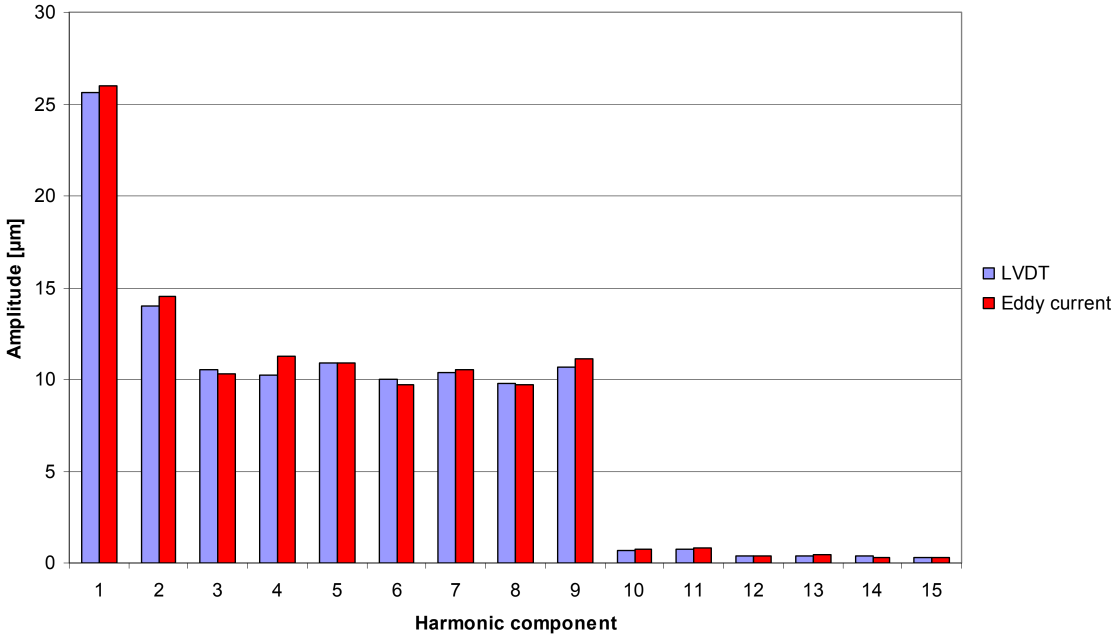

Figure 58. LVDT and eddy current measurements at the rotation frequency of 0.3 Hz in the ccw direction.

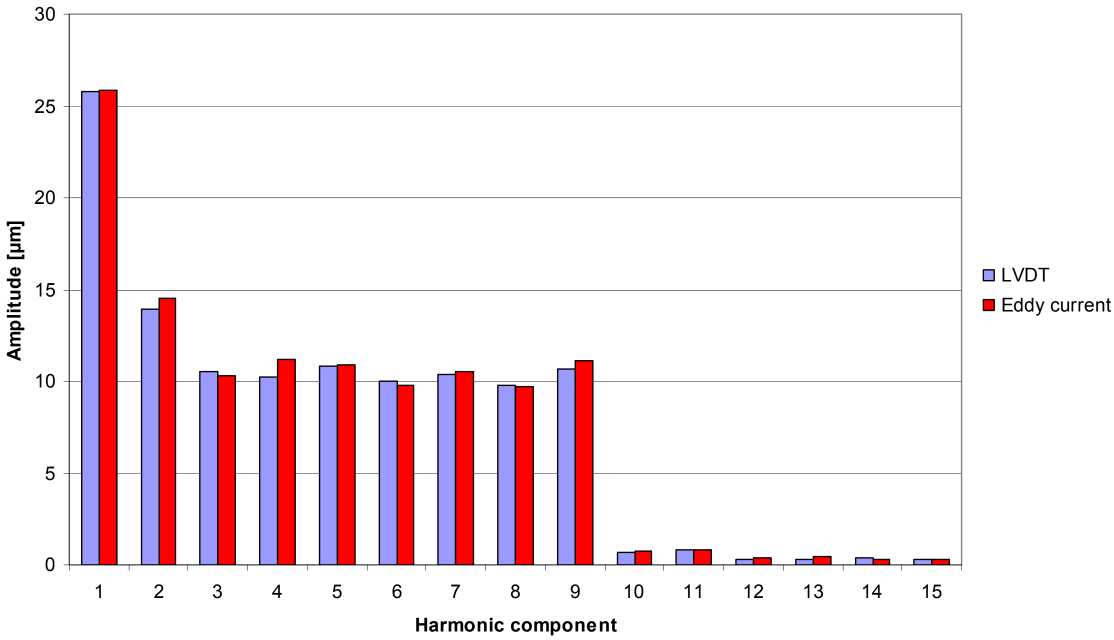

Figure 59. LVDT and eddy current measurements at the rotation frequency of 0.5 Hz in the cw direction.

In the contact based LVDT measurement there is a distinct phenomenon with the first harmonic component in the sequence of the measurements. The first harmonic rises gradually as the measurement continues (Figure 60). This happens in both rotation directions. There is no change in the eddy current measurement.

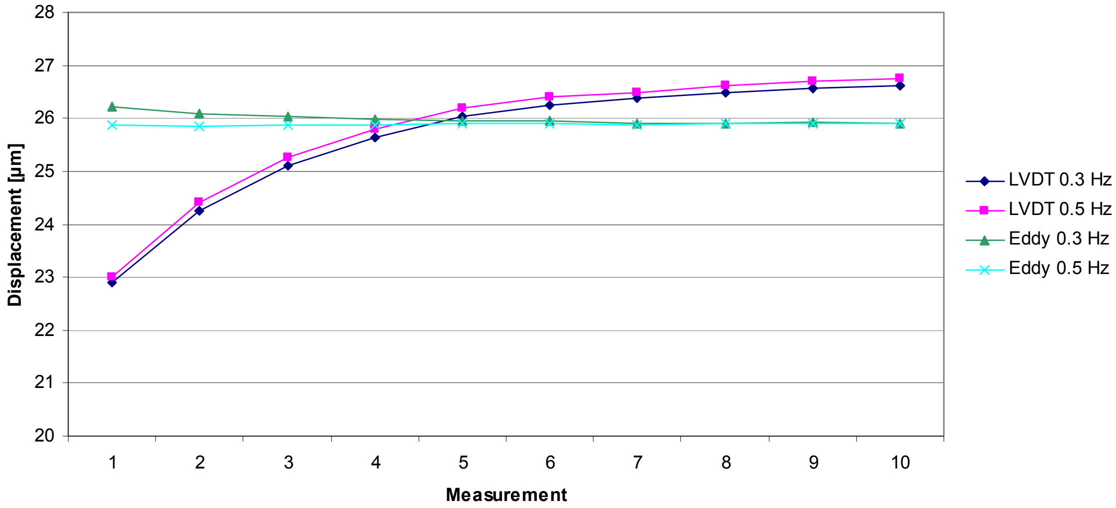

Figure 60. First harmonic component measured with LVDT and eddy current sensors.

In Figure 61 there are the first 15 harmonic components of the runout measured with the eddy current sensor at four different rotation frequencies. The measurement direction is the same as would be with the slide pad measurement.

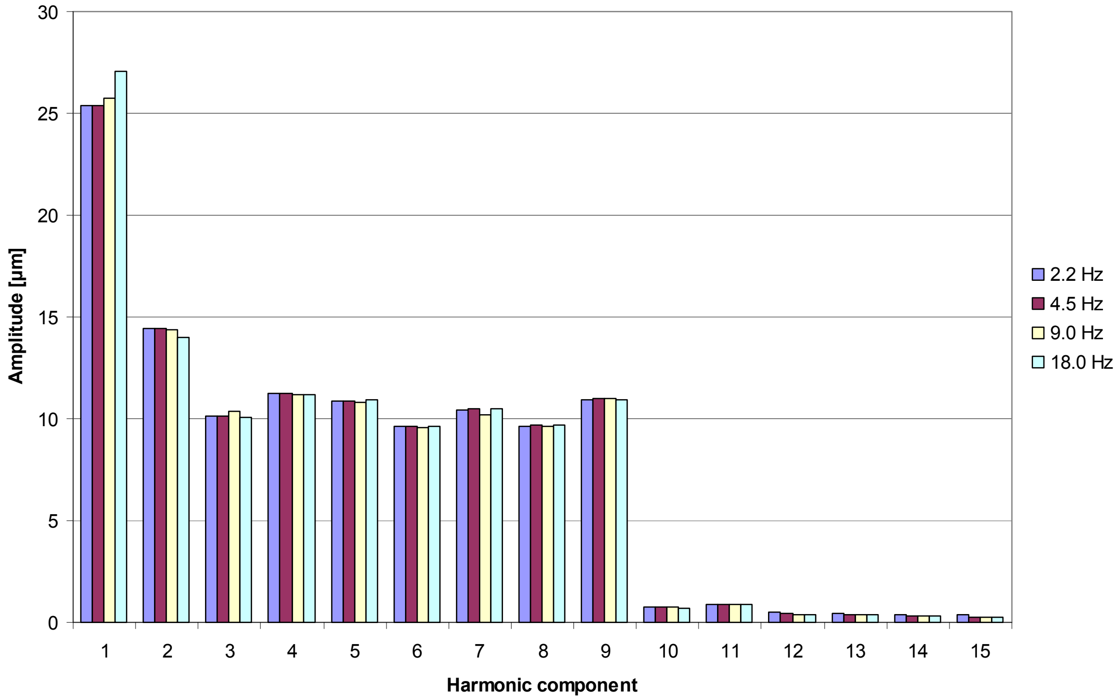

Figure 61. Eddy current measurements at different rotation frequencies.

4.1.3 Slide pad measurement of the disk

In the following measurements the runout of the disk was measured with the slide pad device in the lathe simultaneously with the eddy current probe. Figure 62 shows the runout measured at 4 different rotation frequencies of the disk. The results are an average of 10 measurements. Figure 63 shows the standard deviations of the measurements.

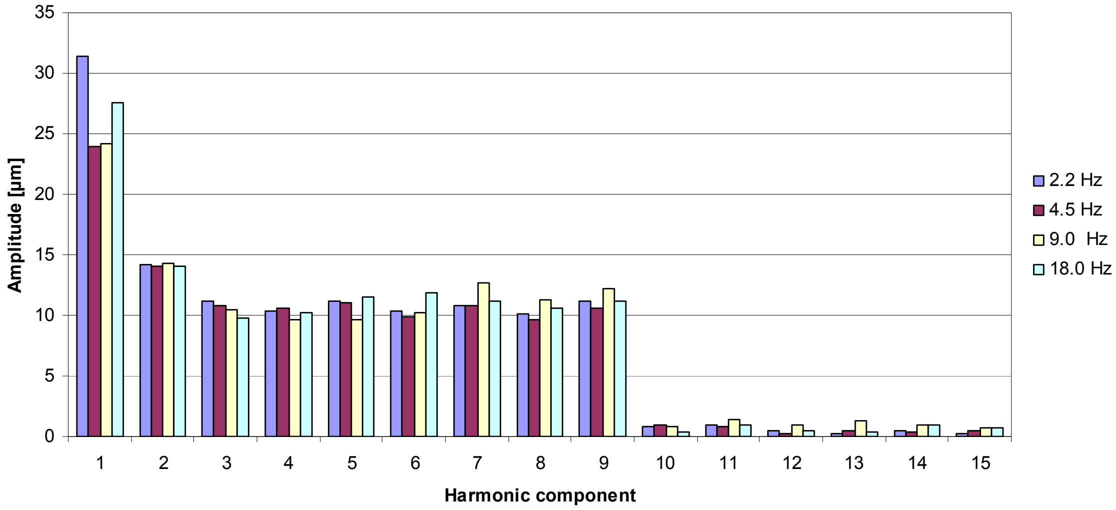

Figure 62. Runout of the disk in different rotation frequencies measured with slide pad.

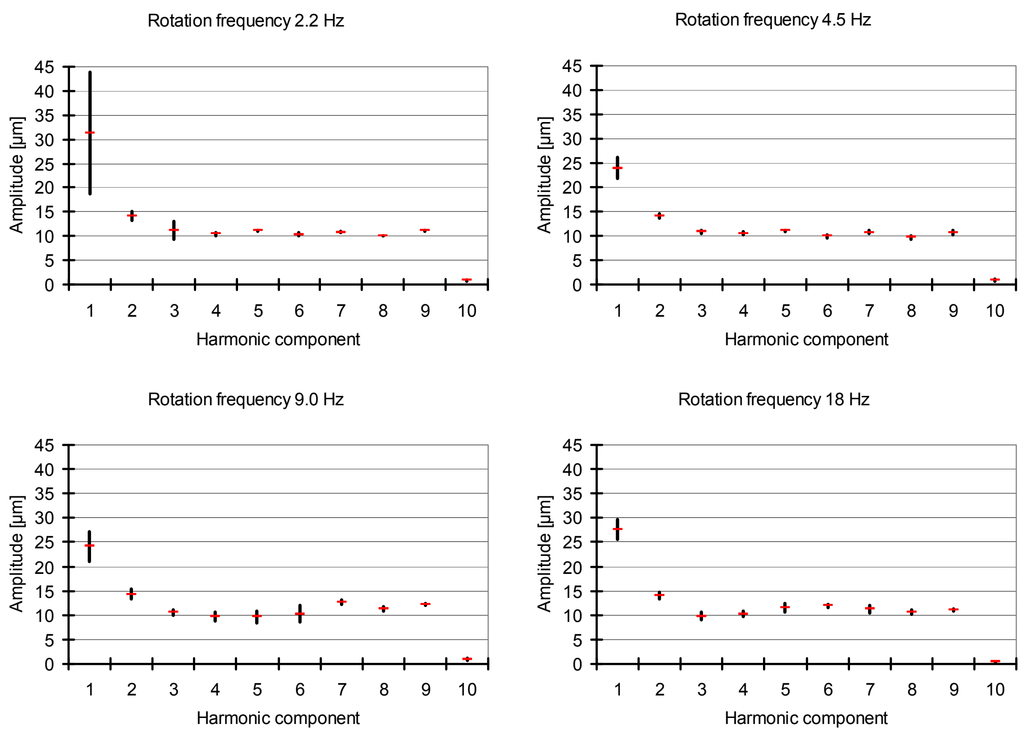

Figure 63. Average and standard deviation of runout at different rotation frequencies.

In Figure 64 to Figure 67 the slide pad measurement at different rotation frequencies is compared with the eddy current measurement which was done simultaneously at the opposite side of the disk.

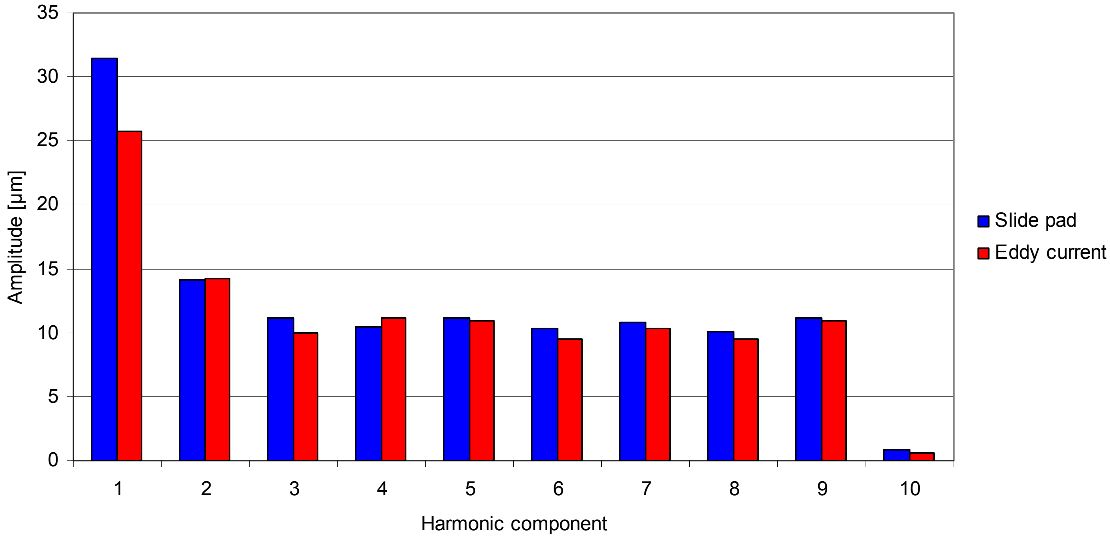

Figure 64. Comparison of measurements at a rotation frequency of 2.2 Hz.

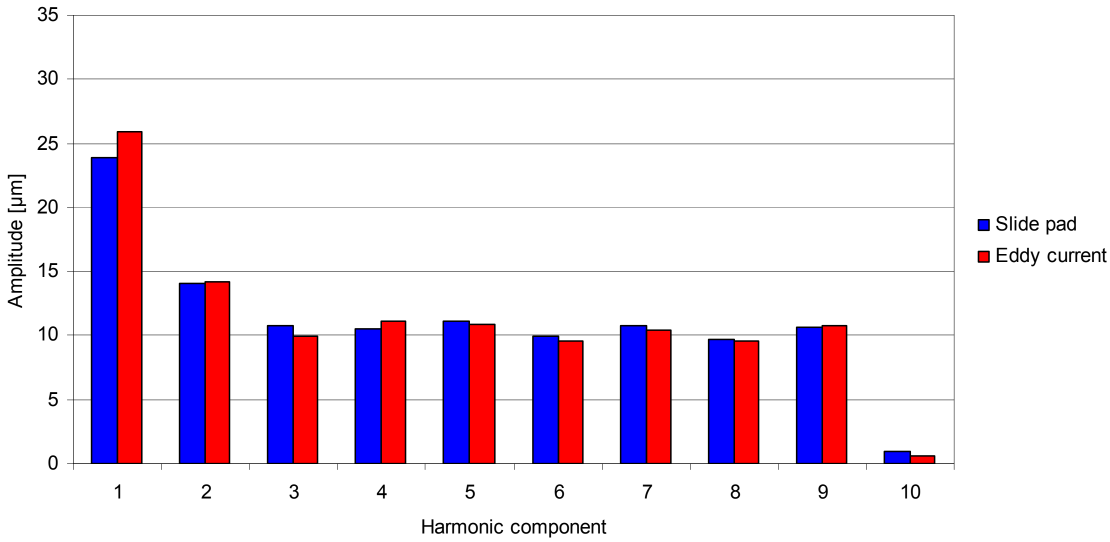

Figure 65. Comparison of measurements at a rotation frequency of 4.5 Hz.

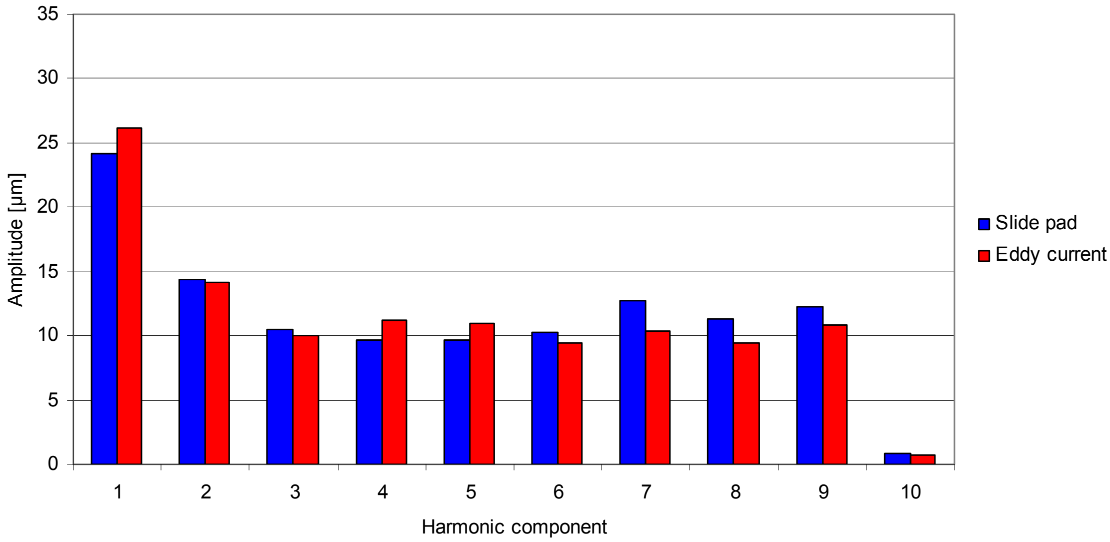

Figure 66. Comparison of measurements at a rotation frequency of 9.0 Hz.

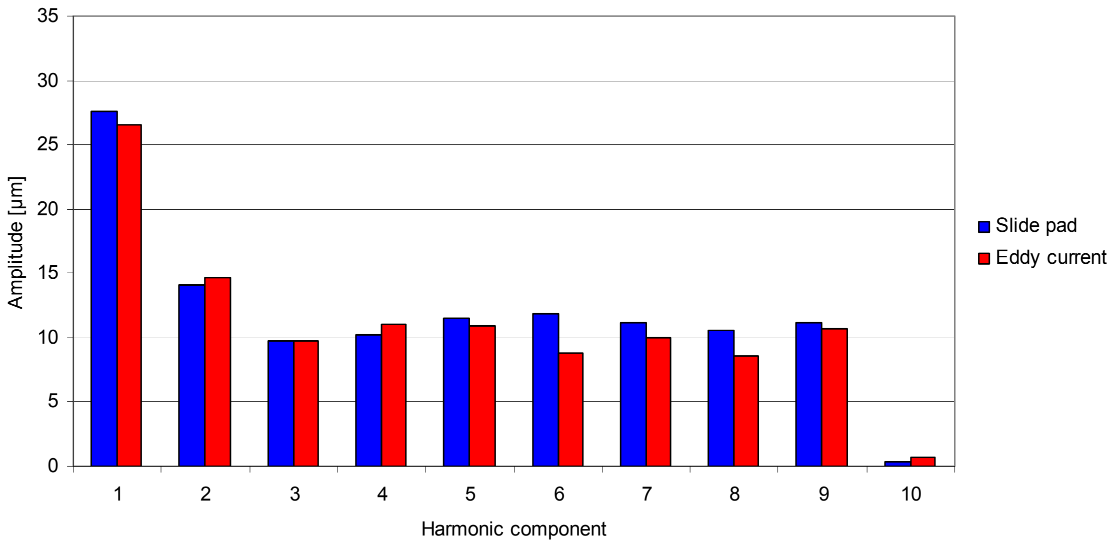

Figure 67. Comparison of measurements at a rotation frequency of 18 Hz.

In Figure 68 the runout is depicted as a displacement around the circumference of the disk. The phase and polarity of the eddy current measurement has been adjusted to match the slide pad measurement.

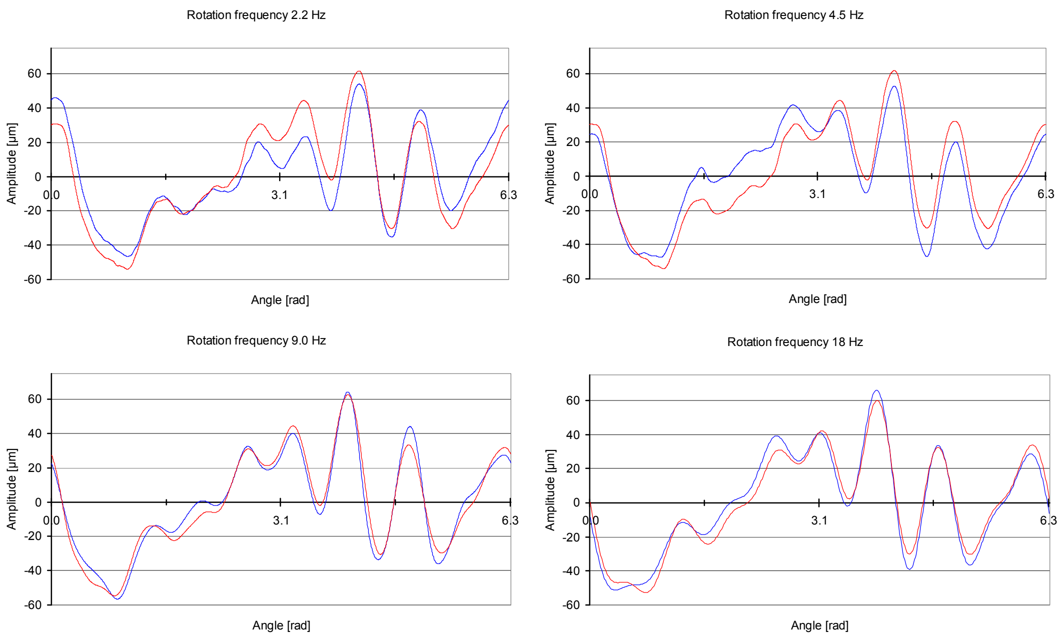

Figure 68. The runout of the disk in relation to the rotation angle measured with eddy current sensor (red) and slide pad (blue).

4.1.4 Measurement of the roll

The runout of the roll surface was measured using both slide pad and eddy current probes. The lowest 50 harmonic components are presented in Figure 69 and Figure 70. The rotation frequency of the roll in this measurement was about 5 Hz.

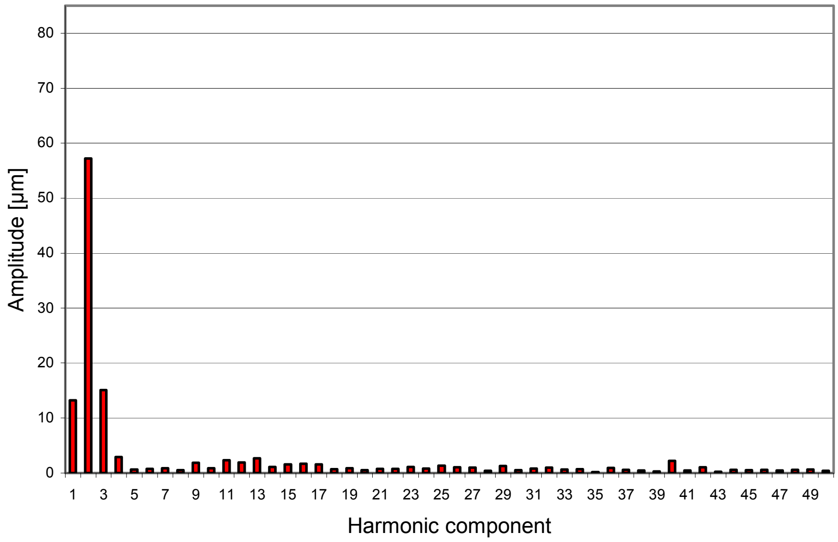

Figure 69. Harmonic components of the roll runout measured using eddy current probe.

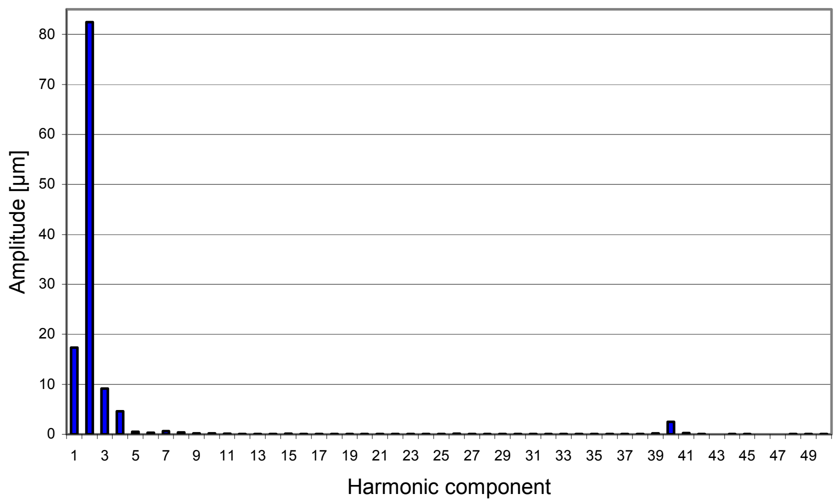

Figure 70. Harmonic components of the roll runout measured using slide pad.

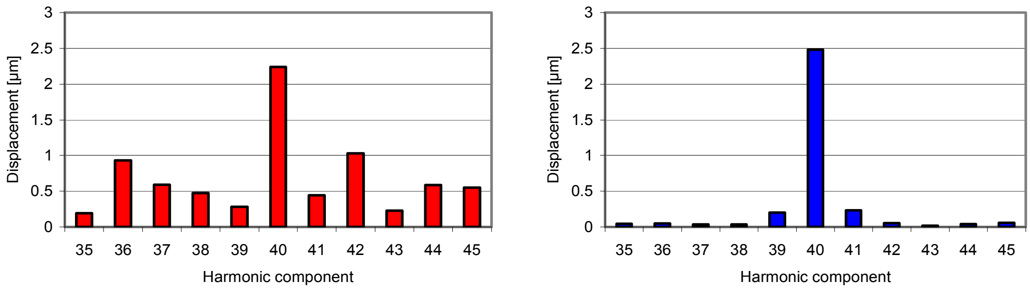

Figure 71. Harmonic components 35…45 of the roll runout measured with an eddy current probe (left) and slide pad (right).

Figure 72 shows the first 4 harmonic components of the roll runout measured with eddy current and slide pad probes at rotation frequencies from 0.5 to 7.2 Hz.

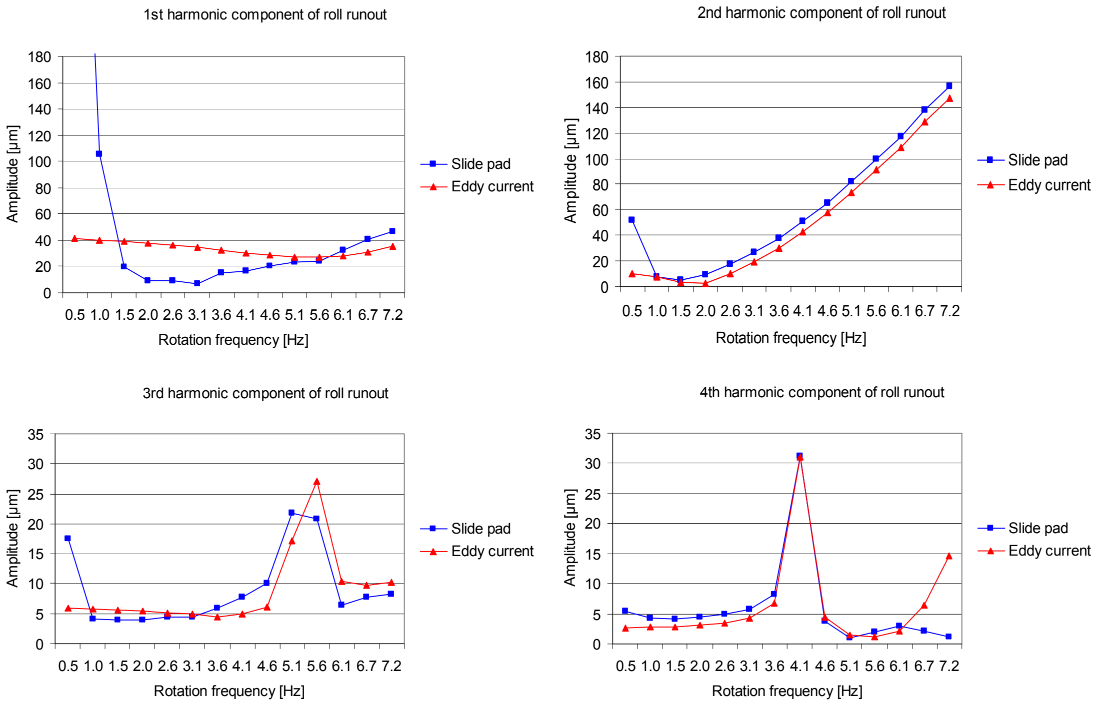

Figure 72. First 4 harmonic components of the roll runout at different rotation frequencies.

4.2 Case measurements

Thermal bending of thermo-roll (Case 1)

The target of this measurement was to find out the behaviour of an oil-heated, peripherally bored cast iron thermo roll in an on-line soft calender at different temperatures. First, the runout of the roll was measured during the papermaking process. The amplitude of the first harmonic of the runout measured in nine equally spaced cross-sections from tending side (TS) of the roll to drive side (DS) is presented in Figure 73 and the phase angle in Figure 74.

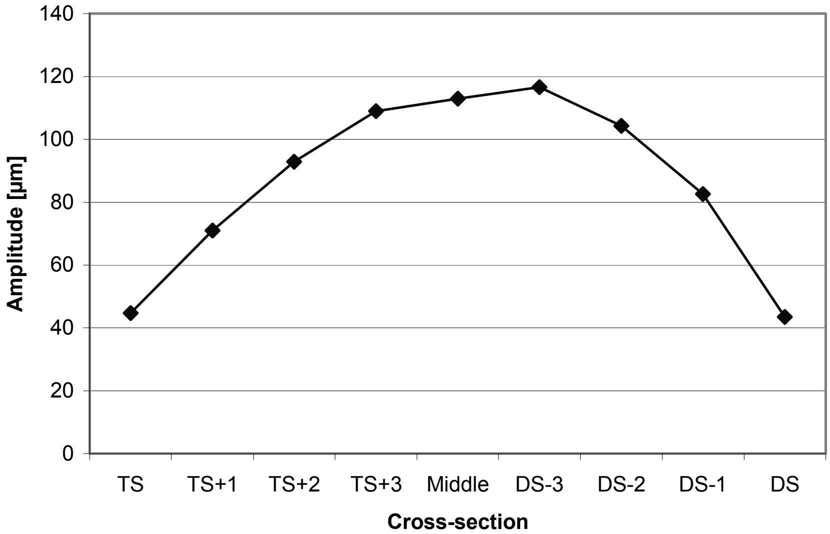

Figure 73. The amplitude of the 1st harmonic component of runout of the thermo roll during papermaking process.

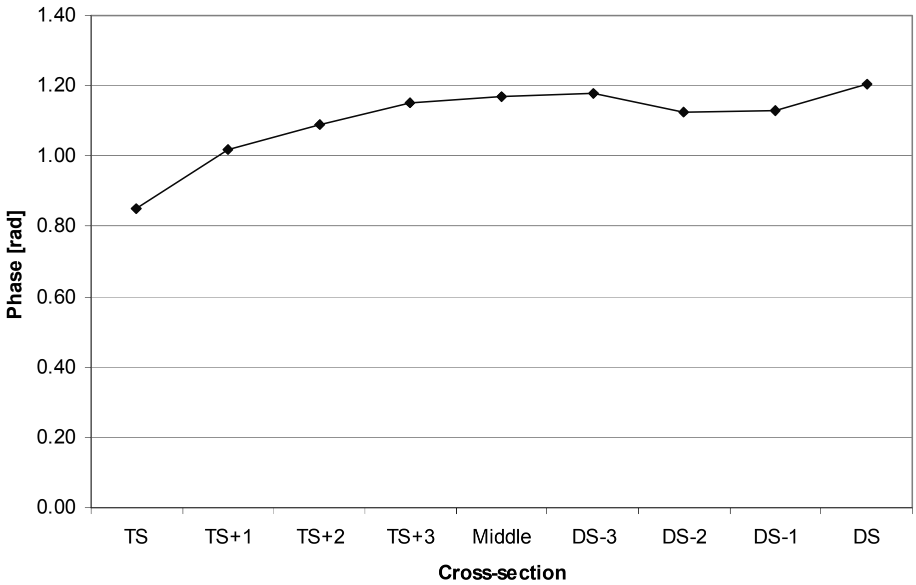

Figure 74. The phase of the 1st harmonic component of runout of the thermo roll.

In Figure 75 the runout measured at the middle cross section of the roll is shown as a displacement in relation to the rotation angle. It can be seen that the 1st harmonic dominates clearly the runout. Considering the polarity of the acceleration sensor (inverted installation) the maximum value of runout amplitude 113 µm is reached at the angle of 2.01 radians (in relation to the trigger point).

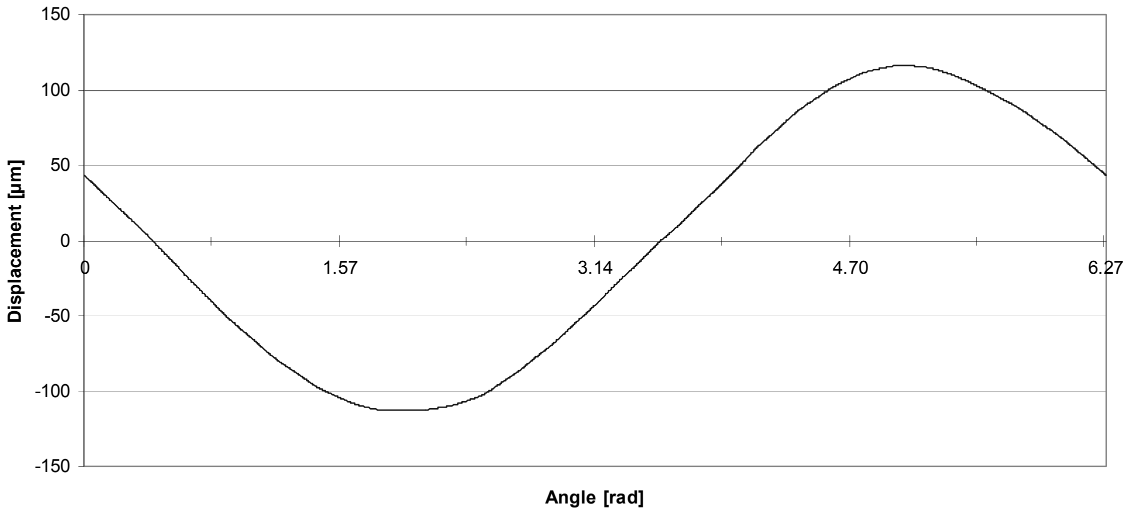

Figure 75. Runout measured at the middle of the roll.

The preceding measurement was done in the nip-direction, i.e., in the line between the centre points of the rolls. The runout was also measured in a direction just about perpendicular to that direction and at the middle cross section the maximum value of runout amplitude was 103 µm.

Figure 76 shows vibrations up to 50 Hz measured at the roll support using acceleration sensors. The roll rotation frequency of 5.8 Hz and especially its

2nd (11.6 Hz) and 7th (40.6 Hz) multiples can be detected. The other two clear peaks at 24.5 and 37.4 Hz are not synchronized with the rotation frequency. The vibration amplitudes at the bearing houses are small and when integrated into displacement the amplitudes are in the region of 1 µm or less even at the lower frequencies. For comparison, the vibration spectrum of the slide pad measurement at the middle of the roll is shown in Figure 77.

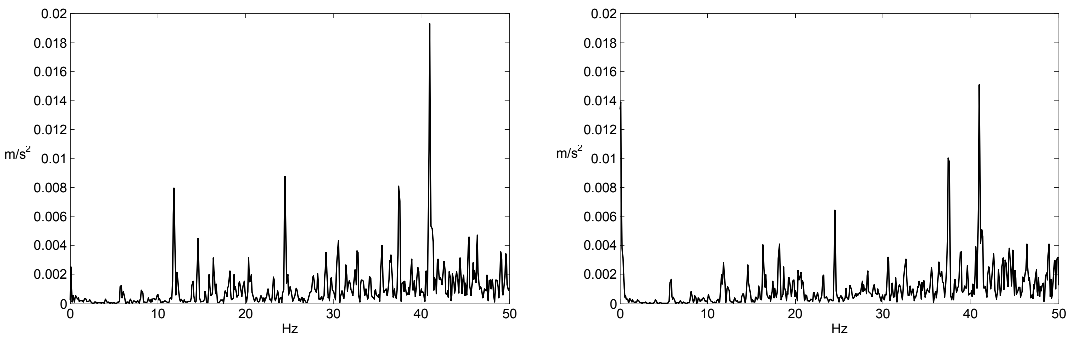

Figure 76. Vibration spectrum measured at the bearing houses (Tending side left, Drive side right).

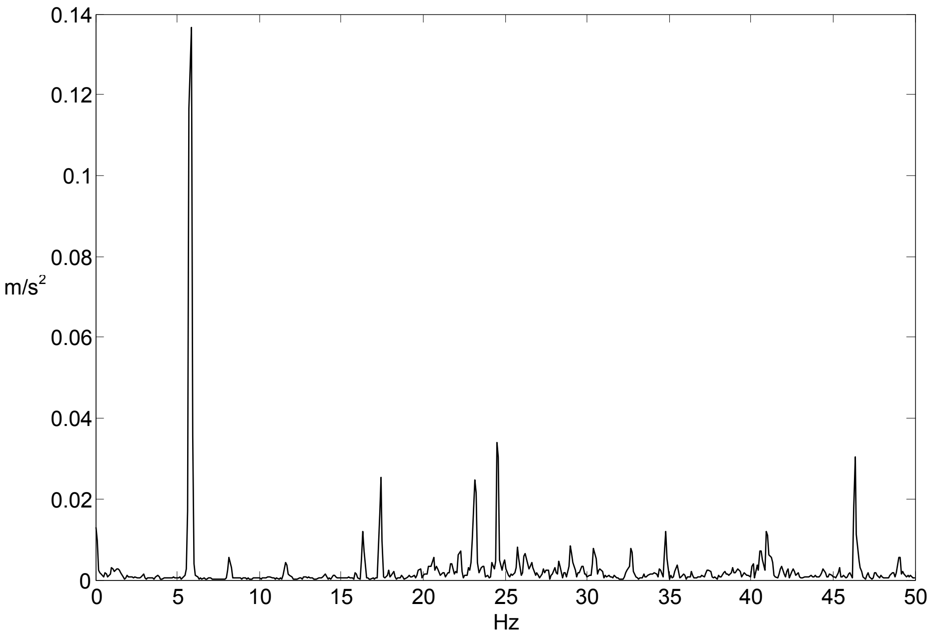

Figure 77. Vibration spectrum of the slide pad measurement.

Immediately after a web break the runout was measured at the centre cross section of the roll when the nip was just opened to see if the paper web has some effect on the runout (Figure 78).

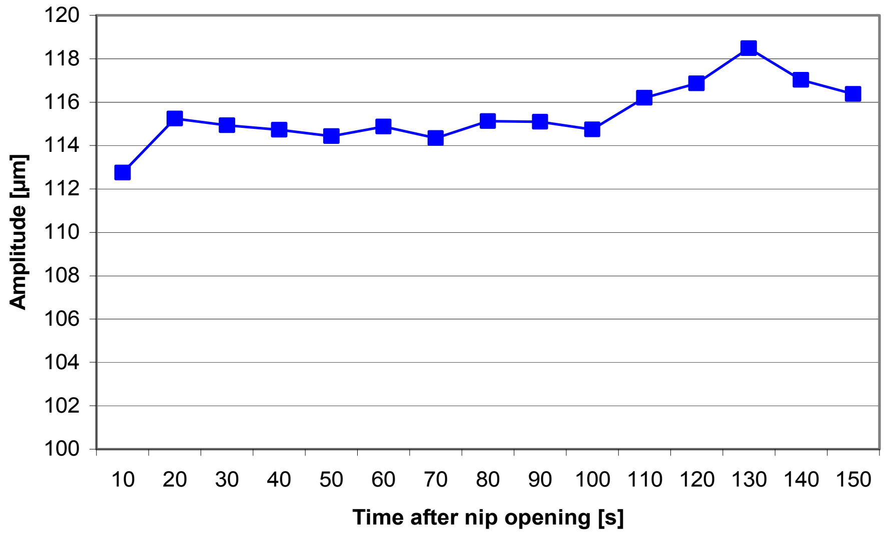

Figure 78. Runout at the middle of the roll after web break.

During the shutdown of the paper machine the runout was first measured at two different running speeds (616 and 1196 m/min) (Figure 79). The temperature of the heating oil was 50 °C.

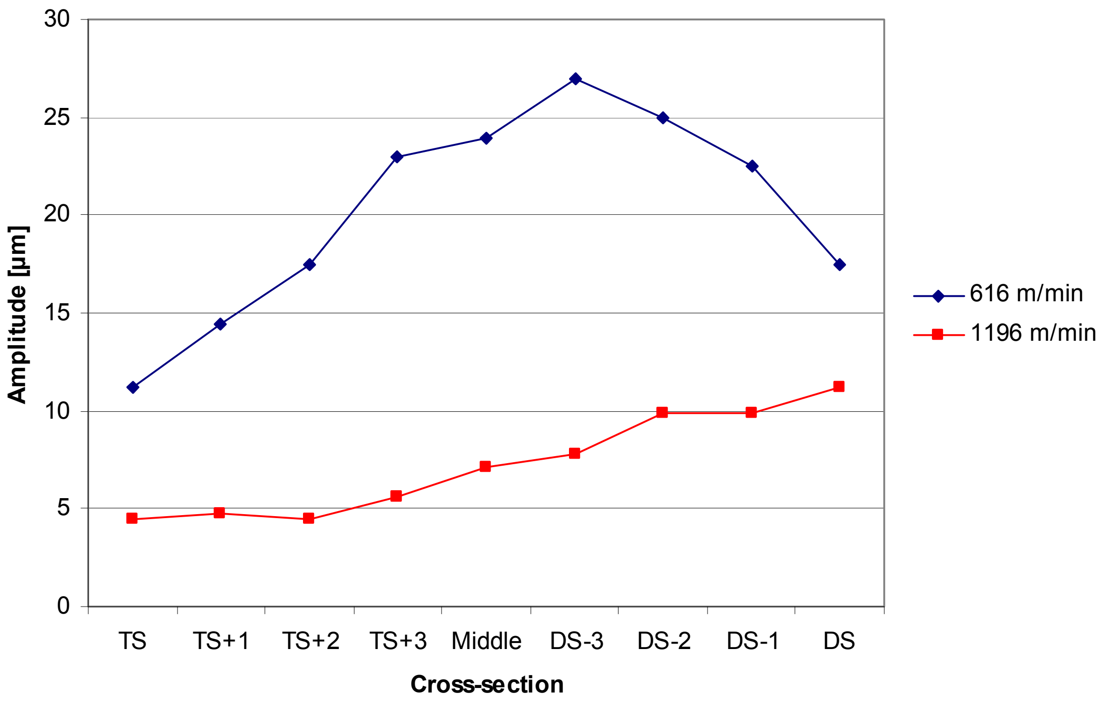

Figure 79. The first harmonic component of the runout of the thermo roll at different running speeds.

The runout of the thermo roll at different temperatures of the heating oil is represented in Figure 80. The runout was measured in nine cross-sections except with the last measurement (220 °C) where there were only five cross-sections measured. The running speed of the thermo roll was 1196 m/min. Cross-section 1 is at the end of the tending side of the roll, 5 at the centre of the roll and 9 at the end of the drive side of the roll.

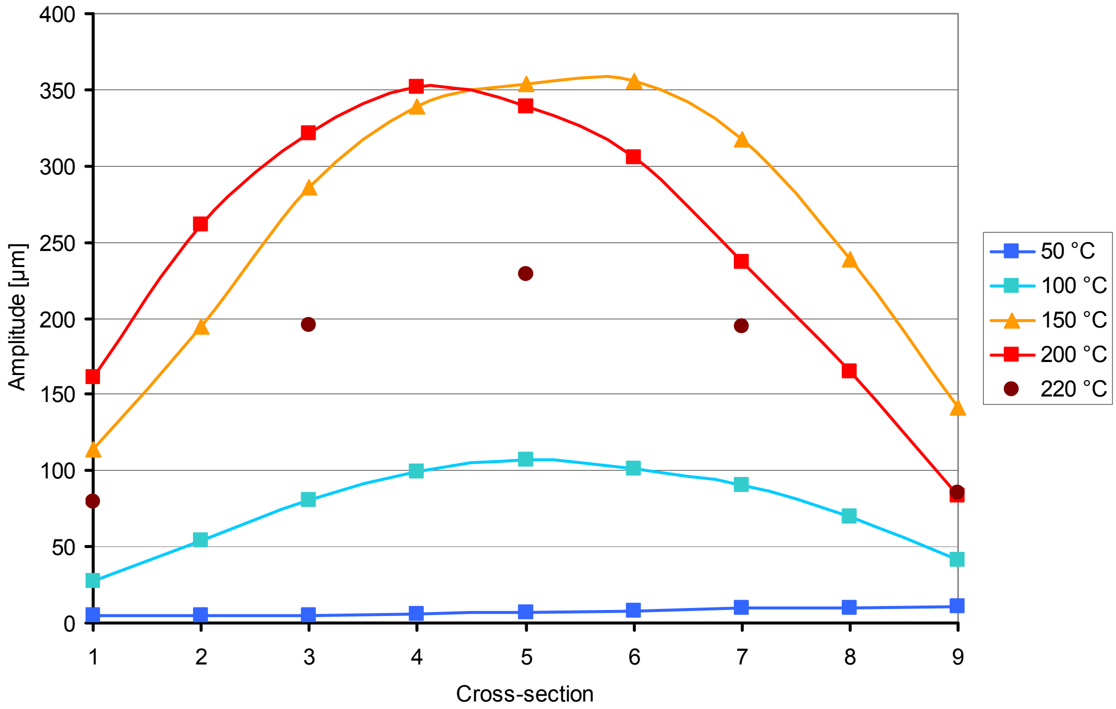

Figure 80. The runout of the thermo roll at different temperatures of the heating oil.

The amplitudes of the 1st harmonic of the runout are presented in Table 5. Due to the schedule of the maintenance break, the number of measured cross-sections was limited in the last two measurements. The variation in the amplitude of the 1st harmonic component during the time lapse of the measurement is shown in Figure 81 and the phase in Figure 82.

Table 5. Amplitude (µm) of the 1st harmonic of the runout at different temperatures.

	Temperature [°C]					
Cross-section	50	100	150	200	220	175
1	4.4	28	110	160	80	
2	4.7	54	190	260	-	
3	4.5	81	290	320	200	
4	5.6	100	340	350	-	
5	7.2	110	350	340	230	190
6	7.8	100	360	310	-	
7	9.9	90	320	240	190	
8	9.9	70	240	170	-	
9	11	41	140	84	86	

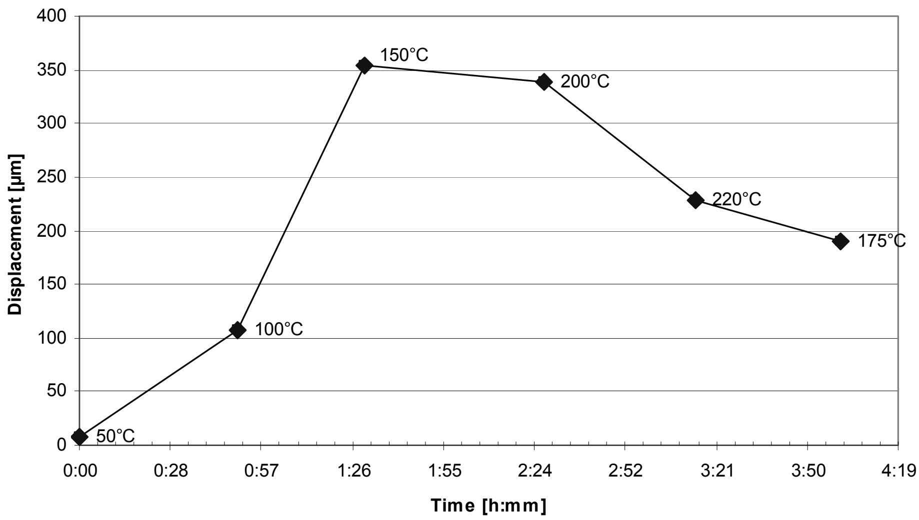

Figure 81. The amplitude of the 1st harmonic component of runout at the middle cross-section of the roll at different temperatures.

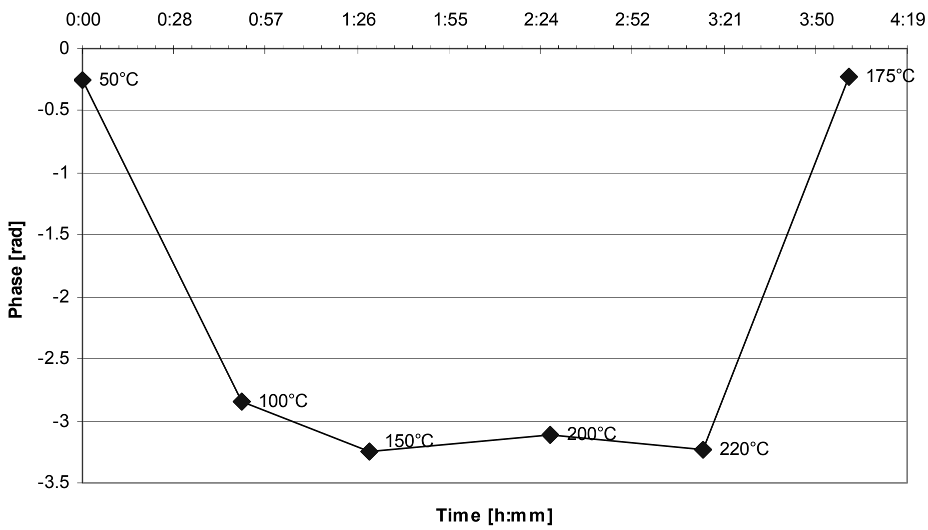

Figure 82. The phase of the 1st harmonic component of runout at the middle cross-section of the roll at different temperatures.

Thermal expansion of thermo roll

Case 2: Off-line multinip calender with forged steel thermo rolls

The target of this measurement was to find out the bending and thermal expansion of forged steel thermo rolls in a multinip calender. The temperatures of the inlet heating oil varied from 110 to 220 °C in a way that the top rolls in the line were the hottest. The 1st harmonic components of the runout of the thermo rolls at nine cross-sections are represented in Figure 83. Figure 84 and Figure 85 show the harmonic components 12 and 24 which could show if there was deformation on the surface of the rolls at the frequency of the heating bores (24 bores).

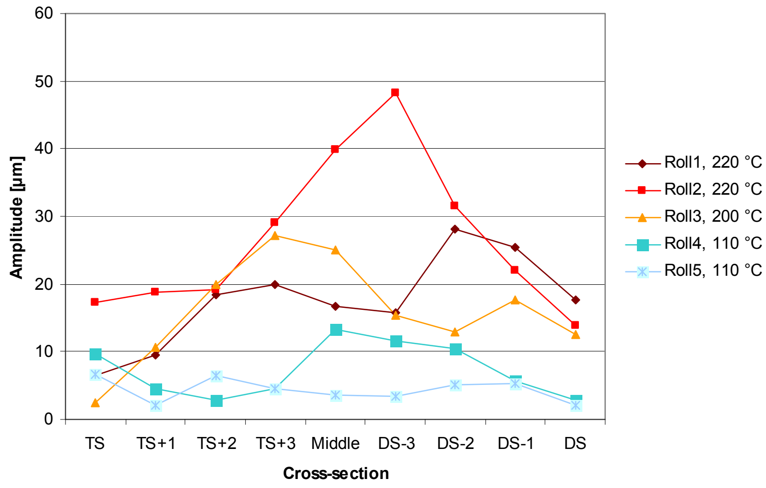

Figure 83. The 1st harmonic component of the runout.

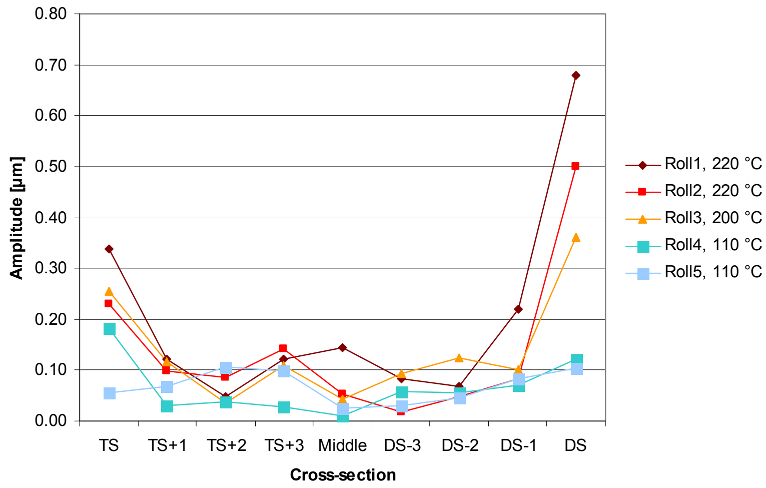

Figure 84. The 12th harmonic component of the runout.

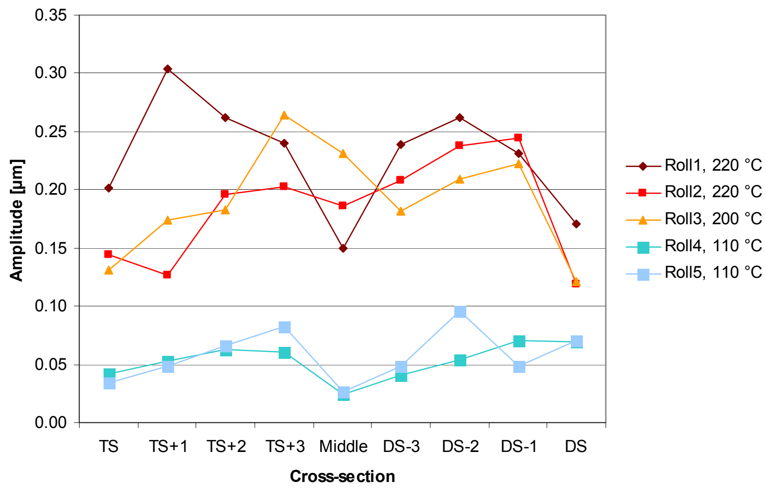

Figure 85. The 24th harmonic component of the runout.

Thermal expansion caused by the peripheral bore layout is evident on the 12th harmonic at the end of the roll with the high temperature rolls (Figure 86) and on the 24th harmonic with the high temperature rolls (Figure 87).

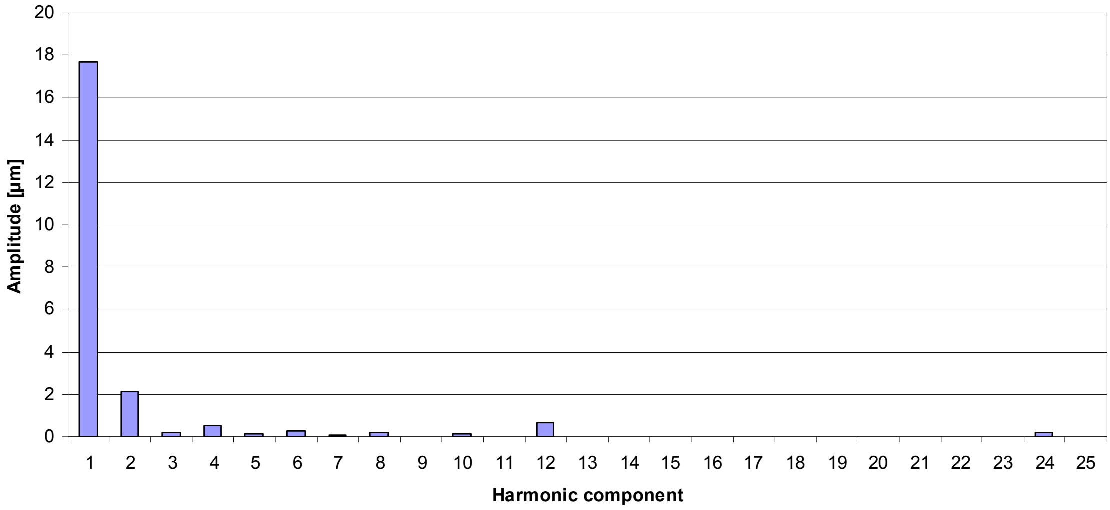

Figure 86. Harmonic components of the runout of the Roll 1 at the drive side end.

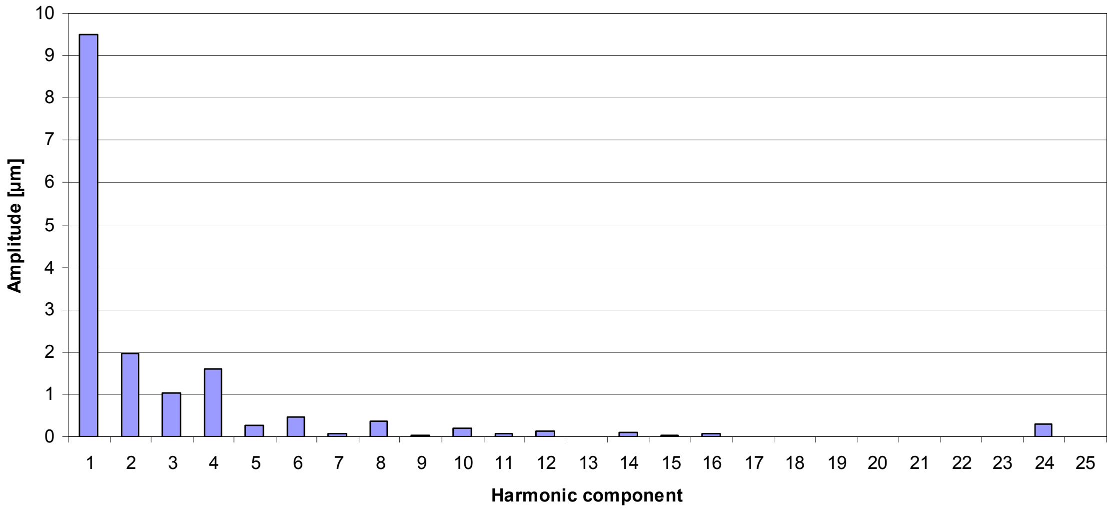

Figure 87. Harmonic components of the runout of the Roll 1 at the cross section "TS+1".

Case 3: On-line multinip calender with cast iron thermo rolls

The target of this measurement was to find out the effect of heating on the runout of an oil-heated, peripherally bored cast iron thermo roll in an on-line multinip calender. The thermo roll had 32 peripheral bores.

In the first measurement the runout of the roll was measured nip open at the normal running speed after the roll had cooled down during the maintenance break. Secondly the runout was measured during the papermaking process with the temperature of the heating oil raised to 257 °C. Comparisons of these measurements are presented in Figure 88 for the first 5 harmonic components and in Figure 89 for the harmonic components 30…34.

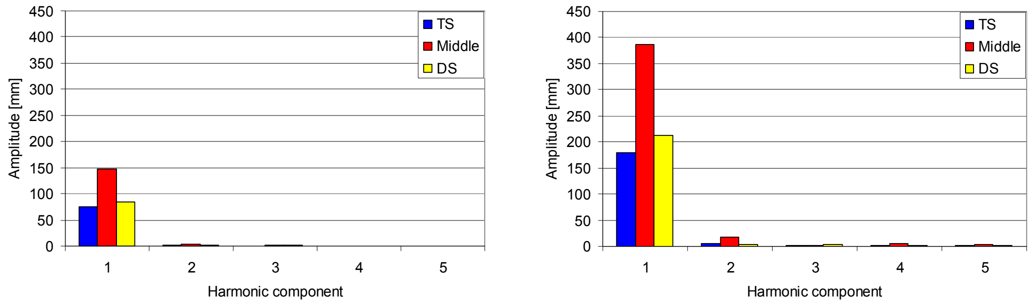

Figure 88. The amplitudes of the first 5 harmonic components of thermo roll runout measured at three cross-sections while the nip was open (left) and during process (right).

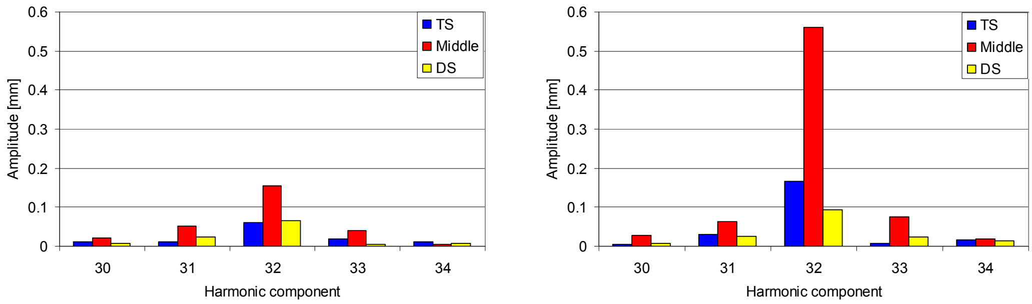

Figure 89. The amplitudes of the harmonic components 30…34 of thermo roll runout measured at three cross-sections while the nip was open (left) and during process (right).

Figure 90 shows the result of the Tapio Paper Machine Analysis of thickness variation. The thickness variation is represented in the frequency domain. Figure 91 is a closer look at the lower frequencies near the rotation frequency (8 Hz) of the roll. Figure 92 shows the spectrum near the frequency of the peripheral bores (32 · 8 Hz =256 Hz). Figure 93 shows the gloss variation in the finished paper.

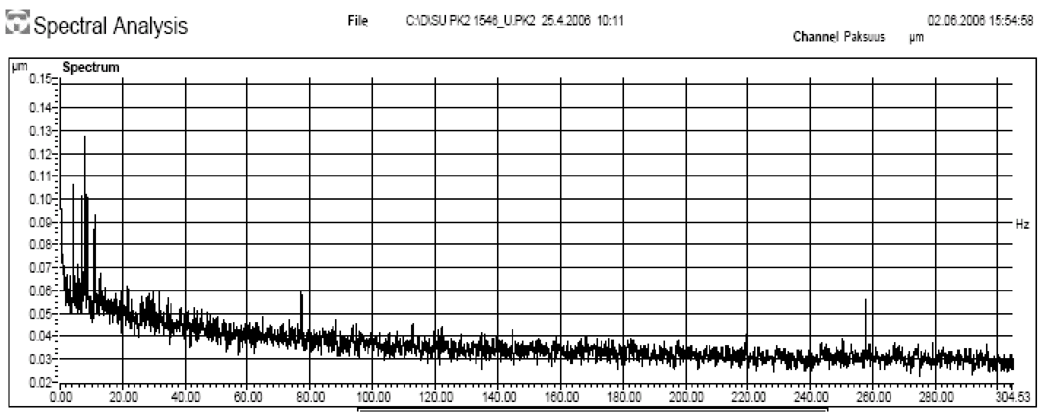

Figure 90. Tapio Paper Machine Analysis of thickness variation.

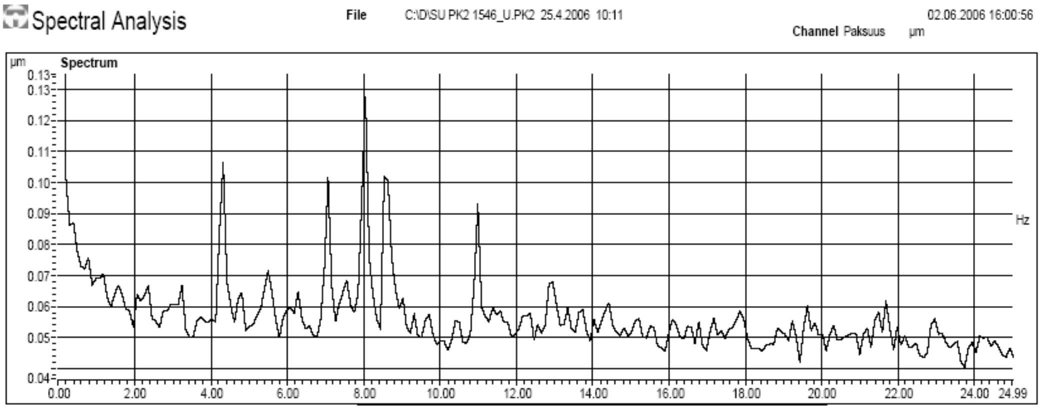

Figure 91. Tapio Paper Machine Analysis shows thickness variation in the range of the rotation frequency of the thermo roll.

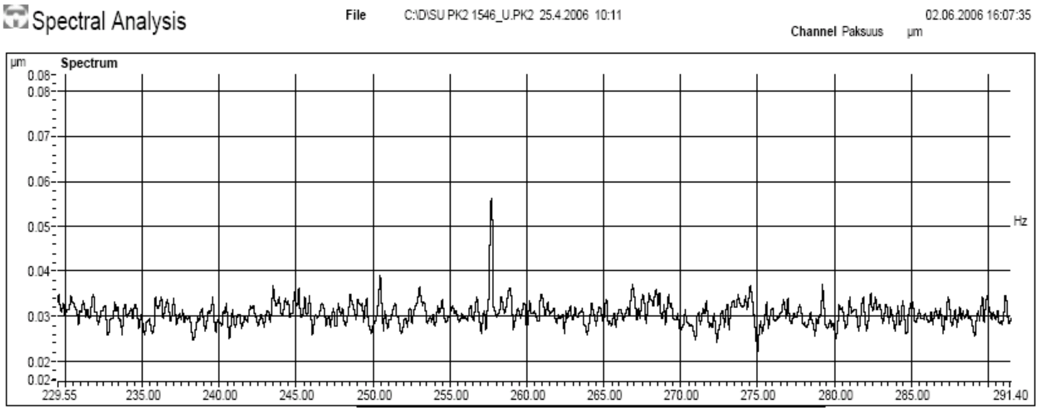

Figure 92. Tapio Paper Machine Analysis shows thickness variation in the range of the frequency of the peripheral bores of the thermo roll.

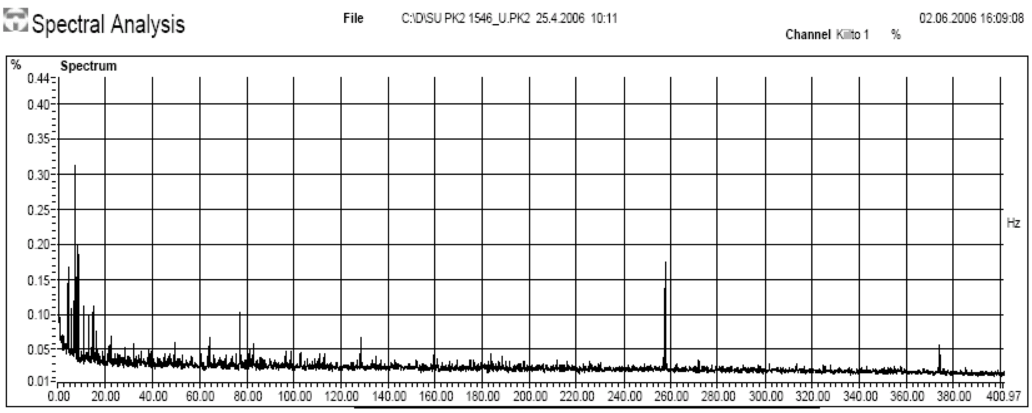

Figure 93. Tapio Paper Machine Analysis of gloss variation.

5 Discussion

5.1 Laboratory measurements

5.1.1 Disk measurement

The roundness profile of the test disk cannot be compared directly with the runout measurements because the runout is always a combination of the geometry of the target and the movement of its centre. Another problem with the test disk is the relative lightness and elasticity of the supporting structure. As a contact based method the slide pad measurement will inevitably affect the rotation of the disk to some extent. The movement of the rotation centre will be different from that of a non-contact method. Yet another problem, when trying to find out the absolute accuracy of the method, is the fact that the reference measurement should be done simultaneously at the same measurement location as the slide pad measurement, which is almost impossible to implement in practice.

The movement of the rotational centre combined with the geometrical shape of the target makes the runout to appear slightly different at different locations. Even the measurement at the opposite direction does not guarantee the uniformity of the results. Figure 94 shows a runout curve measured with an eddy current sensor alone opposite to the slide pad measurement location (red line), simultaneously with slide pad at opposite location (blue line) and alone at the location where the slide pad measurement is done (green line). It can be seen that there are slight differences between the measurements. However, as can be seen in Figure 95, the differences between the lower harmonic components are very small, less than 1 µm.

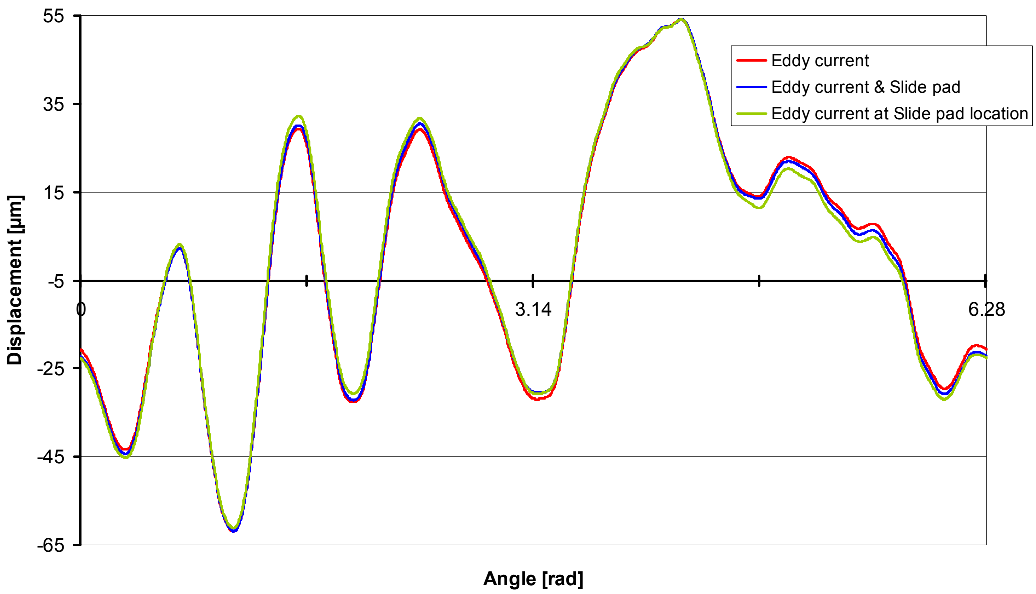

Figure 94. Runout of the test disk measured with eddy current sensor at different locations.

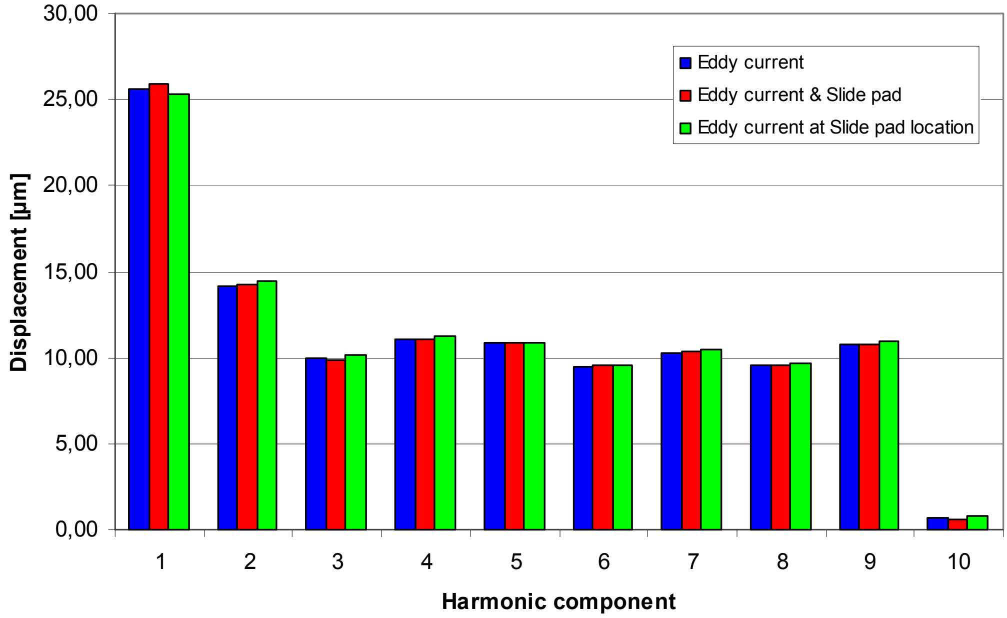

Figure 95. Harmonic components of runout of the test disk measured with eddy current sensor at different locations.

The test disk was used because of its known shape with the distinctive lower harmonic components. The lowest 9 harmonic components of the roundness profile are clearly detectable in the runout measurement and they actually dominated the runout because the eccentricity of the disk in the lathe was minimal and it was well balanced. The error movement of the lathe spindle seemed to be very small. Therefore it is, in practice, acceptable to compare the runout measurement with the roundness profile and also compare different methods with each other.

The measurement with the eddy current sensor in the roundness measurement system indicated that the eddy current sensor is applicable to the runout measurement of the disk. The comparison with the LVDT sensor supported this. Differences between the methods are within the measurement accuracy. The rotation direction and rotation frequency has no effect on the result. The small rise in the first harmonic (Figure 61) is most probably caused by the unbalance of the slightly eccentric disk. The measurements also showed the inconveniencies of these two methods. The eddy current probe must be calibrated *in situ* to the non-moving target surface at a very close proximity. The LVDT sensor can only be used at low rotation frequencies and even then the warm-up of the probe or the target surface causes drift to the result (Figure 60). Both sensors need a fixture to support the device and to bring it near to the surface.

The slide pad measurement gave very reproducible results at different speeds (Figure 62). The deviation was largest at lower frequencies, especially in the 1st harmonic component. There may be several reasons for this. The own movement of the measurer will be seen at low frequencies. The response of the accelerometer at low frequencies is not as good as it is at higher frequencies. A change in friction between static and kinetic friction, called stick-slip, causes erratic behaviour at slow sliding speeds. This can be seen at slow speeds as a difficulty to hold the slide pad steadily on the surface. The error in the speed measurement has a higher influence on the result at lower frequencies. There are also some harmonic components that have a slightly increased level of variance. They may be related to the resonance frequencies of either the disk setup or the measuring device itself. For example, the 6^{th} harmonic component at the rotation frequency of 9.0 Hz and the 3^{rd} harmonic component at the rotation frequency of 18 Hz have the same absolute frequency of 54 Hz. This could indicate the presence of a resonance frequency at 54 Hz. There is always a possibility of a human error as the test disk is narrow compared with the slide pad and it was difficult to hold the device on the surface steadily for a long period. The influence of the measurer is difficult to confirm because it is not easy to keep the device on a moving surface with exactly the same grip and force repeatedly.

The comparison between the slide pad and eddy current measurements (Figure 64 to Figure 67) shows that the differences between the methods were small, within a few micrometers, for the most of the harmonic components. The shape of the displacement curve as a function of the circumferential angle (Figure 68) shows that the phase of the runout is measured correctly. The influence of the deviation in the first harmonic component can be seen in the displacement curve especially at the lower rotation frequencies (2.2 and 4.5 Hz). Otherwise the displacement curves are highly uniform.

5.1.2 Test roll measurement

The shape of the measured roll cross section is strongly elliptic (2^{nd} harmonic). On the higher harmonics there can be seen on both measurements a slight rise of the 40^{th} harmonic with an amplitude of 2.5 µm (Figure 71). This is consistent with the shape that was machined on the surface. A roll resonance frequency is clearly visible in the runout measurement in the form of the rise of certain harmonic components at specific rotation frequencies (Figure 72). Based on the 4^{th} harmonic component, it can be estimated that the resonance frequency is in the region of 16 Hz. The same response can be seen in the 3^{rd} harmonic component in the rotation frequencies of 5.1 and 5.6 Hz as well as in the 2^{nd} harmonic while the speed increases to 7.2 Hz. Higher rotation frequencies could not be measured.

The result of the slide pad measurement differs from the eddy current measurement especially at low rotation frequencies. The result is also slightly biased; the slide pad method gives higher values for runout. Potential causes for this discrepancy are different measurement angle and error in calibration of the eddy current sensor. The eddy current probe was installed at the slide of the grinding machine using a magnetic fixture which made it susceptible to external vibrations. The test roll was made of a scrapped workpiece with fairly inhomogeneous shell structure. The shell thickness, for example, varied significantly.

5.2 Measurements in paper mills

The measurements in the paper machines could clearly verify the phenomena that have been described in the literature. Both the bending of the thermo roll and so-called polygon-effect were detected and measured.

5.2.1 Case 1: On-line soft calender

The measured thermo roll has a significant bend during the process (Figure 73). As could be expected, the runout has its maximum at the middle of the roll and the minimum at the ends. The phase shows that the bending is not quite linear but a little “S-shaped” in the lengthwise direction. The nip contact does not seem to have a great influence on the bending. The runout of the roll is fairly constant both in the direction of the nip and perpendicular to it. Even after the opening of the nip, the runout does not increase remarkably. A slight increase in the first harmonic of the runout after the web break can be seen (Figure 78) indicating a possible effect of the cooling by the paper web during the process.

The vibration measurement of the roll support (Figure 76) does not give much information about the roll bend. The first harmonic component can be detected but the amplitude is very low. This may be due to the successful balancing of the roll. In a typical balancing procedure the target is to minimise the force response at the roll ends. A runout measurement at the middle cross-section of the roll would give much better information (Figure 77).

The measurement at two different speeds (Figure 79) shows that the runout of the roll is actually diminished at a higher running speed which indicates that the roll is balanced at the running speed. There is no notable unbalance in the roll when it is cooled down. When the roll is heated, it bends strongly (Figure 80). The runout increases as the temperature rises as expected. As the temperature rises, the bending increases up to 354 μm while the phase remains almost constant. After that, at 220 °C, the runout of the roll decreases to 228 μm. At the same time, the phase of the runout turns about 180 degrees. This may be due to the thermal balancing of the roll which is implemented by adjusting the heating flow in each peripheral bore using valves at the end of the roll. This arrangement combined with the relatively slow convection of the heat and non-concentric zones of cast-iron may cause the uneven bending of the roll until the temperature became even throughout the roll (Figure 96).

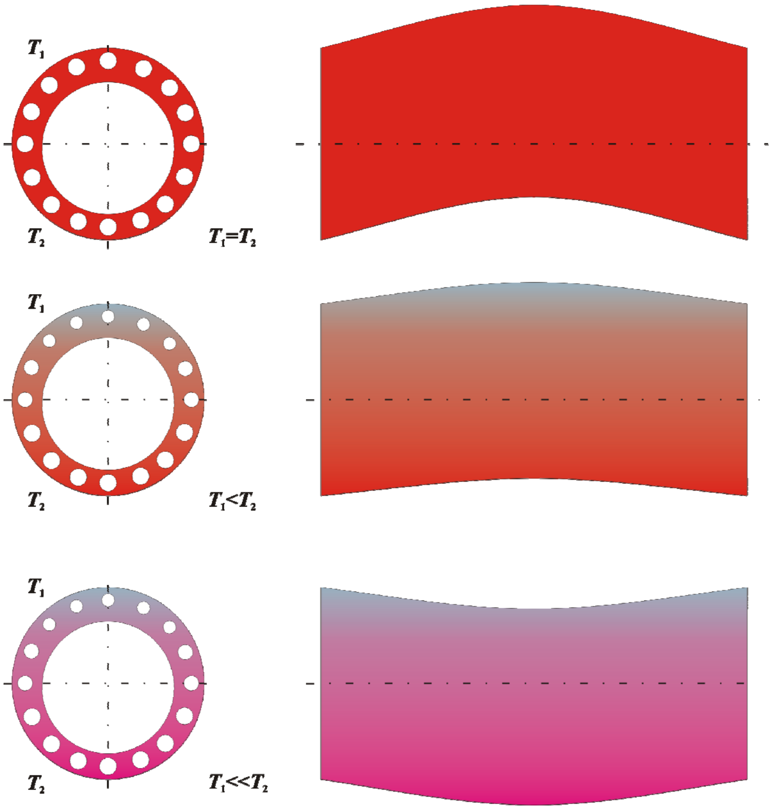

Figure 96 The behaviour of the roll under increasing temperature. Original (up), corrected (middle) and start-up (bottom) situations.

Originally, the roll may have bent in a certain direction when hot (upper illustration in Figure 96). This could have been caused by an uneven thickness of the surface layer (white iron), for example. If this problem was solved by choking the flow of the heating fluid on one side of the roll (middle illustration), the roll would straighten when hot. It is possible that when the paper machine was started after a service break and the temperature of the roll increased, the flow of the heating media was higher on the other side of the roll (bottom illustration). This may have caused the roll to bend in that direction during the heating. When the temperature distributed evenly on the roll shell, the roll straightened again.

5.2.2 Case 2: Off-line multinip calender

The bending of the thermo roll is relatively small; the maximum value of the amplitude in the middle of the second roll is less than 50 µm (Figure 83). This may be due to the homogenous forged steel structure; even at high temperatures the rolls keep their shape. The polygon effect can be clearly detected. It is bigger at the ends of the high temperature rolls (Figure 84) which may be caused by the heat input at the end and by the fact that the paper web takes away some of the heat except for the end zone which therefore is warmer than the rest of the surface ("oxbow effect" (Zwart 1992)). The number of heating bores in the high temperature rolls can be seen in the 24th harmonic component of the runout (Figure 85). The maximum values of the runout are, however, very small.

5.2.3 Case 3: On-line multinip calender

It is evident that the roll bends strongly in the process temperature (Figure 88). Other harmonic components are almost non-existent. In the nip open situation the maximum value of the amplitude of the runout is 147 µm and during the process 386 µm. There is a slight but clear rise in the 32^{nd} harmonic component (Figure 89) which is the number of the peripheral bores.

Both the bending of the roll (1^{st} harmonic) and the peripheral bores (32^{nd} harmonic) can be seen as a thickness and gloss variation of the finished paper near the frequencies of 8 Hz and 256 Hz. There were a total of four nearly identical thermo rolls in the calender and the paper was still modified in the process after leaving the measured thermo roll. This makes it impossible to state definitely that the variations in the finished paper were caused by the measured thermo roll.

5.3 Applicability of the method

The tests proved that the slide pad method has many advantages compared with the traditional displacement measurement methods. The device is easy and fast to take into operation. No calibration for a specific target is needed. The manoeuvrability of the device makes it possible to measure several locations and directions in a short period of time. In some cases, this makes it possible to replace multiple conventional sensors with a single device, assuming that the measurement conditions remain unchanged between the measurements. Measurements can also be made for targets that would otherwise be inaccessible. Prerequisites for the measurement are that the surface of the roll must be accessible and the measurer must be able to get to a distance where the target can be reached with the extension handle. Depending on the circumstances, the distance is 1 to 2 m. The measurement can be made, for example, from the working platform or service elevator.

This study showed that the results achieved with this method are consistent with theories and expectations about the behaviour of the rolls. The rolls bent when heated and typically the bending increased as the temperature was raised. The bending was smaller with the forged steel rolls indicating a more homogeneous structure. The thermal expansion, polygon-effect, caused by the higher than surrounding temperature of the peripheral bores, was clearly detected, as well as the temperature dependency of the phenomena.

The tests indicated that the accuracy of the method is in the micrometer scale when used by an experienced measurer. The accuracy is adequate for the purposes the method is planned for. Notably, at the rotation frequencies of the rolls typical in the paper industry, i.e., from 5 to 10 Hz, the accuracy is good. However, the measurer must have some experience to be able to make reliable and reproducible measurements. During and after the measurement the validity of the data must be verified. This can be done, for example, by using possible other measurements (such as condition monitoring system and quality control measurements) and analysis of the data. The more there are deviations in the measurements, the more problems there may be. It is up to the measurer to observe the results and find out any possible incoherencies. In the laboratory it is possible to compare results with other measurements but in the process environment there is usually only one chance to do the measurement. However, if possible, the measurements should be repeated at least a few times. Because the method is based on the concept that the apparatus is held and supported by hand of the measurer there will always be a chance for human error.

5.4 Applications of the method

The slide pad method makes it possible to measure the movement of the whole roll body instead of the roll support alone. This opens new possibilities to study the behaviour of the rolls during the process. *In situ* runout measurements make it possible to detect and understand the dynamic behaviour of the rolls and the causes of it. Mathematical models can also be used for that purpose but as the demands increase, the more complicated the models become. The theoretical models depend on many physical parameters and their validation and verification requires measurements of the real world systems. There are also variables that cannot be measured reliably, such as the surface temperature of a fast rotating roll. With the slide pad method, however, it is possible to measure the effect of the temperature on the roll runout.

5.4.1 Problem solving

One of the most important fields of application for the slide pad method is problem solving. The problems in paper machines are usually caused by unwanted vibrations which have an effect on both the paper quality and the runnability of the machine. The method can be used for detecting the cause for these vibrations. The measurement of the roll body runout provides more information than an analysis based on the roll support measurements. Speed ramps, i.e., gradual or continuous increase or decrease of rotation frequency, can be used to detect possible unbalance of the roll and thermal ramps to study the bending of the roll. Speed ramps can also be used to find out the resonance frequencies of the roll system. By runout measurement it is possible to find out form errors, such as ovality or barring, in the rolls. When doing the runout analysis it is, however, important to notice the different causes for runout to avoid wrong conclusions.

5.4.2 Online roundness measurement

Perhaps the most interesting geometrical property of the roll would be the run-time roundness profile. Knowing the operational shape of the roll, the profile of any chosen cross-section, would give abundant information about the properties and the behaviour of the roll. It would be useful when trying to improve the behaviour of the roll and thereby the performance of the paper machine. The slide pad measurement could be used for a roundness profile measurement of roll which in some cases would be more useful than a mere runout measurement. Presently the roundness of a roll can only be measured in the workshop.

In the roundness measurement the movement of the workpiece is separated from the surface profile. Conventionally this is done utilising a precision spindle either supporting the probe or the table upon which the workpiece stands (Figure 97).

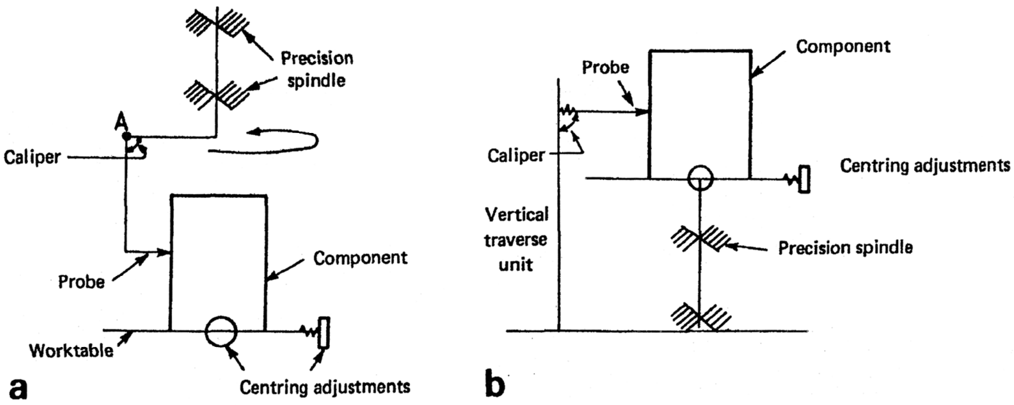

Figure 97. Conventional methods of measuring roundness using rotating probe (a) and rotating table (b)(Whitehouse 1987).

For targets that are too large or heavy to be measured using precision measurement systems, the measurement of roundness usually requires the use of more than one probe and the measurement of runout at different angles. There are an abundance of studies of this subject (Ozono 1974, Gao 1997, Fujimaki 2008). The method usually employs three fixed probes at specific angles and the roundness profile is calculated from the runouts of these probes. Kato et al. (1990) studied a method which employed only one probe that was moved around the workpiece to make several measurements at different angles. The results were in good agreement with those measured by using a roundness measuring system. With the slide pad it would be possible to measure the runout at different angles (Figure 98) if the behaviour of the roll remains unchanged between the measurements.

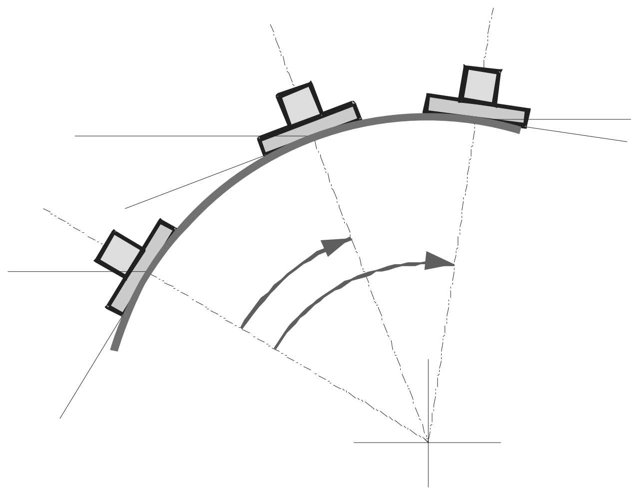

Figure 98. The slide pad at different measuring angles.

5.4.3 Balancing

The balancing is based on the measurement of some quantity related to the unbalance of the workpiece. Usually, the measurement is made at the support of the roll and the forces caused by the unbalance are minimized at the support by adding balancing weights to the ends of the rolls. This may still leave significant displacement at the centre of the roll. With the slide pad it is possible to measure the once-per-revolution amplitude, i.e., the 1st harmonic component, and phase of the runout, which are needed for the balancing, in more than one or two balancing planes. Even more useful is the possibility to balance the rolls on their operational positions and at their actual support. The balancing would then be optimal in runtime conditions.

Thermal balancing

The thermo rolls bend to some extent during the operation due to the heating. It is possible to control the roll bending by controlling the flow of the heating media. With the slide pad it is possible to measure the *in situ* bending of the roll at the process temperature. Presently, it is done at the workshop.

5.4.4 Form compensation

If the roll is bent or has some other geometry errors during the operation, the shape can be corrected by machining. This requires the measurement of the operational shape which can be done with the slide pad method. If the shape is corrected, for example by grinding, it is necessary to be able to measure the needed amount of correction and especially the phase of it.

Hot grinding

It is possible to detect the polygon-effect using the slide pad method. Although the polygon-effect is usually so small that it will probably not cause quality problems to the paper, it is a possible source of excitation of vibrations. The undulation may be difficult to remove even by 3D-grinding but if the roll was ground while it is hot, it could be possible to minimise the polygon-effect. In a patent (von Schweinichen et al. 2006) a manufacturing method for the calender thermo roll is presented where the roll surface is treated and the roll balanced while hot. According to the patent, when the surface treatment and balancing of the rolls is carried out at a temperature corresponding to the operating temperature, heat-caused deformations of the rolls during operation are prevented. The heat transfer of a roll operating at increased operational temperature onto a paper web can be simulated by cooling the roll surface. The method includes also determining a profile of the roll in the hot state and transferring it as a negative profile onto the roll while the roll is in the workshop temperature.

5.5 Suggestions for further development

To ease the assembly, the structure of the slide pad is now such that the accelerometer is attached upside down to the “ceiling” of the slide pad (Figure 99). This makes it prone to vibrations. The structure may act as a spring and affect the measurement. This may even explain some of the variations in the disk measurements. It would be relatively easy to modify the structure by attaching the accelerometer directly to the base plate. In any case, the resonance frequencies of the structure of the device should be determined.

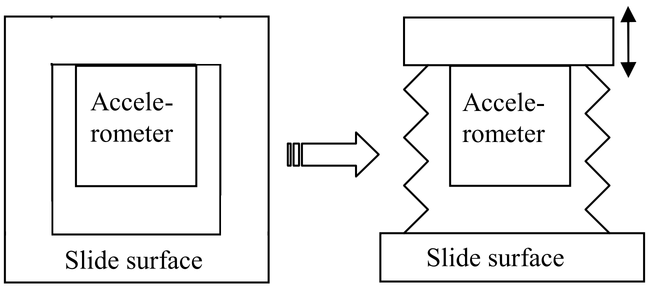

Figure 99. Structure of the slide pad may act as a spring.

The importance of the structure to the measurement comes evident considering the effect of the heat to the old construction (Figure 30). High temperature rapidly changed the properties of the structure deteriorating the result.

To study the movement and alignment of the slide pad relative to the target surface during the measurement, an additional accelerometer perpendicular to the current one can be mounted on the device. This will provide more information for the estimation of the accuracy of the method.

The analysis of the measured data is based on the averaging and synchronisation of the measurement to one revolution of the target. At the present, the acceleration data are averaged in the time domain and the averaged data are then double integrated to displacement. If the rotation frequency of the target varies during the measurement, the number of measured points per rotation varies as well. Therefore the data must be resampled before averaging to obtain the same number of points per rotation. A more accurate method would be to perform the integration of the acceleration data on each rotation separately and then do the averaging in the frequency domain for the harmonic components of the consecutive rotations.

To further add confidence to the method, a reference measurement in the process conditions should be done. The target should be chosen so that the reference measurement is possible. The target should be easily accessible, preferably from the plant floor so that there is no need for vibration prone supports. A capacitance based method could be appropriate for the reference measurement. The movement of the reference sensor itself should be measured in any case.

Some of the variables related to the hand held method could be further studied. The effect of the variables, such as the holding force and the movement of the slide pad during the measurement, could be analysed using a “mechanised measurer” to eliminate the human influence on them.

6 Summary

In a paper machine there are hundreds of rolls for various tasks. In the calender the paper web is pressed in the nip, i.e., between a pair or multiple pairs of rolls, under heavy load and high temperature to give paper desired structure and finish. The temperature in the nip is controlled using heated rolls, thermo rolls. Geometry and rotational error of the rolls will be duplicated on the paper web and may be a cause for several different calendering problems like profile problems (gloss, caliper, moisture) and barring. Also, as the machine speeds and widths are increasing, even higher demands are made on the dynamic properties of rolls. Besides the quality problems, unwanted vibrations cause runnability problems.

Errors in the roll geometry and rotation appear as a runout. The runout is a very practical and directly measurable parameter which is defined as the movement of the surface of a rotating object in relation to a fixed datum. The motion of a surface is a combination of both the physical properties of the target, such as eccentricity or surface geometry, and vibrations. The runout of a thermo roll is caused, for example, by roundness error, eccentricity, unbalance, initial curvature, uneven thermal expansion and errors in bearing.

The behaviour of the roll is highly dependent on the process parameters and the operational environment. Some of the most important factors affecting the behaviour are

- rotation frequency
- temperature
- support

However, the measurements of the rolls are usually done in the workshop conditions during the normal maintenance operations. The roundness measurement of the roll, for example, is typically done in the grinding machine at a low speed. Only using special workshop test equipment the dynamic behaviour of a roll can also be measured at higher speeds. High temperatures can not be reproduced in the workshop and the rolls are usually mounted on the support of the machine tool. With the nip rolls, the contact with the other roll has its own influence in the behaviour. Thus, to find out the true dynamic behaviour of the rolls requires that the measurements should be done in the real operating conditions during the papermaking process. Typical, indirect measurement of the vibration through the bearing houses does not provide enough information about the behaviour of the roll body during the operation and about the causes for the vibration.

In the *in situ* measurements the main difficulties arise from the support and fixture of the sensors. The sensor must be placeable close to the surface of the roll and yet the support of the sensor must be rigid. Some sensors also require on-site calibration to the measured surface. The vibrations conducting through the sensor support may distort the signal which calls for actions to compensate the own movement of the sensor from the signal. High surface velocities restrict the usage of contact sensors and combined with the shiny roll surface makes also the laser optic methods practically unusable.

In this study, a device and a method for the *in situ* measurement of a roll shell runout based on the radial acceleration measurement of the surface was described. The objective of this research was to confirm experimentally that with the developed device and method it would be possible to measure the runout of the paper machine rolls in the process conditions with an adequate accuracy. A number of measurements were done to demonstrate the applicability of the method. The method was used to make *in situ* measurements of the phenomena in the rotating rolls that were difficult or impossible to measure earlier.

The device consists of a polymer based slide pad which is in contact with the moving surface, an accelerometer attached to the slide pad and an extension handle for the user to hold the device on the target surface. During the measurement, the measurer positions the slide pad on the surface of the target and keeps the probe still with a light pressure for the duration of the measurement. The acceleration signal, along with a trigger signal, is collected using a PC-based data acquisition system.

The analysis of the measured data is based on the averaging and synchronisation of the displacement to one revolution of the target. As a result of the trigger analysis, the rotation frequency of the target and an average number of measured points per revolution are found out. The acceleration data are divided to sequences of one revolution using the trigger signal. To be able to average the data that is measured during consequent revolutions, the number of points per a revolution should be the same. Therefore the data are resampled and a certain number of equally spaced points are interpolated for each revolution. Finally, the averaged data are integrated twice using FFT to get the displacement signal. FFT is also used to analyse the harmonic content of the signal.

A series of laboratory and *in situ* measurements were done to study the performance of the method in measuring the runout of cylindrical and rotationally symmetrical objects. First, a series of laboratory measurements for a workpiece with a known geometry were done to study the accuracy and functionality of the method. A test disk was measured, in addition to the slide pad device, with a Taylor Hobson Talyrond 31C roundness geometry measurement system, a LVDT probe and an eddy current sensor. Secondly, a series of *in situ* measurements in paper mills were done to study the usability of the method in actual cases. The objective of the on-site measurements was to find out how the calender thermo rolls behave in the papermaking process when heated. There were two main effects to look for: thermal bending and possible undulations on the roll surface in the locations where the heating bores exists.

The slide pad measurement of the test disk gave very reproducible results at the different speeds. The deviation was largest at the lower frequencies, especially at the 1st harmonic component. The comparison between the slide pad and eddy current measurements showed that the differences between the methods were small, within a few micrometers, for the most of the harmonic components. The shape of the displacement curve as a function of the circumferential angle showed that the phase of the runout was also measured correctly.

The measurements in the paper machines could clearly verify the phenomena that have been described in the literature. Both the bending of the thermo roll and so-called polygon-effect were detected and measured. The tests proved that the slide pad method has many advantages compared with the traditional displacement measurement methods. The most useful benefits of the method are

- the device is easy and fast to take into operation
- no calibration for a specific target is needed
- the manoeuvrability of the device is good

It is possible to measure several locations and directions in a short period of time. In some cases, this makes it possible to replace multiple conventional sensors with a single device, assuming that the measurement conditions remain unchanged between the measurements. Measurements can also be made for targets that would otherwise be inaccessible.

The tests indicated that the accuracy of the method is in the micrometer scale when used by an experienced measurer. The accuracy is adequate for the purposes the method is designed. Notably, at the rotation frequencies of the rolls typical in the paper industry, i.e., from 5 to 10 Hz, the accuracy is good.

The slide pad method makes it possible to measure the movement of the whole roll body instead of the roll support alone. This opens new possibilities to study the behaviour of the rolls during the process. The *in situ* runout measurement makes it possible to detect and understand the dynamic behaviour of the rolls and the causes of it. The method can be used, for example, for applications related to

- problem solving in the paper quality and runnability issues
- online geometry measurement and shape correction
- balancing
- validation and verification of the theoretical models

The roll behaviour is vital information for the process development purposes. If the running speed of the machine is to be raised, it is necessary to find out the rolls that may become bottlenecks because of excessive vibration. Measurements can also be used to detect the need for roll maintenance. Information about the runtime geometry and behaviour can be used for the planning of the future maintenance operations.

References

Albrecht, A., Park, S. S., Altintas, Y., Pritschow, G., High frequency bandwidth cutting force measurement in milling using capacitance displacement sensors, International Journal of Machine Tools & Manufacture 45 (2005) pp. 993-1008, Elsevier.

Alciatore, D. G., Histand, M. B., Introduction to Mechatronics and Measurement Systems, 3rd edition, McGraw-Hill 2007, ISBN 007-125407-2.

Bishop, R. H., The Mechatronics Handbook, 2nd Edition, Mechatronic Systems, Sensors and Actuators, ISBN: 9780849392573, CRC Press 2008.

Brierley, P., Hopkins, H.G., Peel, J.D., Thermal deformations of machine calender rolls, Paper Technology and Industry, August 1977

Brüel & Kjær, Primer: Measuring Vibration, Denmark 1982.

Brüel & Kjær, Technical Review No. 2, Denmark 1987.

Cambell, W.R., Shaft Runout under Eddy Current Non-Contact Probes, Proceedings Machinery Vibration Monitoring and Analysis Meeting, April 19-21, 1983.

Castro, H.F.F., A method for evaluating spindle rotation errors of machine tools using a laser interferometer, Measurement 41 (2008) pp. 526-537, Elsevier.

Charles, J. A., Diagnostic tools for Yankee dryers, 2000 TAPPI Engineering Conference, Atlanta, Georgia, USA, September 2000.

Cotsaftis, M., Keskinen, E., Miettinen, J., Nuutila, O. & Salmenperä, P. 2005. Vibration analysis of rotors in rolling contact, 2005 ASME International Design Engineering, Technical Conferences & Computers and Information in Engineering Conference, IDETC/CIE 2005, September 24-28, 2005, Long Beach, CA, USA 1 10 p.

Doebelin, E.O., Measurement Systems: Application and Design, Fourth Edition, ISBN 0-07-100697-4, McGraw-Hill, 1990.

Taylor Hobson, Exploring roundness: a fundamental guide to the measurement of cylindrical form, Leicester: Taylor Hobson Ltd, 2006.

Flack, R.D., Rooke, J.H., Bielk, J.R., Gunter, E.J., Comparison of the Unbalance Responses of Jeffcott Rotors With Shaft Bow and Shaft Runout, Journal of Mechanical Design, Transactions of The ASME, 1981.

Fujimaki, K., Sase, H. and Mitsui, K., Effects of sensor noise in digital signal processing of the three-point method, Measurement Science and Technology 19, IOP Publishing 2008.

Gao, W., Kiyono, S., On-machine roundness measurement of cylindrical workpiece by the combined three-point method, Measurement Vol. 21, No. 4, pp. 147-156, Elsevier, 1997.

Gatzwiller, K. B., Ginn, K.B., Betts, A. & Morel, S. Practical Aspects of Successful Laser Doppler Vibrometry based Measurements, DEGA 2003.

Girão, P. M. B., Postolache, O. A., Faria, J. A., Pereira, J. M. C. D., An Overview and a Contribution to the Optical Measurement of Linear Displacement, IEEE Sensors Journal, Vol. 1, No. 4, December 2001.

Jang, G., Kim, D. and Oh, J-E, New Frequency Domain Method of Nonrepeatable Runout Measurement in a Hard Disk Drive Spindle Motor, IEEE Transactions on Magnetics, Vol. 35, No. 2, March 1999.

Jeong, G.-B., Kim, D. H., Jang, D. Y., Real time monitoring and diagnosis system development in turning through measuring a roundness error based on three-point method, International Journal of Machine Tools & Manufacture 45 (2005) pp. 1494-1503, Elsevier.

ISO 1101:2004, Geometrical Product Specifications (GPS).

Jokio, M., editor, Papermaking science and technology, Book 10 : Papermaking : part 3, finishing, Fapet, Helsinki, 1999. 361 p., ISBN 952-5216-10-1.

Juhanko, J. Dynamic behaviour of a paper machine roll, Licentiate's thesis, Helsinki University of Technology. Espoo, 1999, 82 pp.

Järvenpää, V.-M., Järvinen, V., Salmenperä, P. & Yuan, L. 2007. Experimental analysis of non-linear roll contact, Proceedings of the IMAC-XXV, A Conference & Exposition on Structural Dynamics, February 19-22, 2007, Orlando, Florida, USA 7 p.

Järvinen, V., Miettinen, J., Keskinen, E., Cotsaftis, M. and Hirvonen M. Wireless Sensing System for Modal Testing Of Rolling Cylinders. Society for Experimental Mechanics ANNUAL CONFERENCE on Experimental and Applied Mechanics, June 4-6, 2001, Portland, Oregon.

Kato, H., Nakano, Y. and Nomura, Y., Development of In-situ Measuring System of Circularity in Precision Cylindrical Grinding, Bulletin of Japan Society of Precision Engineering, Vol. 24, No. 2 (June 1990).

Kivinen, Juha-Matti, A Variable Parameter Facility for Dynamic Testing of Polymer Covered Paper Machine Rolls, Tampere University of Technology Publications 347, Tampere 2001.

Kuosmanen, P., Predictive 3D grinding method for reducing paper quality variations in coating machines. Helsinki University of Technology Publications in Machine Design 2/2004.

Kuosmanen, P. & Väänänen P., New Highly Advanced Roll Measurement Technology, Proceedings of 5th international conference on new available techniques, The world pulp and paper week, pp. 1056-1063, Stockholm, Sweden, June 1996.

Larsson, M., Engström, G., Vidal, D., Zou, X., Impact of calendering on coating structures. Nordic Pulp and Paper Research Journal, Vol 22 no.2, 2007.

Lin, J., Bissonnette, M.R., Cochard, M., New proximity probe and accelerometer for machine monitoring, Conf. Proc. IRIS Rotating Machine Technical Conference IRMC, March 10-13, 1998.

Matbase, http://www.matbase.com, 4.9.2009.

The Mathworks, Inc., Online Matlab reference, Version 7.4.0.287 (R2007a), 2007

Metso paper, http://www.metso.com, 24.6.2009.

Micro-epsilon, http://www.micro-epsilon.com, 24.6.2009.

Möhle, H., Buschmann, G., Müller, G., Vibrationen an Papierrollmaschinen, 1970.

Okuyama, E., Nosaka, N., Aoki, J., Radial motion measurement of a high-revolution spindle motor, Measurement 40 (2007) pp. 64-74, Elsevier.

Onwubolu, G. C., Mechatronics: Principles and Applications, ISBN 0750663790, 9780750663793, Butterworth-Heinemann, 2005.

Ozono, S., On a new method of roundness measurement on the three point method. Proceedings of the ICPE, Tokyo, p. 457 – 462, 1974.

Randall, R.B., Frequency Analysis, 3rd edition, ISBN 87 87355 07 8, Brüel & Kjaer, September 1987.

Rothenbacher, P., Vomhoff, E., Mass centering of chilled cast-iron rolls, Tappi journal, July 1985.

Rothenbacher, P., Vomhoff, E., Report on improved balancing methods for chilled cast iron rolls, Pulp & Paper Canada, 87:3, 1986.

von Schweinichen et al., Roll, in particular, Calender Roll, US Patent 7,018,512 B2, Mar. 28, 2006.

Shigley, J. E., Uicker, J. J. Jr., Theory of Machines and Mechanisms, McGraw-Hill 1981, ISBN 0-07-056884-7

SHW Casting Technologies, Inc., Techical Newsletter No. 7 September 2003.

SHW Casting Technologies, Inc., Techical Newsletter No. 8 October 2003.

SHW Casting Technologies, Inc., Techical Newsletter No. 17 August 2005.

SHW Casting Technologies, Inc., http://www.shwinc.com, 26.4.2009

Slocum, A., Precision Machine Design, ISBN: 0872634922, Society of Manufacturing Engineers 1992.

Smith, Graham T., Industrial Metrology: Surfaces and Roundness, ISBN 1852335076, Springer-Verlag, London 2002.

Smith, P.T., Vallance, R.R., Marsh, E.R., Correcting capacitive displacement measurements in metrology applications with cylindrical artifacts, Precision Engineering 29 (2005) 324–335.

Stachowiak, G. W., Batchelor, A. W., Engineering tribology, Third Edition, ISBN 978-0-7506-7836-0, Elsevier 2005.

Tatar, K., Gren,. P., Measurement of milling tool vibrations during cutting using laser vibrometry, International Journal of Machine Tools & Manufacture 48 (2008) pp. 380-387. Elsevier.

Taylor, James I., The Vibration Analysis Handbook, ISBN 0-9640517-2-9, VCI 2003.

Tian, G. Y., Zhao, Z. X., Baines, R. W., Corcoran, P., Blind Sensing, Manufacturing Engineer, August 1997.

Vinicki, J., Barring induced vibration, Sound and Vibration, Vol. 35, No. 9, 2001. p. 26-28, ISSN: 0038-1810.

Wang, H., Valdivia-Hernandez, R., Shaft Runout Inspection by a Fiber Optic Displacement Sensor, Fiber and Integrated Optics, Vol 14, pp. 159-169, 1995.

Widmaier, T., Salmela, T., Kuosmanen, P., Juhanko, J., Kärhä, P., Uusimäki, J., Reducing thickness variation of hot rolled steel strip by non-circular back-up roll geometry, Ironmaking & Steelmaking, Volume 36, Number 2, February 2009 , pp. 133-140(8).

Wirtz, W., Advanced Thermo Rolls for High Speed Modern Calenders, 7th International conference on New Available Technologies, June 4-6, 2002, Stockholm, Sweden.

Yuan, L., Järvenpää, V.M. & Keskinen, E. 2006. Roll vibration analysis with nip contact. Proceedings of the 7th International Conference on Rotor Dynamics, September 25-28, 2006, Vienna, Austria 6 p.

Zaoralek, M., Improved high temperature calender roll, Annual meeting – Technical Section, Canadian Pulp and Paper Association, Preprints, n pt B, 1991, p. 107-110. ISSN:0316-6732.

Zaoralek, M., Higher precision for high temperature calender rolls, PAPTAC 90th Annual Meeting, 2004.

Zwart, J., Farrel, W.R., Oxbow effect and surface temperature profiles of calendar rolls, Pulp and Paper Canada, Vol 92, No 2, 1992. p. 30-36.

ISBN 978-952-248-259-4
ISBN 978-952-248-260-0 (PDF)
ISSN 1795-2239
ISSN 1795-4584 (PDF)